SCATTERING OF ELASTIC WAVES AROUND A COMPRESSIONAL SOURCE

by

Donald Leavy

B.Sc., Physics, Universite de Montreal,

(1968)

SUBMITTED IN PARTIAL FULFILLMENT

OF THE REQUIREMENTS FOR THE

DEGREE OF MASTER OF

SCIENCE

at the

MASSACHUSETTS INSTITUTE OF TECHNOLOGY

February, 1972

Signature of Author _____

Department of Earth and Planetary Sciences, December, 1971

Certified by _____ 3, 1971

Thesis Supervisor

Accepted by _____

Chairman Departmental Committee on Graduate Students

SCATTERING OF ELASTIC WAVES AROUND A COMPRESSIONAL SOURCE

by

Donald Leavy

Submitted to the Department of Earth and Planetary Sciences on February, 1972 in partial fulfillment of the requirements for the degree of Master of Science.

ABSTRACT

We use the method of small perturbation to study the scattered wave generated by an arbitrary three dimensional inhomogeneous medium in the vicinity of a spherical compressional source. Two models of the medium inside the source are considered: a homogeneous solid and a fluid. It is only when scattering occurs within a boundary layer around the source, of radius a few times the one of the source, that we might expect the two models to give different results.

A spherical coordinate system is used to express the displacement field in terms of potentials. This leads us to a simple relation between the structure of the first order scattered wave and the structure of the medium, namely a given spherical harmonic of the medium parameters excited the same harmonic of the two spheroidal potentials. Moreover, no torsional waves (as defined in Chapter I) are generated to that order.

Special attention is given to the cases where scattering occurs within a wavelength and many wavelengths from the source. In particular, in the first case, we study the contribution of scattering to the anomalous SH wave which usually seems to originate near a compressional source and the result is applied to the Love waves from Boxcar nuclear explosion.

Thesis Supervisor: Keiiti Aki

Title: Professor of Geophysics

ACKNOWLEDGEMENTS

I wish to express my gratitude to Professor K. Aki for his help and his guidance through all the stages of this study. His moral support coupled to his experimental expertise made possible a rewarding experience from the human and scientific points of view.

Special thanks are due to Professor T. Madden who not only helped to clarify some basic concepts at an early phase of this work, but also made some useful suggestions concerning the possible methods of investigating the problem.

I wish to acknowledge the financial support for this work which was given by the Advanced Research Project Agency monitor by Air Force Office of Scientific Research through contract number F44620-70-C-0103.

TABLE OF CONTENTS

APPENDICES

LIST OF FIGURES

CHAPTER I

Introduction

1.1 Formulation of the problem

The purpose of this paper is to study the scattered displacement field due to an inhomogeneous distribution of medium parameters around a compressional source. A model of the experimental set-up is sketched below (Fig. 1)

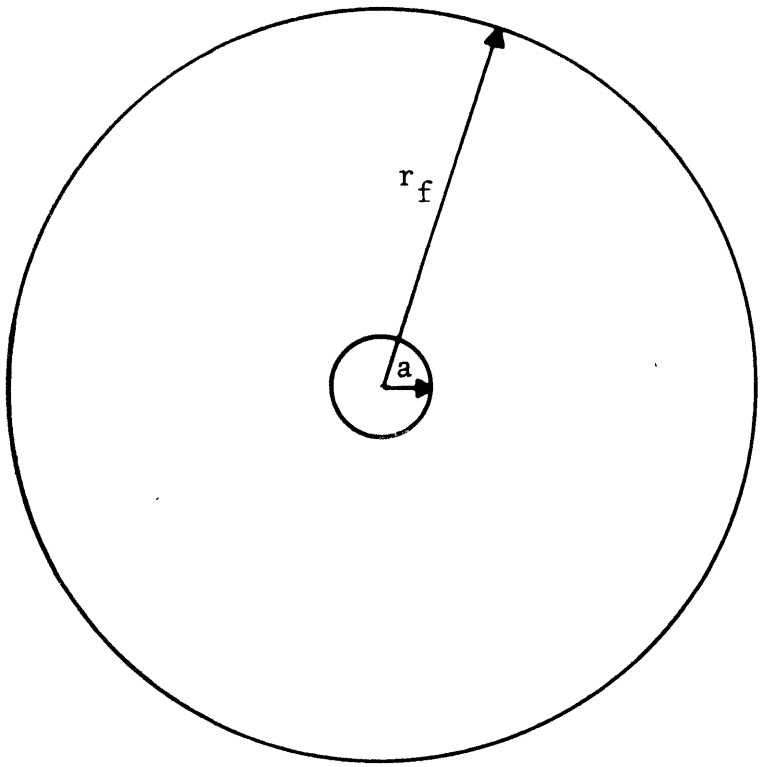

Figure 1. Experimental set-up

The distribution of stresses on the surface of a spherical cavity of radius "a" is modified by the production of an explosion in its interior.

The radius "a" is chosen such that Hooke's law is obeyed in the medium r > a which is formed by an infinite, isotropic, and inhomogeneous solid. An important assumption implied in the preceding model is that we will not consider the transformation of the field by the earth's surface.

Let us consider a model in which the distributions of parameters are inhomogeneous only within a sphere of radius r_f outside of which lies a homogeneous solid characterized by (ρ_0, μ_0, λ_0). Then, following an analysis apparently started by Sezawa (1927), we can show that, in a spherical coordinate system having its origin at the center of the source cavity, a complete decomposition of the displacement field in the region $r > r_f$, can be expressed in the following way:

Let $\vec{s}_\omega$ be the Fourier transform with respect to time of the displacement field, then

$$\vec{s}_\omega = \nabla\psi + \nabla\times\vec{a}_r r\psi_1 + \nabla\times\nabla\times\vec{a}_r r\psi_2$$

where $\vec{a}_r$ is the unit vector in the radial direction and, in standard notation (e.g. Morse and Feshback (1953)), we have that

$$(\psi,\psi_1,\psi_2) = (c_0 h_0(k_\alpha r),0,0)$$

$$+ \sum_{n=1}^{\infty} \sum_{m=0}^{n} (c^1_{nm} h_n(k_\alpha r), d^1_{nm} h_n(k_\beta r), f^1_{nm} h_n(k_\beta r))$$

$$\cdot P^m_n(\cos\theta)\cos m\phi$$

$$+ (c^2_{nm} h_n(k_\alpha r), d^2_{nm} h_n(k_\beta r), f^2_{nm} h_n(k_\beta r))$$

$$\cdot P^m_n(\cos\theta)\sin m\phi \qquad (1.1.1)$$

The fields ψ and ψ_2 are respectively called the spheroidal compressional and shear potential whereas ψ_1 is the torsional potential. Displacements corresponding to ψ_1 have no radial component while those corresponding to ψ_2 have a radial component which dies out quickly proportional to r^{-2}. Furthermore, there is no rotation around a radial axis associated with ψ_2.

Let us assume that in the medium $r > r_f$ we have placed a network of three components seismometers and thus have obtained partial or complete information of the (c^σ_{nm}, d^σ_{nm}, f^σ_{nm}) coefficients specified above. Then, the problem that naturally arises is to find which class the parameters of the source and the medium must belong to in order to be consistent with the observed coefficients.

1.2 The parameters of the source and the medium

An explosive source has been modelled by a sudden application of a uniform pressure since Sharpe (1942). This is basically the initial condition that we shall use in the present study to model the source of energy.

However, secondary seismic sources associated with explosion have been considered in recent years in order to explain the anomalous production of shear waves near the source. In this respect, Geyer and Martner (1969) have concluded, after fifteen years of field observation, that the production of SH waves near an explosive source seems to be the rule rather than the exception. Though a review of the mechanisms likely to excite these SH waves will appear in a paper by Aki and Tsai (1971), let us summarize them briefly since they bear directly on the inverse problem set up in the first section. They may be classified into the following three categories

1. Direct effect of explosion

Here we include all the processes inside the non-elastic domain of an explosion. Though no quantitative estimate of their efficiency has yet been worked out, we may expect an azimuthal asymmetry if the rocks in the immediate vicinity of the shot point are inhomogeneous, anisotropic or are set in motion along pre-existing cracks,

joints and faults. Even for a homogeneous isotropic medium, the radiation asymmetry may be caused by the Taylor instability (Wright and Carpenter 1962) or by formation of new cracks (Kisslinger, Mateker and McEvilly, 1961).

2. Release of pre-existing stress

The explosion may have modified the pre-existing stress distribution around the cavity. In this connection, two different models for this process have been studied.

a. The cavity model

Due to the shock induced fracture zone created by the explosion, the initial stress field around the source will be relaxed so as to meet the new equilibrium configuration inside the cavity. Archambeau and Sammis (1970) have worked out the anomalous field generated by this process in the case of the Rainier and Bilby nuclear explosion. They found, using reasonable values for the parameters, a good quantitative fit with field observations.

b. Trigger model

Aki et al (1969) suggested that a fault displacement triggered by the Benham explosion would explain fairly well the structure of the seismogram obtained for that nuclear event. Field observations near the source, aftershock studies and long period Love wave spectra observed at long distances, support the faulting hypothesis in that

case.

3. Scattering

It is often assumed in seismology that the earth has a layered structure with uniform thicknesses. By symmetry, no SH wave can be generated from a spherical compressional source buried in such a medium. Since the assumption of laterally homogeneous earth is obviously an extreme idealization especially at shallow depths, we must consider the generation of SH waves through scattering by the laterally inhomogeneous medium around the compressional source. In this connection, Smith (1963) argued in favor of the mode conversion in the elastic domain near the shot point on the basis of observed similarity between P, SV and SH spectra for the frequency range 0.5 to 2.5 cps.

One aim of this study is to provide a quantitative estimate of the efficiency of this process. But, in order to do so, we must specify the distributions of parameters in the medium. This point represents, no doubt, the core of the difficulty in the calculation. A hint of its solution is provided by the observation of the main compressional wave. Indeed, in order to obtain a good zero order approximation of the main body waves, one often replaces the real earth by a model having its average properties. Because of the success of this modelling technique, it suggests

that the medium is slightly inhomogeneous and that we should try to exploit this fact in order to gain greater flexibility in the evaluation of the scattered wave. This can be done by using the Born's approximation or method of small perturbation. The main advantage of this technique is that it permits us to analyze the scattered field generated by an arbitrary structure of the medium provided this structure does not deviate much from some given homogeneous model.

But, in order to carry out this program, we must also specify the properties of the medium inside the source. Indeed, a wave scattered in $r > a$ may impinge on the source and be scattered again depending on its properties. In that respect we shall study two models of the source. First, we shall discuss the case where the medium inside the source is a homogeneous solid having the same value of the parameters as the medium $r > r_f$. Incidentally, these parameters $(\rho_0, \mu_0, \lambda_0)$, will also be taken to represent the zero order structure of the medium $a < r < r_f$. Then, since a more realistic model of the medium inside the source is a fluid, we will try to investigate in which ways does a source of zero rigidity modify the field obtained in the first case.

1.3 Summaries of the following chapters

So, following this plan, chapter II will present a detailed derivation of the first approximation to the

displacement field we obtain by using the method of small perturbation. There, we will find it convenient to analyze the distributions of parameters in spherical harmonics in order to express the field as in Eq. 1.1.1. In that respect, we will reach two important results. First, to the approximation considered, no torsional waves are generated by the inhomogeneities. But, of more consequence still, we will show that a given pair $(c_{nm}^{\sigma}, f_{nm}^{\sigma})$ in Eq. 1.1.1 depends only on the (n,m,σ) harmonic of the medium parameters. For example, let us suppose that in $r > r_f$ we record a wave specified by the source, (c_0), together with a scattered wave specified by the coefficients say (c_{21}^{1}, f_{21}^{1}). Then, to the order considered, we can say that the structure of the medium can be expressed as

$$(\rho,\mu,\lambda) = (\rho_0,\mu_0,\lambda_0) + (\rho_{21}^{1}(r),\mu_{21}^{1}(r),\lambda_{21}^{1}(r)) \cdot P_2^1(\cos\theta)\cos\phi \qquad (1.3.1)$$

We therefore remark that this fact permits us to make a great step in the solution of the inverse problem.

Though, in this paper, we will be mainly concerned with the case where the seismometers are situated in the homogeneous region $r > r_f$, we will briefly mention, before closing the second chapter, how to generalize the results

to the case where the receivers lie inside the inhomogeneities.

Chapter III will be devoted to the evaluation of the scattered wave for some particular models. But, before going into a detailed calculation of the coefficients of 1.1.1 for a given structure, we will find it worthwhile to study the spectrum at the low and high frequency limits. To be more specific, we will first investigate the case where all the inhomogeneities are concentrated near the source i.e. such that

$$k_\alpha r_f << 1 \tag{1.3.2}$$

Secondly we will consider a medium formed by the first n order spherical harmonics of the parameters, but we will restrict their radial variation to the interior of two spheres of radius r_ℓ and r_f such that

$$k_\alpha r_f > k_\alpha r_\ell >> n^2 \tag{1.3.3}$$

The interest in these particular limits stems from the fact that, in these cases, we can expand the exact first order scattered wave in asymptotic series in terms of the parameters k times the radius of the scatterer. Then, we need only to keep the dominant term in these series in order

to describe the main contribution to the displacement field.

In this respect, we will reach an important result in the case where the scattering occurs near the source. Indeed we will show that the wave scattered by the spherical harmonics of the rigidity of order n = 2 depends on the frequency only through the spectrum of the source. Moreover, they are particularly sensitive to the inhomogeneities near the source. To give an example of this, let us consider a model specified by 1.3.1 together with the constraint 1.3.2. Then, for that case, the coefficients of 1.1.1, to the order considered, are

$$c_0 = G \quad \text{(the spectrum of the source)}$$

$$c^1_{21} = G \left(- \frac{4}{5} \frac{1}{(\lambda_0 + 2\mu_0)} \right) \int_a^{r_f} \frac{\mu^1_{21}}{r_0} \, dr_0$$

$$f^1_{21} = G \left(- \frac{2}{5} \frac{1}{\mu_0} \frac{k_\beta}{k_\alpha} \right) \int_a^{r_f} \frac{\mu^1_{21}}{r_0} \, dr_0$$

Furthermore, we will show that this group of harmonics (n=2) is the only one possessing such a characteristic. All the scattered waves generated by the other harmonics of the parameters have a low frequency cut-off. Therefore, we

see that these components of a given structure might prove to be the most efficient scatterer of long waves near the source. From that point of view, we will place some severe constraints on the possible structure that may cause the anomalous SH waves discussed in Section 1.2.

We will then turn our attention to the high frequency case and examine which type of structure may generate a substantial scattered wave. In this connection we will find it convenient to separate the displacement field in four components: the transmitted and reflected compressional and shear wave. In studying the first component we will be lead to consider the effect of structure varying slowly over many wavelengths. We will then compare the scattered wave obtained by the Born's approximation with the one we would calculate by using the methods of geometrical optics. In our investigation of the other components of the scattered waves, we will see that if the medium has some periodic structure, then some parts of the spectrum may be greatly enhanced relative to others, depending on the so-called Bragg's conditions.

Finally, having obtained these results, we will be in a better position to analyze the spectrum of a given structure for all frequencies.

The purpose of chapter IV is twofold. First to give a brief account of the case where the medium inside the source is a fluid. We will see there that in practice, the

influence of the fluid cavity is restricted to waves scattered within a boundary layer around the source, of radius less than ten times the one of the cavity. We will then consider the body forces equivalent and seismic moment for the scattering process likely to contribute to the anomalous SH signal discussed previously. In this connection, we will try to estimate the efficiency of this process in the case of the Boxcar nuclear explosion.

In the concluding chapter, we will discuss the possible ways of applying and improving the following analysis.

Various appendices have been added which will permit, it is hoped, the saving some of the time of a reader who wants to go into the details of the calculations.

CHAPTER II

Formal Derivation of the Scattered Wave Using The Method of Small Perturbations

2.1 Application of the method of small perturbation to the elastic wave problem

Let

$\tilde{\tilde{S}}$: the strain dyadic

$\tilde{\tilde{T}}$: the stress dyadic

$\vec{s}$: the displacement vector

Then, Newton's law without the body force term can be written as

$$\rho \frac{\partial^2 \vec{s}}{\partial t^2} = \nabla \cdot \tilde{\tilde{T}} \qquad (2.1.1)$$

We shall assume the medium to be isotropic so that we have the stress-strain relation

$$\tilde{\tilde{T}} = 2\mu \tilde{\tilde{S}} + \lambda |\tilde{\tilde{S}}| \tilde{\tilde{I}} \qquad (2.1.2)$$

where

$\tilde{\tilde{I}}$: the unit dyadic

$|\tilde{\tilde{S}}|$: the trace of $\tilde{\tilde{S}} \equiv \nabla \cdot \vec{s}$

μ, λ: the Lamé's constants.

Therefore, we can rewrite Eq. 1 as

$$\rho \frac{\partial^2 \vec{s}}{\partial t^2} = 2\nabla\mu \cdot\cdot \tilde{\tilde{S}} + 2\mu\nabla\cdot\tilde{\tilde{S}} + \nabla\lambda \cdot\cdot |\tilde{\tilde{S}}|\tilde{\tilde{I}} + \lambda\nabla\cdot|\tilde{\tilde{S}}|\tilde{\tilde{I}} \qquad (2.1.3)$$

Let us assume that within the inhomogeneous sphere ($r_f > r > a$) (see Fig. 1), the parameters are described by

$$\rho = \rho_0 + \varepsilon\rho_1$$

$$\mu = \mu_0 + \varepsilon\mu_1$$

$$\lambda = \lambda_0 + \varepsilon\lambda_1$$

where

$$\left(\varepsilon \frac{\rho_1}{\rho_0}\ ,\ \varepsilon \frac{\mu_1}{\mu_0}\ ,\ \varepsilon \frac{\lambda_1}{\lambda_0}\right) << (1,1,1)$$

The region $r > r_f$ and $r < a$ will be characterized by constant parameters

$$(\rho,\mu,\lambda) = (\rho_0,\mu_0,\lambda_0) \quad \text{for } r > r_f$$

$$(\rho,\mu,\lambda) = (\rho^-,\mu^-,\lambda^-) \quad \text{for } r < a$$

With the hope that the displacement field depends analytically

on ε as $\varepsilon \to 0$ we might try the following asymptotic expansion of $\vec{s}$

$$\vec{s} = \vec{s}_0 + \varepsilon\vec{s}_1 + \varepsilon^2\vec{s}_2 + \ldots \qquad \text{for } r > a$$

So, we can rewrite Eq. 3, for $r > a$, as follows

$$\begin{aligned}(\rho_0+\varepsilon\rho_1)\,\frac{\partial^2}{\partial t^2}(\vec{s}_0+\varepsilon\vec{s}_1+..) = {} & 2\varepsilon\nabla\mu_1\cdot\cdot(\tilde{\tilde{S}}_0+\varepsilon\tilde{\tilde{S}}_1+..) \\ & +2(\mu_0+\varepsilon\mu_1)\nabla\cdot(\tilde{\tilde{S}}_0+\varepsilon\tilde{\tilde{S}}_1+..) \\ & +\varepsilon\nabla\lambda_1\cdot\cdot(|\tilde{\tilde{S}}_0|+\varepsilon|\tilde{\tilde{S}}_1|+..)\tilde{\tilde{I}} \\ & +(\lambda_0+\varepsilon\lambda_1)\nabla\cdot(|\tilde{\tilde{S}}_0|+\varepsilon|\tilde{\tilde{S}}_1|+..)\tilde{\tilde{I}}\end{aligned} \qquad (2.1.4)$$

Collecting terms of the same order in ε, we have for $r > a$

a) The zero order equation

$$\rho_0\,\frac{\partial^2\vec{s}_0}{\partial t^2} - 2\mu_0\nabla\cdot\tilde{\tilde{S}}_0 - \lambda_0\nabla\cdot|\tilde{\tilde{S}}_0|\tilde{\tilde{I}} = 0 \qquad (2.1.5)$$

b) The first order equation

$$\rho_0 \frac{\partial^2 \vec{s}_1}{\partial t^2} - 2\mu_0 \nabla\cdot\tilde{\tilde{S}}_1 - \lambda_0 \nabla\cdot|\tilde{\tilde{S}}_1|\tilde{\tilde{I}} =$$

$$= -\rho_1 \frac{\partial^2 \vec{s}_0}{\partial t^2} + 2\nabla\mu_1 \cdot\cdot \tilde{\tilde{S}}_0 + 2\mu_1 \nabla\cdot\tilde{\tilde{S}}_0$$

$$+\nabla\lambda_1 \cdot\cdot |\tilde{\tilde{S}}_0|\tilde{\tilde{I}} + \lambda_1 \nabla\cdot|\tilde{\tilde{S}}_0|\tilde{\tilde{I}} \qquad (2.1.6)$$

In the region r < a if we use the expansion

$$\vec{s} = \vec{s}_0^- + \varepsilon \vec{s}_1^- + \varepsilon^2 \vec{s}_2^- + \ldots$$

the displacement field must then satisfy

c) The zero order equation

$$\rho^- \frac{\partial^2 \vec{s}_0^-}{\partial t^2} - 2\mu^- \nabla\cdot\tilde{\tilde{S}}_0^- - \lambda^- \nabla\cdot|\tilde{\tilde{S}}_0^-|\tilde{\tilde{I}} = 0 \qquad (2.1.7)$$

d) The first order equation

$$\rho^- \frac{\partial^2 \vec{s}_1^-}{\partial t^2} - 2\mu^- \nabla\cdot\tilde{\tilde{S}}_1^- - \lambda^- \nabla\cdot|\tilde{\tilde{S}}_1^-|\tilde{\tilde{I}} = 0 \qquad (2.1.8)$$

Perturbation of the boundary conditions

We must also meet, at r = a, the continuity of stress and displacement.

A) Continuity of stress

We must have that

$$2\mu \vec{a}_r \cdot\cdot \tilde{\tilde{S}} + \lambda \vec{a}_r \cdot\cdot |\tilde{\tilde{S}}| \tilde{\tilde{I}} \Big|_{r=a^-}$$

$$= 2\mu \vec{a}_r \cdot\cdot \tilde{\tilde{S}} + \lambda \vec{a}_r \cdot\cdot |\tilde{\tilde{S}}| \tilde{\tilde{I}} \Big|_{r=a^+} \qquad (2.1.9)$$

where

$\vec{a}_r$ is the unit vector in the radial direction

If we substitute the asymptotic expansion of the displacement field in Eq. 9 and collect the terms of the same order in ε, we obtain

a) The zero order boundary condition on stress

$$2\mu \vec{a}_r \cdot\cdot \tilde{\tilde{S}}_0 + \lambda \vec{a}_r \cdot\cdot |\tilde{\tilde{S}}_0| \tilde{\tilde{I}} \Big|_{r=a^-}$$

$$= 2\mu_0 \vec{a}_r \cdot\cdot \tilde{\tilde{S}}_0 + \lambda_0 \vec{a}_r \cdot\cdot |\tilde{\tilde{S}}_0| \tilde{\tilde{I}} \Big|_{r=a^+} \qquad (2.1.10)$$

b) The first order boundary condition on stress

$$2\mu^{-}\vec{a}_r\cdot\cdot\tilde{\tilde{S}}_1^{-} + \lambda^{-}\vec{a}_r\cdot\cdot|\tilde{\tilde{S}}_1^{-}|\tilde{\tilde{I}}\Big|_{r=a^{-}}$$

$$= 2\mu_1\vec{a}_r\cdot\cdot\tilde{\tilde{S}}_0 + \lambda_1\vec{a}_r\cdot\cdot|\tilde{\tilde{S}}_0|\tilde{\tilde{I}}$$

$$+2\mu_0\vec{a}_r\cdot\cdot\tilde{\tilde{S}}_1 + \lambda_0\vec{a}_r\cdot\cdot|\tilde{\tilde{S}}_1|\tilde{\tilde{I}}\Big|_{r=a+} \qquad (2.1.11)$$

B) Continuity of displacement at r = a

Case 1. At a solid-solid interface the three components of the displacement must be continuous, i.e.

$$\vec{s}_0^{-} + \varepsilon\vec{s}_1^{-} + ..\Big|_{r=a^{-}} = \vec{s}_0 + \varepsilon\vec{s}_1 + ..\Big|_{r=a^{+}}$$

Collecting the order in ε we have that

$$\vec{s}_0^{-}\Big|_{r=a^{-}} = \vec{s}_0\Big|_{r=a^{+}} \qquad (2.1.12)$$

$$\vec{s}_1^{-}\Big|_{r=a^{-}} = \vec{s}_1\Big|_{r=a^{+}} \qquad (2.1.13)$$

Case 2. At a fluid-solid interface (e.g. fluid cavity), the normal component of the displacement must be continuous, i.e.

$$\vec{a}_r\cdot(\vec{s}_0^{-} + \varepsilon\vec{s}_1^{-} + ..\Big|_{r=a^{-}} = \vec{a}_r\cdot(\vec{s}_0 + \varepsilon\vec{s}_1 + ..\Big|_{r=a^{+}}$$

Collecting the order in ε, we have that

$$\vec{a}_r \cdot \vec{s}_0^- \Big|_{r=a^-} = \vec{a}_r \cdot \vec{s}_0 \Big|_{r=a^+} \tag{2.1.14}$$

and

$$\vec{a}_r \cdot \vec{s}_1^- \Big|_{r=a^-} = \vec{a}_r \cdot \vec{s}_1 \Big|_{r=a^+} \tag{2.1.15}$$

The next step, then, is to solve the set of equations 5, 6, 7, 8 subject to the boundary conditions 10, 11, 12, 13 or 10, 11, 14, 15 depending on whether we consider a solid or a fluid cavity in $r < a$.

2.2 Solution of the zero order equations

We have to solve the following set of equations

For $r > a$

$$\rho_0 \frac{\partial^2 \vec{s}_0}{\partial t^2} - 2\mu_0 \nabla \cdot \tilde{\tilde{S}}_0 - \lambda_0 \nabla \cdot |\tilde{\tilde{S}}_0| \tilde{\tilde{I}} = 0 \tag{2.2.1}$$

for $r < a$

$$\rho^- \frac{\partial^2 \vec{s}_0^-}{\partial t^2} - 2\mu^- \nabla \cdot \tilde{\tilde{S}}_0^- - \lambda^- \nabla \cdot |\tilde{\tilde{S}}_0^-| \tilde{\tilde{I}} = 0 \tag{2.2.2}$$

subject to the boundary conditions

$$2\mu^{-}\vec{a}_r \cdot\cdot \tilde{\tilde{S}}_0^{-} + \lambda^{-}\vec{a}_r \cdot\cdot |\tilde{\tilde{S}}_0^{-}|\tilde{\tilde{I}}\Big|_{r=a^{-}}$$

$$= 2\mu_0\vec{a}_r \cdot\cdot \tilde{\tilde{S}}_0 + \lambda_0\vec{a}_r \cdot\cdot |\tilde{\tilde{S}}_0|\tilde{\tilde{I}}\Big|_{r=a^{+}} \qquad (2.2.3)$$

and

$$\vec{s}_0^{-}\Big|_{r=a^{-}} = \vec{s}_0\Big|_{r=a^{+}} \quad \text{(for solid-solid interface)} \qquad (2.2.4)$$

or

$$\vec{a}_r \cdot \vec{s}_0^{-}\Big|_{r=a^{-}} = \vec{a}_r \cdot \vec{s}_0\Big|_{r=a^{+}} \quad \text{(for fluid-solid interface)} \qquad (2.2.5)$$

Initial condition representing an explosion

Since Sharpe's (1942) model has been verified experimentally to give a fair representation of the compressional wave generated by an explosion, we will use it in order to represent our initial condition.

It consists of specifying a uniform radial pressure on the surface r = a, i.e.

$$2\mu_0\vec{a}_r \cdot\cdot \tilde{\tilde{S}}_0 + \lambda_0\vec{a}_r \cdot\cdot |\tilde{\tilde{S}}_0|\tilde{\tilde{I}}\Big|_{r=a^{+}} = T_{rr}(t)\vec{a}_r \qquad (2.2.6)$$

The solution of this well-known problem is outlined in Appendix I. It is shown there that if $\vec{s}_{0\omega}$ is the Fourier transform of $\vec{s}_0$ with respect to time, which will

be expressed in the following as

$$\vec{s}_{0\omega} \leftrightarrow \vec{s}_0 \ ,$$

then the displacement field can be written as

$$\vec{s}_{0\omega} = \nabla\psi_0 \tag{2.2.7}$$

and the compressional potential ψ_0 can be expressed as follows

$$\psi_0 = G\ h_0(k_\alpha r) \tag{2.2.8}$$

where G is the spectrum of the source and $h_0(k_\alpha r)$ is the zero order spherical Bessel function (see Appendix I for definition).

2.3 The first order equation

We can, now, solve the set of first order equations, i.e.

$$\rho_0 \frac{\partial^2 \vec{s}_1}{\partial t^2} - 2\mu_0 \nabla\cdot\tilde{\tilde{S}}_1 - \lambda_0 \nabla\cdot|\tilde{\tilde{S}}_1|\tilde{\tilde{I}}$$

$$= -\rho_1 \frac{\partial^2 \vec{s}_0}{\partial t^2} + 2\nabla\mu_1 \cdot\cdot\, \tilde{\tilde{S}}_0 + 2\mu_1 \nabla\cdot\tilde{\tilde{S}}_0$$

$$+\nabla\lambda_1 \cdot\cdot\, |\tilde{\tilde{S}}_0|\tilde{\tilde{I}} + \lambda_1 \nabla\cdot|\tilde{\tilde{S}}_0|\tilde{\tilde{I}} \tag{2.3.1}$$

for the medium r > a, and

$$\rho^- \frac{\partial^2 \vec{s}_1^-}{\partial t^2} - 2\mu^- \nabla \cdot \tilde{\tilde{S}}_1^- - \lambda^- \nabla \cdot |\tilde{\tilde{S}}_1^-| \tilde{\tilde{I}} = 0 \qquad (2.3.2)$$

inside the source, i.e. r < a

subject to the boundary conditions

$$2\mu^- \vec{a}_r \cdot\cdot \tilde{\tilde{S}}_1^- + \lambda^- \vec{a}_r \cdot\cdot |\tilde{\tilde{S}}_1^-| \tilde{\tilde{I}} \Big|_{r=a^-}$$

$$= 2\mu_1 \vec{a}_r \cdot\cdot \tilde{\tilde{S}}_0 + \lambda_1 \vec{a}_r \cdot\cdot |\tilde{\tilde{S}}_0| \tilde{\tilde{I}}$$

$$+ 2\mu_0 \vec{a}_r \cdot\cdot \tilde{\tilde{S}}_1 + \lambda_0 \vec{a}_r \cdot\cdot |\tilde{\tilde{S}}_1| \tilde{\tilde{I}} \Big|_{r=a^+} \qquad (2.3.3)$$

and

$$\vec{s}_1^- \Big|_{r=a^-} = \vec{s}_1 \Big|_{r=a^+} \text{ (for solid-solid interface)} \qquad (2.3.4)$$

or

$$\vec{a}_r \cdot \vec{s}_1^- \Big|_{r=a^-} = \vec{a}_r \cdot \vec{s}_1 \Big|_{r=a^+} \text{ (for fluid-solid interface)} \qquad (2.3.5)$$

The inhomogeneous term in 2.3.1, which might be thought of as a body force, denotes the fact that the main wave (i.e. the zero order solution) is being transformed at each point of the inhomogeneous sphere into a shear and a compressional wave.

The stress

$$2\mu_1 \vec{a}_r \cdot\cdot \tilde{\tilde{S}}_0 + \lambda_1 \vec{a}_r \cdot\cdot |\tilde{\tilde{S}}_0| \tilde{\tilde{I}}$$

in the boundary condition, might be assimilated to a new source at the surface of the cavity due to the inhomogeneous distributions of parameters there.

In order to simplify the evaluation of the scattered field we will split the problem into two parts:

Let

$$\vec{s}_1 = \vec{s}_{11} + \vec{s}_{12}$$

and

$$\vec{s}_1^- = \vec{s}_{11}^- + \vec{s}_{12}^-$$

where

a) $\vec{s}_{11}$ and $\vec{s}_{11}^-$ satisfy the inhomogeneous equations with homogeneous boundary conditions, i.e., for r > a

$$\rho_0 \frac{\partial^2 \vec{s}_{11}}{\partial t^2} - 2\mu_0 \nabla \cdot \tilde{\tilde{S}}_{11} - \lambda_0 \nabla \cdot |\tilde{\tilde{S}}_{11}| \tilde{\tilde{I}}$$

$$= -\rho_1 \frac{\partial^2 \vec{s}_0}{\partial t^2} + 2\nabla\mu_1 \cdot\cdot \tilde{\tilde{S}}_0$$

$$+ 2\mu_1 \nabla \cdot \tilde{\tilde{S}}_0 + \nabla\lambda_1 \cdot\cdot |\tilde{\tilde{S}}_0| \tilde{\tilde{I}} \qquad (2.3.6)$$

and for $r < a$

$$\rho^- \frac{\partial^2 \vec{s}_{11}^-}{\partial t^2} - 2\mu^- \nabla\cdot\tilde{\tilde{S}}_{11}^- - \lambda^- \nabla\cdot|\tilde{\tilde{S}}_{11}^-|\tilde{\tilde{I}} = 0 \qquad (2.3.7)$$

subject to the boundary conditions

$$2\mu^- \vec{a}_r\cdot\cdot\tilde{\tilde{S}}_{11}^- + \lambda^- \vec{a}_r\cdot\cdot|\tilde{\tilde{S}}_{11}^-|\tilde{\tilde{I}}\Big|_{r=a^-}$$

$$= 2\mu_0 \vec{a}_r\cdot\cdot\tilde{\tilde{S}}_{11} + \lambda_0 \vec{a}_r\cdot\cdot|\tilde{\tilde{S}}_{11}|\tilde{\tilde{I}}\Big|_{r=a^+} \qquad (2.3.8)$$

and

$$\vec{s}_{11}^-\Big|_{r=a^-} = \vec{s}_{11}\Big|_{r=a^+} \text{ (for solid-solid interface)} \qquad (2.3.9)$$

or

$$\vec{a}_r\cdot\vec{s}_{11}^-\Big|_{r=a^-} = \vec{a}_r\cdot\vec{s}_{11}\Big|_{r=a^+} \text{ (for fluid-solid interface)} \qquad (2.3.10)$$

In the following, I will call $\vec{s}_{11}$ the "body perturbation" contribution to the scattered wave.

b) $\vec{s}_{12}$ and $\vec{s}_{12}^-$ satisfy the homogeneous equations with inhomogeneous boundary conditions, i.e.

$$\rho_0 \frac{\partial^2 \vec{s}_{12}}{\partial t^2} - 2\mu_0 \nabla\cdot\tilde{\tilde{S}}_{12} - \lambda_0 \nabla\cdot|\tilde{\tilde{S}}_{12}|\tilde{\tilde{I}} = 0 \qquad (2.3.11)$$

for $r > a$

and

$$\rho^- \frac{\partial^2 \vec{s}_{12}^-}{\partial t^2} - 2\mu^- \nabla\cdot\tilde{\tilde{S}}_{12}^- - \lambda^- \nabla\cdot|\tilde{\tilde{S}}_{12}^-|\tilde{\tilde{I}} = 0 \qquad (2.3.12)$$

for $r < a$

subject to the boundary conditions

$$2\mu^- \vec{a}_r\cdot\cdot\tilde{\tilde{S}}_{12}^- + \lambda^- \vec{a}_r\cdot\cdot|\tilde{\tilde{S}}_{12}^-|\tilde{\tilde{I}}\Big|_{r=a^-}$$

$$= 2\mu_0 \vec{a}_r\cdot\cdot\tilde{\tilde{S}}_{12} + \lambda_0 \vec{a}_r\cdot\cdot|\tilde{\tilde{S}}_{12}|\tilde{\tilde{I}}$$

$$+ 2\mu_1 \vec{a}_r\cdot\cdot\tilde{\tilde{S}}_0 + \lambda_1 \vec{a}_r\cdot\cdot|\tilde{\tilde{S}}_0|\tilde{\tilde{I}}\Big|_{r=a^+} \qquad (2.3.13)$$

and

$$\vec{s}_{12}^-\Big|_{r=a^-} = \vec{s}_{12}\Big|_{r=a^+} \text{ (for solid-solid interface)} \qquad (2.3.14)$$

or

$$\vec{a}_r\cdot\vec{s}_{12}^-\Big|_{r=a^-} = \vec{a}_r\cdot\vec{s}_{12}\Big|_{r=a^+} \text{ (for fluid-solid interface} \qquad (2.3.15)$$

In the following, I will call $\vec{s}_{12}$ the "surface perturbation" contribution to the scattered wave.

We can verify that

$$\vec{s}_1 = \vec{s}_{11} + \vec{s}_{12}$$

and

$$\vec{s}_1 = \vec{s}_{11} + \vec{s}_{12}$$

by simply summing the two preceding sets of equations.

2.4 Body perturbation with a solid cavity

As a first approximation to our problem we will assume that the medium inside the source ($r < a$) is a homogeneous solid having the same value of the parameters as the medium $r > r_f$ i.e. for $r < a$

$$(\rho, \mu, \lambda) = (\rho_0, \mu_0, \lambda_0)$$

The case where we have a fluid inside the cavity will be discussed in Chapter IV and it will be shown there that in practice the two models do not differ much quantitatively.

In this case, in order to find the body perturbation part of the scattered wave, we have to solve

$$\rho_0 \frac{\partial^2 \vec{s}_{11}}{\partial t^2} - 2\mu_0 \nabla \cdot \tilde{\tilde{S}}_{11} - \lambda_0 \nabla \cdot |\tilde{\tilde{S}}_{11}| \tilde{\tilde{I}}$$

$$= -\rho_1 \frac{\partial^2 \vec{s}_0}{\partial t^2} + 2\nabla \mu_1 \cdot\cdot \tilde{\tilde{S}}_0 + 2\mu_1 \nabla \cdot \tilde{\tilde{S}}_0$$

$$+ \nabla \lambda_1 \cdot\cdot |\tilde{\tilde{S}}_0| \tilde{\tilde{I}} + \lambda_1 \nabla \cdot |\tilde{\tilde{S}}_0| \tilde{\tilde{I}} \qquad (2.4.1)$$

which is valid here throughout space.

In the model just described, the boundary conditions, eq. 2.3.8 and 2.3.9, are redundant. Indeed, we have to use them only in the case where the medium $r < a$ has parameters different from $(\rho_0, \mu_0, \lambda_0)$. In such cases (e.g. a fluid cavity), they permit us to determine the conditon that must be met at $r = a$ by a scattered wave impinging on the source (see Fig. 2).

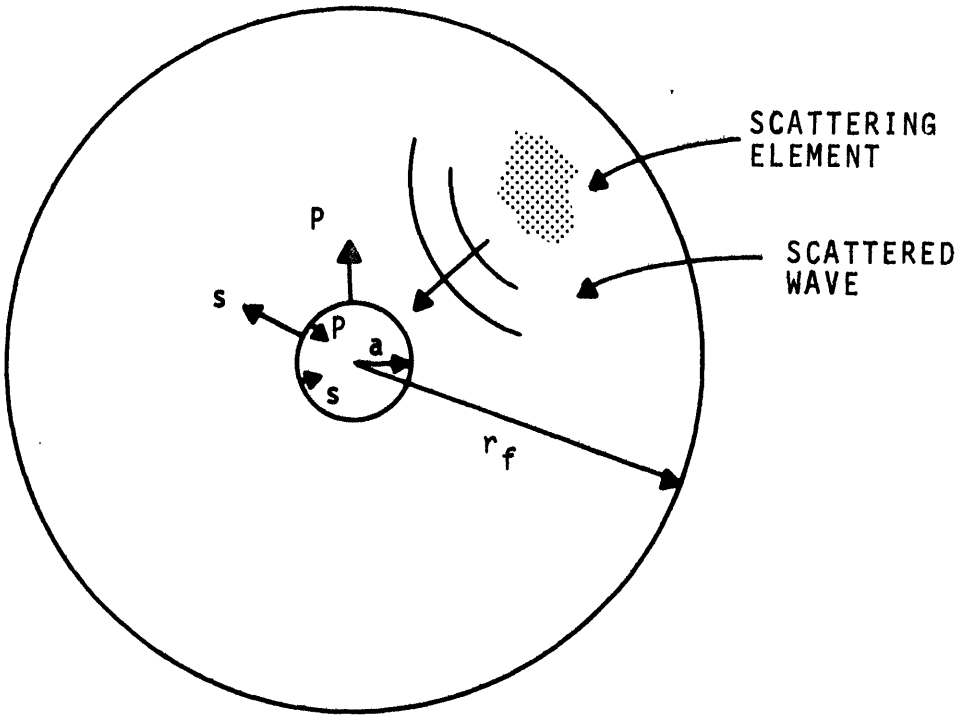

Figure 2. A wave scattered in the inhomogeneous sphere might impinge on the cavity $r < a$ and be scattered again

Taking into account the fact that the main wave has only radial motion we can rewrite 2.4.1 in the form

$$\rho_0 \frac{\partial^2 \vec{s}_{11}}{\partial t^2} - 2\mu_0 \nabla\cdot\tilde{\tilde{S}}_{11} - \lambda_0 \nabla\cdot|\tilde{\tilde{S}}_{11}|\tilde{\tilde{I}}$$

$$= \left[-\rho_1\left(\frac{\lambda_0+2\mu_0}{\rho_0}\right) + 2\mu_1+\lambda_1\right] \frac{\partial}{\partial r} \frac{1}{r^2} \frac{\partial r^2 s_r^0}{\partial r} \vec{a}_r$$

$$+ 2\frac{\partial \mu_1}{\partial r} \frac{\partial s_r^0}{\partial r} \vec{a}_r + \frac{\partial \lambda_{11}}{\partial r}\left[\frac{1}{r^2} \frac{\partial r^2 s_r^0}{\partial r}\right] \vec{a}_r$$

$$+ \frac{2}{r} \frac{\partial \mu_1}{\partial \theta} \frac{s_r^0}{r} \vec{a}_\theta + \frac{1}{r} \frac{\partial \lambda_{11}}{\partial \theta} \left[\frac{1}{r^2} \frac{\partial r^2 s_r^0}{\partial r}\right] \vec{a}_\theta$$

$$+ \frac{2}{r \sin\theta} \frac{\partial \mu_1}{\partial \phi} \frac{s_r^0}{r} \vec{a}_\phi + \frac{1}{r \sin\theta} \frac{\partial \lambda_{11}}{\partial \phi} \cdot$$

$$\left[\frac{1}{r^2} \frac{\partial r^2 s_r^0}{\partial r}\right] \vec{a}_\phi \qquad (2.4.2)$$

Analysis of the parameters

We shall assume that at each radius r we can decompose the inhomogeneous parameters in spherical harmonics, i.e.

$$(\rho_1,\mu_1,\lambda_1) = (\rho_{00}(r),\mu_{00}(r),\lambda_{00}(r))$$

$$+ \sum_{n=1}^{\infty} \sum_{m=0}^{n} [(\rho_{nm}^1,\mu_{nm}^1,\lambda_{nm}^1) \cos m\phi$$

$$+ (\rho_{nm}^2,\mu_{nm}^2,\lambda_{nm}^2)\sin m\phi] P_n^m(\cos\theta)$$

where

$$(\rho_{n,0},\mu_{n,0},\lambda_{n,0}) = \frac{2n+1}{4\pi} \int_{-\pi}^{\pi}\int_{0}^{\pi} (\rho_1,\mu_1,\lambda_1)\cdot$$

$$P_n(\cos\ \theta)\sin\ \theta d\theta d\phi$$

and

$$(\rho^1_{nm},\mu^1_{nm},\lambda^1_{nm}) = \frac{2n+1}{2\pi}\frac{(n-m)!}{(n+m)!} \int_{-\pi}^{\pi}\int_{0}^{\pi} (\rho_1,\mu_1,\lambda_1)\cos\ m\phi\cdot$$

$$P^m_n(\cos\ \theta)\sin\ \theta\ d\theta d\phi$$

$$(\rho^2_{nm},\mu^2_{nm},\lambda^2_{nm}) = \frac{2n+1}{2\pi}\frac{(n-m)!}{(n+m)!} \int_{-\pi}^{\pi}\int_{0}^{\pi} (\rho_1,\mu_1,\lambda_1)\sin\ m\phi\cdot$$

$$P^m_n(\cos\ \theta)\sin\ \theta d\theta d\phi$$

Since 2.4.2 is linear, its solution will be the sum of the contributions from each harmonic of the parameters. So, let us consider a general term in our decomposition, i.e.

$$(\rho_1,\mu_1,\lambda_1) = (\rho^1_{nm},\mu^1_{nm},\lambda^1_{nm})\ \cos\ m\phi\ P^m_n(\cos\ \theta)$$

with $n > 0$

The case of pure radial variation of the parameters (i.e. n = 0) will be treated afterwards.

We can then rewrite 2.4.2 as

$$\rho_0 \frac{\partial^2 \vec{s}_{11}}{\partial t^2} - 2\mu_0 \nabla\cdot\tilde{\tilde{S}}_{11} - \lambda_0 \nabla\cdot|\tilde{\tilde{S}}_{11}|\tilde{\tilde{I}}$$

$$= P_n^m(\cos\theta)\cos m\phi \left\{ \left[-\rho_{nm}^1 \left(\frac{\lambda_0 + 2\mu_0}{\rho_0} \right) + 2\mu_{nm}^1 + \lambda_{nm}^1 \right] \right.$$

$$\left. \cdot \frac{\partial}{\partial r} \frac{1}{r^2} \frac{\partial r^2 s_r^0}{\partial r} + 2 \frac{\partial \mu_{nm}^1}{\partial r} \frac{\partial s_r^0}{\partial r} + \frac{\partial \lambda_{nm}^1}{\partial r} \frac{1}{r^2} \frac{\partial r^2 s_r^0}{\partial r} \right\} \vec{a}_r$$

$$+ \frac{\partial}{\partial\theta} P_n^m(\cos\theta)\cos m\phi \left\{ 2\mu_{nm}^1 \frac{s_r^0}{r^2} + \frac{\lambda_{nm}^1}{r^3} \frac{\partial r^2 s_r^0}{\partial r} \right\} \vec{a}_\theta$$

$$+ \frac{P_n^m(\cos\theta)}{\sin\theta} \frac{\partial}{\partial\phi} \cos m\phi \left\{ 2\mu_{nm}^1 \frac{s_r^0}{r^2} + \frac{\lambda_{nm}^1}{r^3} \frac{\partial r^2 s_r^0}{\partial r} \right\} \vec{a}_\phi$$

(2.4.3)

Green's functions

We would like to find the solution to the equation

$$\rho_0 \frac{\partial^2 \vec{s}_{11}^g}{\partial t^2} - 2\mu_0 \nabla\cdot\tilde{\tilde{S}}_{11}^g - \lambda_0 \nabla\cdot|\tilde{\tilde{S}}_{11}^g|\tilde{\tilde{I}}$$

$$= P_n^m(\cos\theta)\cos m\phi \; A\delta(r-r_0)\vec{a}_r$$

$$+ \frac{\partial}{\partial\theta} P_n^m(\cos\theta)\cos m\phi \; B\delta(r-r_0)\vec{a}_\theta$$

$$+ \frac{P_n^m(\cos\theta)}{\sin\theta} \frac{\partial}{\partial\phi} \cos m\phi \; B\delta(r-r_0)\vec{a}_\phi \qquad (2.4.4)$$

where $\delta(r-r_0)$ is the Dirac's delta function and A, B are constants.

The solution $\vec{s}^g_{11}$ can be expressed in the following way:

Let

$$\vec{s}^g_{11\omega} \leftrightarrow \vec{s}^g_{11}$$

then

$$\vec{s}^g_{11\omega} = \nabla K + \nabla\times\nabla\times\vec{a}_r rH \qquad (2.4.5)$$

where

$$K = \left[- \frac{Ar_0^2}{i(\lambda_0+2\mu_0)} \frac{dj_n(k_\alpha r_0)}{dk_\alpha r_0} h_n(k_\alpha r) \right.$$

$$\left. - \frac{B(n)(n+1)r_0^2}{i(\lambda_0+2\mu_0)} \frac{j_n(k_\alpha r_0)}{k_\alpha r_0} h_n(k_\alpha r) \right] P_n^m(\cos\theta)\cos m\phi$$

$$\text{for } r > r_0$$

$$= \left[- \frac{Ar_0^2}{i(\lambda_0+2\mu_0)} \frac{d\, h_n(k_\alpha r_0)}{dk_\alpha r_0} j_n(k_\alpha r) \right.$$

$$\left. - \frac{B(n)(n+1)r_0^2}{i(\lambda_0+2\mu_0)} \frac{h_n(k_\alpha r_0)}{k_\alpha r_0} j_n(k_\alpha r) \right] P_n^m(\cos\theta)\cos m\phi$$

$$\text{for } r < r_0 \qquad (2.4.6)$$

and

$$H = \left[-\frac{Ar_0^2}{i\mu_0} \frac{j_n(k_\beta r_0)}{k_\beta r_0} h_n(k_\beta r) \right.$$

$$\left. -\frac{Br_0^2}{i\mu_0} \left(\frac{j_n(k_\beta r_0)}{k_\beta r_0} + \frac{dj_n(k_\beta r_0)}{dk_\beta r_0} \right) h_n(k_\beta r) \right] \cdot$$

$$P_n^m(\cos\theta)\cos m\phi \qquad \text{for } r > r_0$$

$$= \left[-\frac{Ar_0^2}{i\mu_0} \frac{h_n(k_\beta r_0)}{k_\beta r_0} j_n(k_\beta r) \right.$$

$$\left. -\frac{Br_0^2}{i\mu_0} \left(\frac{h_n(k_\beta r_0)}{k_\beta r_0} + \frac{dh_n(k_\beta r_0)}{dk_\beta r_0} \right) j_n(k_\beta r) \right] \cdot$$

$$P_n^m(\cos\theta)\cos m\phi \qquad \text{for } r < r_0 \qquad (2.4.7)$$

The validity of these formulas may be confirmed by checking that

1. They satisfy the wave equation in $r > r_0$ and $r < r_0$
2. They are radiating at ∞ and are finite at $r = 0$
3. $\vec{s}^g_{11\omega}$ is continuous at $r = r_0$ i.e.

$$\vec{s}^g_{11\omega}\Big|_{r_0^-} = \vec{s}^g_{11\omega}\Big|_{r_0^+}$$

4. They satisfy the proper jump in stress across $r = r_0$ i.e.

$$- \left[2\mu_0 \vec{a}_r \cdot\cdot \tilde{\tilde{S}}^g_{11\omega} + \lambda_0 \vec{a}_r \cdot\cdot |\tilde{\tilde{S}}^g_{11\omega}| \tilde{\tilde{I}}\right]_{r=r_0^+}$$

$$+ \left[2\mu_0 \vec{a}_r \cdot\cdot \tilde{\tilde{S}}^g_{11\omega} + \lambda_0 \vec{a}_r \cdot\cdot |\tilde{\tilde{S}}^g_{11\omega}| \tilde{\tilde{I}}\right]_{r=r_0^-}$$

$$= P_n^m(\cos\theta)\cos m\phi \; A \; \vec{a}_r$$

$$+ \frac{\partial}{\partial\theta} P_n^m(\cos\theta)\cos m\phi \; B\vec{a}_\theta + \frac{P_n^m(\cos\theta)}{\sin\theta} \frac{\partial}{\partial\phi} \cos m\phi \; B \; \vec{a}_\phi$$

A more inductive procedure to find these Green's functions is detailed in Appendix II.

Making use of these Green's functions, we can therefore write the solution of eq. 2.4.3 in the following way

Let

$$\vec{s}_{11} \leftrightarrow \vec{s}_{11\omega}$$

then, for $r > r_f$

$$\vec{s}_{11\omega} = \nabla\psi^B + \nabla\times\nabla\times\vec{a}_r r\psi_2^B$$

where

$$\psi^B = \frac{P_n^m(\cos\theta)\cos m\phi}{i(\lambda_0+2\mu_0)} h_n(k_\alpha r)$$

$$\int_a^{r_f} -\left\{\left[-\rho^1_{nm}\left(\frac{\lambda_0+2\mu_0}{\rho_0}\right) + 2\mu^1_{nm} + \lambda^1_{nm}\right]\frac{\partial}{\partial r_0}\frac{1}{r_0^2}\frac{\partial r_0^2 s^0_{r_0\omega}}{\partial r_0}\right.$$

$$+ 2\frac{\partial \mu^1_{nm}}{\partial r_0}\frac{\partial s^0_{r_0\omega}}{\partial r_0} + \frac{\partial \lambda^1_{nm}}{\partial r_0}\frac{1}{r_0^2}\frac{\partial r_0^2 s^0_{r_0\omega}}{\partial r_0}\left.\right\} r_0^2 \frac{dj_n(k_\alpha r_0)}{dk_\alpha r_0}$$

$$-\left[2\mu^1_{nm}\frac{s^0_{r_0\omega}}{r_0^2} + \frac{\lambda^1_{nm}}{r_0^3}\frac{\partial r_0^2 s^0_{r_0\omega}}{\partial r_0}\right] n(n+1) r_0^2 \frac{j_n(k_\alpha r_0)}{k_\alpha r_0}\, dr_0$$

(2.4.8)

and

$$\psi_2^B = \frac{P_n^m(\cos\theta)\cos m\phi}{i\mu_0} h_n(k_\beta r)$$

$$\int_a^{r_f} -\left\{\left[-\rho^1_{nm}\left(\frac{\lambda_0+2\mu_0}{\rho_0}\right)+2\mu^1_{nm}+\lambda^1_{nm}\right]\frac{\partial}{\partial r_0}\frac{1}{r_0^2}\frac{\partial r_0^2 s^0_{r_0\omega}}{\partial r_0}\right.$$

$$+2\frac{\partial \mu^1_{nm}}{\partial r_0}\frac{\partial s^0_{r_0\omega}}{\partial r_0} + \frac{\partial \lambda^1_{nm}}{\partial r_0}\frac{1}{r_0^2}\frac{\partial r_0^2 s^0_{r_0\omega}}{\partial r_0}\left.\right\} r_0^2 \frac{j_n(k_\beta r_0)}{k_\beta r_0}$$

$$-\left[\frac{2\mu^1_{nm}}{r_0^2} s^0_{r_0\omega} + \frac{\lambda^1_{nm}}{r_0^3}\frac{\partial r_0^2 s^0_{r_0\omega}}{\partial r}\right] r_0^2 \left(\frac{j_n(k_\beta r_0)}{k_\beta r_0} + \frac{dj_n(k_\beta r_0)}{dk_\beta r_0}\right) dr_0$$

(2.4.9)

where $s^0_{r_0\omega}$ is the Fourier transform of the displacement contained in the main wave. The j_n and h_n are the spherical Bessel functions as defined in Appendix II.

The expression for ψ_2^B can be somewhat simplified by rewriting it in the following form (see Appendix III).

$$\psi_2^B = -\frac{P_n^m(\cos\theta)}{i\mu_0}\cos m\phi\, h_n(k_\beta r)\left[\frac{2\mu^1_{nm}}{r_0^2}s^0_{r_0\omega} + \frac{\lambda^1_{nm}}{r_0^3}\frac{\partial r_0^2 s^0_{r_0\omega}}{\partial r_0}\right]$$

$$r_0^2\,\frac{j_n(k_\beta r_0)}{k_\beta r_0}\Bigg|_a^{r_f} + \frac{P_n^m(\cos\theta)\cos m\phi}{i\mu_0}\,h_n(k_\beta r)\cdot$$

$$\int_a^{r_f}\left\{-\left[-\rho^1_{nm}\left(\frac{\lambda_0+2\mu_0}{\rho_0}\right) + 2\mu^1_{nm}\right]\frac{\partial}{\partial r_0}\,\frac{1}{r_0^2}\,\frac{\partial r_0^2 s^0_{r_0\omega}}{\partial r_0}\right.$$

$$\left. -2r_0^2\left[\frac{\partial}{\partial r_0}\left(\frac{s^0_{r_0\omega}}{r_0}\right)\right]\left[\frac{\partial}{\partial r_0}\,\frac{\mu^1_{nm}}{r_0}\right]\right\} r_0^2\,\frac{j_n(k_\beta r_0)}{k_\beta r_0}\,dr_0 \qquad (2.4.10)$$

In these expressions, $k_\beta = \frac{\omega}{\beta} = \frac{\omega}{(\mu_0/\rho_0)^{1/2}}$

The case n = 0

When all the parameters vary only in the radial direction i.e.

$$(\rho_1,\mu_1,\lambda_1) = (\rho_{00}(r),\mu_{00}(r),\lambda_{00}(r))$$

Then, eq. 2.4.2 reads

$$\rho_0 \frac{\partial^2 \vec{s}_{11}}{\partial t^2} - 2\mu_0 \nabla\cdot\tilde{\tilde{S}}_{11} - \lambda_0 \nabla\cdot|\tilde{\tilde{S}}_{11}|\tilde{\tilde{I}}$$

$$= \left[-\rho_{00}\left(\frac{\lambda_0+2\mu_0}{\rho_0}\right) + 2\mu_{00}+\lambda_{00}\right] \frac{\partial}{\partial r} \frac{1}{r^2} \frac{\partial r^2 s_r^0}{\partial r} \vec{a}_r$$

$$+ 2 \frac{\partial \mu_{00}}{\partial r} \frac{\partial s_r^0}{\partial r} \vec{a}_r + \frac{\partial \lambda_1}{\partial r}\left[\frac{1}{r^2} \frac{\partial r^2 s_r^0}{\partial r}\right] \vec{a}_r \tag{2.4.11}$$

By following somewhat the same procedure as before and as detailed in Appendix IV, we obtain, for $r > r_f$

$$\vec{s}_{11\omega} = \nabla\psi^B \tag{2.4.12}$$

where

$$\psi^B = \frac{h_0(k_\alpha r)}{i(\lambda_0+2\mu_0)} \int_a^{r_f} \left\{ \left[-\rho_{00}\left(\frac{\lambda_0+2\mu_0}{\rho_0}\right)+2\mu_{00}+\lambda_{00}\right] \right.$$

$$\frac{\partial}{\partial r_0} \frac{1}{r_0^2} \frac{\partial r_0^2 s^0_{r_0\omega}}{\partial r_0}$$

$$\left. +2 \frac{\partial \mu_{00}}{\partial r_0} \frac{\partial s^0_{r_0\omega}}{\partial r_0} + \frac{\partial \lambda_{00}}{\partial r_0} \frac{1}{r_0^2} \frac{\partial r_0^2 s^0_{r_0\omega}}{\partial r_0} \right\} r_0^2 j_1(k_\alpha r_0) dr_0 \tag{2.4.13}$$

This completes our evaluation of the body perturbation.

2.5 Surface perturbation

Now let us evaluate the part of the scattered wave coming from the inhomogeneous boundary conditions.

For that, we have to solve the system of equations:

$$\rho_0 \frac{\partial^2 \vec{s}_{12}}{\partial t^2} - 2\mu_0 \nabla\cdot\tilde{\tilde{S}}_{12} - \lambda_0 \nabla\cdot|\tilde{\tilde{S}}_{12}|\tilde{\tilde{I}} = 0$$

for $r > a$ (2.5.1)

$$\rho_0 \frac{\partial^2 \vec{s}_{12}}{\partial t^2} - 2\mu_0 \nabla\cdot\tilde{\tilde{S}}^-_{12} - \lambda_0 \nabla\cdot|\tilde{\tilde{S}}^-_{12}|\tilde{\tilde{I}} = 0$$

for $r < a$ (2.5.2)

subject to the boundary conditions:

$$2\mu_0 \vec{a}_r\cdot\tilde{\tilde{S}}^-_{12} + \lambda_0 \vec{a}_r\cdot|\tilde{\tilde{S}}^-_{12}|\tilde{\tilde{I}}\Big|_{r=a^-}$$

$$= 2\mu_0 \vec{a}_r\cdot\tilde{\tilde{S}}_{12} + \lambda_0 \vec{a}_r\cdot|\tilde{\tilde{S}}_{12}|\tilde{\tilde{I}}$$

$$+ 2\mu_1 \vec{a}_r\cdot\tilde{\tilde{S}}_0 + \lambda_1 \vec{a}_r\cdot|\tilde{\tilde{S}}_0|\tilde{\tilde{I}}\Big|_{r=a^+} \quad (2.5.3)$$

with

$$\vec{s}^-_{12}\Big|_{r=a^-} = \vec{s}_{12}\Big|_{r=a^+} \quad (2.5.4)$$

In order to solve this boundary value problem, we can follow Sato's (1949) result as detailed in Appendix V.

As shown there, if we consider the general term

$$(\rho_1(a),\mu_1(a),\lambda_1(a)) = (\rho^1_{nm}(a),\mu^1_{nm}(a),\lambda^1_{nm}(a))\cdot$$

$$P^m_n(\cos\theta)\cos m\phi \quad \text{for } n > 0$$

then, the displacement field solution of 2.5.1 can be written as follows:

Let

$$\vec{s}_{12\omega} \leftrightarrow \vec{s}_{12}$$

then for $r > a$

$$\vec{s}_{12\omega} = \nabla\psi^s + \nabla\times\nabla\times\vec{a}_r r\psi^s_2$$

where

$$\psi^s = -\frac{P^m_n(\cos\theta)\cos m\phi}{i(\lambda_0+2\mu_0)} h_n(k_\alpha r)\cdot$$

$$\left(2\mu^1_{nm}(a)\ \frac{\partial s^0_{a\omega}}{\partial a} + \frac{\lambda^1_{nm}}{a^2}\ \frac{\partial a^2 s^0_{a\omega}}{\partial a}\ \right)a^2\ \frac{dj_n(k_\alpha a)}{dk_\alpha a}$$

(2.5.5)

and

$$\psi_2^s = - \frac{P_n^m(\cos\theta)\cos m\phi}{i\mu_0} h_n(k_\beta a) \cdot$$

$$\left(2\mu_{nm}^1(a) \frac{\partial s_{a\omega}^0}{\partial a} + \frac{\lambda_{nm}^1}{a^2} \frac{\partial a^2 s_{a\omega}^0}{\partial a}\right) a^2 \frac{j_n(k_\beta a)}{k_\beta a} \qquad (2.5.6)$$

The special case where the perturbed parameters have no angular dependence i.e.

$$(\rho_1(a), \mu_1(a), \lambda_1(a)) = (\rho_{00}(a), \mu_{00}(a), \lambda_{00}(a))$$

can be handled in a similar way (see Appendix V).

In that case, the displacement field for r > a can be expressed in the form

$$\vec{s}_{12\omega} = \nabla\psi^s \qquad (2.5.7)$$

where

$$\psi^s = \frac{h_0(k_\alpha r)}{i(\lambda_0+2\mu_0)} \left(2\mu_{00}(a) \frac{\partial s_{a\omega}^0}{\partial a} + \frac{\lambda_{00}(a)}{a^2} \frac{\partial a^2 s_{a\omega}^0}{\partial a}\right) a^2 j_1(k_\alpha a) \qquad (2.5.8)$$

2.6 Equivalence of a surface perturbation to a body perturbation

We would like to demonstrate that the formulas we

obtain for the wave emitted at the surface r = a, ($\vec{s}_{12}$), could have been obtained using the expression we have for the body perturbation ($\vec{s}_{11}$).

Let us consider the following two inhomogeneous models specified by

$$(\rho_1,\mu_1,\lambda_1) = ({}^1\rho^1_{nm}(r),{}^1\mu^1_{nm}(r),{}^1\lambda^1_{nm})P^m_n(\cos\theta)\cos m\phi$$

and

$$(\rho_2,\mu_2,\lambda_2) = ({}^2\rho^1_{nm}(r),{}^2\mu^1_{nm}(r),{}^2\lambda^1_{nm})P^m_n(\cos\theta)\cos m\phi$$

Let us fix the relation between the two models by

$$({}^2\rho^1_{nm}(r),{}^2\mu^1_{nm}(r),{}^2\lambda^1_{nm}(r)) = ({}^1\rho^1_{nm}(r+\Delta),{}^1\mu^1_{nm}(r+\Delta),{}^1\lambda^1_{nm}$$

$$\cdot(r+\Delta))$$

where Δ is arbitrarily small (see Fig. 3).

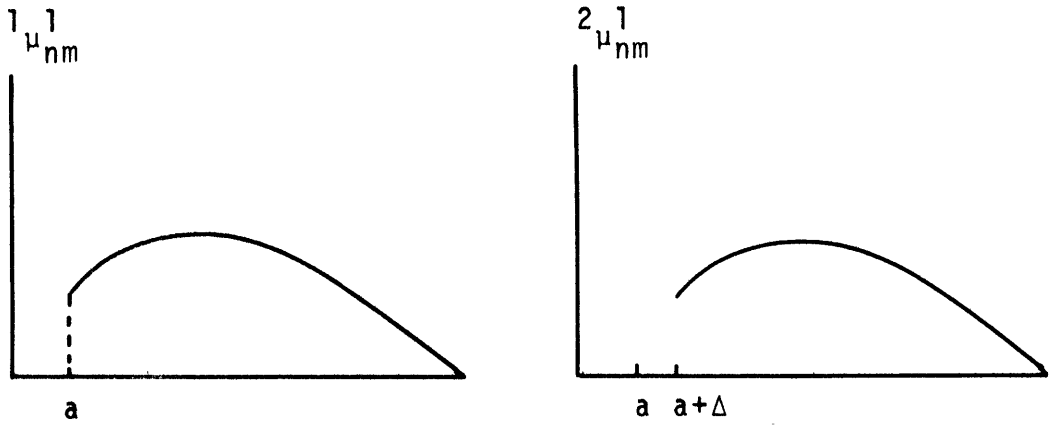

Figure 3. Two models differing slightly and specified by $^2\mu^1_{nm}(r) = {}^1\mu^1_{nm}(r+\Delta)$ where Δ is very small

Since in the second model

$$(^2\rho^1_{nm}(a), ^2\mu^1_{nm}(a), ^2\lambda^1_{nm}(a)) = (0,0,0)$$

no wave is emitted at r = a. But, we must have that

$$\frac{\partial\, ^2\mu^1_{nm}}{\partial r} = {}^1\mu^1_{nm}\delta(r-(a+\Delta)) + \frac{\partial\, ^1\mu^1_{nm}}{\partial r}\,(r+\Delta)$$

and

$$\frac{\partial\, ^2\lambda^1_{nm}}{\partial r} = {}^1\lambda^1_{nm}\delta(r-(a+\Delta)) + \frac{\partial\, ^1\mu^1_{nm}}{\partial r}\,(r+\Delta)$$

If we substitute these expressions in the formulas 2.4.8 and 2.4.9 we obtain after passing to the limit $\Delta \to 0$

$$\psi^{B_2} = \psi^{s_1} + \psi^{B_1}$$

and

$$\psi_2^{B_2} = \psi_2^{s_1} + \psi_2^{B_1}$$

where ψ^{B_2} and $\psi_2^{B_2}$ are respectively the compressional and shear potential coming from the body perturbations of the second model whereas ψ^{s_1} and ψ^{B_1} are the surface and body perturbation of the compressional wave generated by the first model and $\psi_2^{s_1}$, $\psi_2^{B_1}$ the corresponding shear potential.

This shows that the wave emitted at the surface is caused by the jump in the value of the parameters that occurs there.

2.7 Summary of the preceding results

For a compressional source acting at the surface of a spherical cavity characterized by $(\rho_0, \mu_0, \lambda_0)$, the displacement field in the region

$$r > r_f$$

can be given by

$$\vec{s}_\omega = \nabla\psi + \nabla\times\nabla\times r\vec{a}_r\psi_2$$

where

$$\psi = Gh_0(k_\alpha r) + \varepsilon c_{00}h_0(k_\alpha r)$$

$$+ \sum_{n=1}^{\infty}\sum_{m=0}^{n}(\varepsilon c^1_{nm}\cos m\phi + \varepsilon c^2_{nm}\sin m\phi)h_n(k_\alpha r)P^m_n(\cos\theta)$$

and

$$\psi_2 = \sum_{n=1}^{\infty}\sum_{m=0}^{n}(\varepsilon f^1_{nm}\cos m\phi + \varepsilon f^2_{nm}\sin m\phi)h_n(k_\beta r)P^m_n(\cos\theta)$$

where

$Gh_0(k_\alpha r)$ is the zero order solution (2.7.1)

$$c_{00} = \frac{1}{i(\lambda_0+2\mu_0)}\left(2\mu_{00}(a)\frac{\partial s^0_{a\omega}}{\partial a} + \frac{\lambda_{00}(a)}{a^2}\frac{\partial a^2 s^0_{a\omega}}{\partial a}\right)a^2 j_1(k_\alpha a)$$

$$+ \frac{1}{i(\lambda_0+2\mu_0)}\int_a^{r_f}\left\{\left[-\rho_{00}\left(\frac{\lambda_0+2\mu_0}{\rho_0}\right) + 2\mu_{00}+\lambda_{00}\right]\right.$$

$$\cdot \frac{\partial}{\partial r_0}\frac{1}{r_0^2}\frac{\partial r_0^2 s^0_{r_0\omega}}{\partial r_0}$$

$$\left. +2\frac{\partial\mu_{00}}{\partial r_0}\frac{\partial s^0_{r_0\omega}}{\partial r_0} + \frac{\partial\lambda_{00}}{\partial r_0}\frac{1}{r_0^2}\frac{\partial r_0^2 s^0_{r_0\omega}}{\partial r_0}\right\}r_0^2 j_1(k_\alpha r_0)dr_0$$

(2.7.2)

$$c^{\sigma}_{nm} = -\left(2\mu^{\sigma}_{nm}(a)\ \frac{\partial s^{0}_{a\omega}}{\partial a} + \frac{\lambda^{\sigma}_{nm}}{a^2}\ \frac{\partial a^2 s^{0}_{a\omega}}{\partial a}\right)\frac{a^2}{i(\lambda_0+2\mu_0)}\ \frac{dj_n(k_\alpha a)}{dk_\alpha a}$$

$$+ \frac{1}{i(\lambda_0+2\mu_0)}\int_a^{r_f} -\left\{\left[-\rho^{\sigma}_{nm}\left(\frac{\lambda_0+2\mu_0}{\rho_0}\right)+2\mu^{\sigma}_{nm}+\lambda^{\sigma}_{nm}\right]\right.$$

$$\cdot\frac{\partial}{\partial r_0}\ \frac{1}{r_0^2}\ \frac{\partial r^2 s^{0}_{r_0\omega}}{\partial r_0}$$

$$\left. + 2\frac{\partial \mu_{nm}}{\partial r_0}\ \frac{\partial s^{0}_{r_0\omega}}{\partial r_0} + \frac{\partial \lambda^{\sigma}_{nm}}{\partial r_0}\ \frac{1}{r_0^2}\ \frac{\partial r^2 s^{0}_{r_0\omega}}{\partial r_0}\right\} r_0^2\ \frac{dj_n(k_\alpha r_0)}{dk_\alpha r_0}$$

$$-\left[\frac{2\mu_{nm}}{r_0^2}\ s^{0}_{r_0\omega} + \frac{\lambda^{\sigma}_{nm}}{r_0^3}\ \frac{\partial r_0^2 s^{0}_{r_0\omega}}{\partial r_0}\right]\cdot$$

$$(n)(n+1)r_0^2\ \frac{j_n(k_\alpha r_0)}{k_\alpha r_0}\ dr_0 \qquad (2.7.3)$$

$$f^{\sigma}_{nm} = -\left(2\mu^{\sigma}_{nm}(a)\ \frac{\partial s^{0}_{a\omega}}{\partial a} - 2\mu^{\sigma}_{nm}(a)\ \frac{s^{0}_{a\omega}}{a}\right)\frac{a^2}{i\mu_0}\ \frac{j_n(k_\beta a)}{k_\beta a}$$

$$+ \frac{1}{i\mu_0}\int_a^{r_f}\left\{-\left[-\rho^{\sigma}_{nm}\left(\frac{\lambda_0+2\mu_0}{\rho_0}\right)+2\mu^{\sigma}_{nm}\right]\right.$$

$$\left.\frac{\partial}{\partial r_0}\ \frac{1}{r_0^2}\ \frac{\partial r^2 s^{0}_{r_0\omega}}{\partial r_0} - 2r_0^2\left[\frac{\partial}{\partial r_0}\ \frac{s^{0}_{r_0\omega}}{r_0}\right]\left[\frac{\partial}{\partial r_0}\ \frac{\mu^{\sigma}_{nm}}{r_0}\right]\right\}$$

$$\cdot r_0^2\ \frac{j_n(k_\beta r_0)}{k_\beta r_0}\ dr_0 \qquad (2.7.4)$$

where $\sigma = 1,2$, and we have assumed that

$$(\mu^{\sigma}_{nm}, \lambda^{\sigma}_{nm}) = (0,0) \quad \text{at } r = r_f$$

We have to remark that these formulas are valid only when the receiver position is outside the inhomogeneities. When this is not the case, we have to take into account of the reflected wave generated outside a sphere having for radius the distance of the receiver to the center of the cavity. In this case, more general formulas must be used, as outlined in Appendix VI.

Some of the main conclusions that we can reach by examining the preceding formulas are that the first order scattered wave

1. does not contain any torsional vibration as defined in Chapter I
2. Each spherical harmonic of the perturbed medium parameters generates the same and only the same spherical harmonic of the scattered wave.
3. The amplitude of the scattered shear wave does not depend on the elastic parameter λ.

Our next task is to evaluate the coefficients c^{σ}_{nm}, f^{σ}_{nm} for some particular models.

CHAPTER III

Evaluation of the Coefficients of the Scattered Wave

3.1 Introduction

There are two classes of model for which we can use asymptotic expansion of the spherical Bessel functions in order to evaluate the coefficients of the scattered wave. First there is the case where all the inhomogeneities are within a wavelength from the source. The next section will be devoted to that subject and the related one concerning the anomalous production of SH waves near the source. Then, there is the case where the scattering occurs many wavelengths from the source. In our investigation of this subject in section 3.3, we will pay special attention to the various resonances that might occur in such regions. But in general, only parts of the spectrum of the scattered wave can be analyzed through these two extreme approximations. So, in section 3.4, we will try to obtain numerically the complete spectrum for a given structure.

3.2 Scattering near the source

We would like to estimate the scattered wave generated by the inhomogeneous distribution of material parameters surrounding the source. To do so, let us assume that the

radius of the inhomogeneous sphere (r_f) is much smaller than a wavelength, i.e.

$$k_\alpha r_f << 1 \tag{3.2.1}$$

Then, in order to evaluate the coefficients ($c^\sigma_{nm}, f^\sigma_{nm}$) as given in section 2.7, we can use the near field asymptotic expansion of the spherical Bessel functions. This work is outlined in Appendix VII. For the term of lowest order in $k_\alpha r$, the results are as follows:

a) The compressional coefficients

$$c_{00} = \frac{G}{(\lambda_0+2\mu_0)}\int_a^{r_f} \rho_{00}\left(\frac{\lambda_0+2\mu_0}{\rho_0}\right)\frac{k_\alpha^2 r_0}{3} - \frac{28\mu_{00}k_\alpha^2 r_0}{30}$$

$$-\lambda_{00}k_\alpha^2 r_0\, dr_0 \tag{3.2.2}$$

$$c^\sigma_{1m} = \frac{G}{(\lambda_0+2\mu_0)}\int_a^{r_f} -\rho^\sigma_{1m}\left(\frac{\lambda_0+2\mu_0}{\rho_0}\right)\frac{k_\alpha}{3} + \frac{8}{15}\,\mu^\sigma_{1m}k_\alpha dr_0 \tag{3.2.3}$$

$$c^\sigma_{nm} = \frac{-G}{\lambda_0+2\mu_0}\,6n(n-1)\,\frac{2^n n!}{(2n+1)!}\int_a^{r_f} k_\alpha^{n-2} r_0^{n-2}\,\frac{\mu^\sigma_{nm}}{r_0}\,dr_0 \tag{3.2.4}$$

for $n > 1$

b) The shear coefficients

$$f_{1m}^{\sigma} = \frac{G}{\mu_0} \int_a^{r_f} -\rho_{1m}^{\sigma} \left(\frac{\lambda_0 + 2\mu_0}{\rho_0} \right) \frac{k_\alpha}{3} + \frac{2}{5} \frac{k_\beta^2}{k_\alpha} \mu_{1m}^{\sigma} dr_0 \qquad (3.2.5)$$

$$f_{nm}^{\sigma} = - \frac{G}{\mu_0} \frac{6(n-1)2^n n!}{(2n+1)!} \int_a^{r_f} \frac{k_\beta^{n-1}}{k_\alpha} r_0^{n-2} \frac{\mu_{nm}^{\sigma}}{r_0} dr_0$$

for $n > 1$ (3.2.6)

where G is the spectrum of the source as defined in Appendix I. Moreover, I have assumed, to calculate these coefficients that the value of the parameters at r_f is 0 (e.g. $\mu_{nm}^{\sigma}(r_f) = 0$)

If we examine the frequency dependence of these coefficients, we remark that the ones that have the lowest order in kr are related to the $P_2^m(\cos \theta)$ harmonic of the rigidity. Indeed, we have for n = 2:

$$c_{2m}^{\sigma} = - \frac{4}{5} \frac{G}{\lambda_0 + 2\mu_0} \int_a^{r_f} \frac{\mu_{2m}^{\sigma}}{r_0} dr_0 \qquad (3.2.7)$$

and

$$f_{2m}^{\sigma} = - \frac{2}{5} \frac{G}{\mu_0} \frac{k_\beta}{k_\alpha} \int_a^{r_f} \frac{\mu_{2m}^{\sigma}}{r_0} dr_0 \qquad (3.2.8)$$

It is a remarkable fact that they depend on frequency only through the spectrum of the source whereas all the other coefficients have a low frequency cut-off. Furthermore, due to the 1/r weight in the integral, they are particularly sensitive to the inhomogeneities near the source.

Observations of the scattered wave in the far field and the production of SH waves

Let us examine the low frequency end of the spectrum of a signal observed in the far field. We remark that, in general, we will observe two main contributions to the displacement field. First, of course, there will be the signal coming from the zero order solution that is the main compressional wave. But secondly, a scattered wave caused by the $(2,n,\sigma)$ harmonics of the rigidity will also contribute to that part of the spectrum. Now, since this scattered wave seems to originate near the source, its compressional part will be hidden in the main wave displacement field. On the other hand, arrival time difference will permit us to distinguish its shear component. So, this suggests to have a closer look at the observed production of SH waves near the source: let us then examine a seismogram obtained by Geyer and Martner, (1969), which illustrates this phenomena.

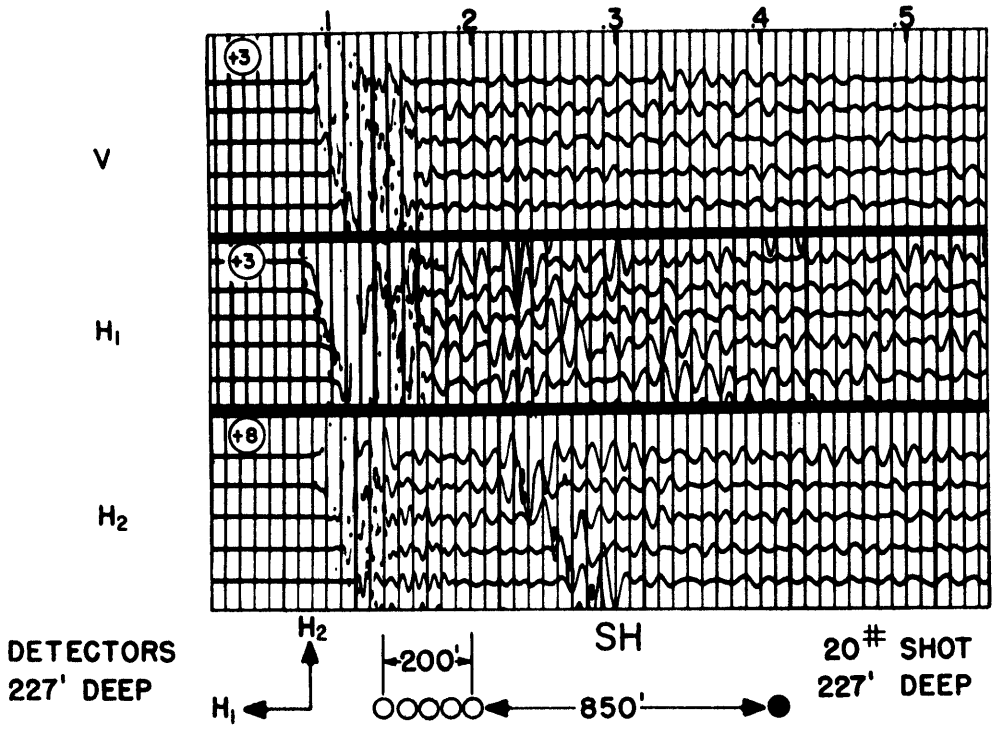

"Figure 4 shows a record from area D in west Texas. The record is from a horizontal downhole spread with five instrument holes spaced 50 ft. apart. The nearest seismometer was 850 ft. from the shothole, where a charge of 20 lb. was shot at a depth of 227 ft which was the same depth as the detectors. Orientation of the horizontal seismometers is shown. There is a strong SH wave on the H_2 component at a time of about 0.23 sec, and the moveout indicates a velocity of of about 4000 ft/sec."

Now, let us try to explain this observation through scattering near the source. If we consider the scattered wave due to the $(2,m,\sigma)$ harmonics of the rigidity we obtain

the displacement field:

$$\vec{s}_\omega = \vec{a}_r P_2^m(\cos\theta)\begin{Bmatrix}\cos m\phi\\ \sin m\phi\end{Bmatrix}\left[\varepsilon c_{2m}^\sigma \frac{\partial}{\partial r} h_2(k_\alpha r)+\varepsilon(n)(n+1)\cdot\right.$$

$$\left. f_{2m}^\sigma \frac{h_2(k_\beta r)}{r}\right]$$

$$+\vec{a}_\theta \frac{\partial}{\partial\theta} P_2^m(\cos\theta)\begin{Bmatrix}\cos m\phi\\ \sin m\phi\end{Bmatrix}\left[\varepsilon c_{2m}^\sigma \frac{h_2(k_\alpha r)}{r}\right.$$

$$\left.+\varepsilon \frac{f_{2m}^\sigma}{r} \frac{\partial r h_2(k_\alpha r)}{\partial r}\right]$$

$$+\vec{a}_\phi \frac{P_2^m(\cos\theta)}{\sin\theta} \begin{Bmatrix}-m\sin m\phi\\ m\cos m\phi\end{Bmatrix}\left[\varepsilon c_{2m}^\sigma \frac{h_2(k_\alpha r)}{r}\right.$$

$$\left.+\varepsilon \frac{f_{2m}^\sigma}{r} \frac{\partial r h_2(k_\beta r)}{\partial r}\right] \qquad (3.2.9)$$

where, in the radial component, $\sigma = 1$ corresponds to $\cos m\phi$ and $\sigma = 2$ to $\sin m\phi$, and where

$$P_2^0 = \frac{1}{4}(3\cos 2\theta + 1)$$

$$P_2^1 = \frac{3}{2}\sin 2\theta$$

$$P_2^2 = \frac{3}{2}(1 - \cos 2\theta)$$

In the experiment detailed above, we can assume that the receivers are in the far field, i.e. $k_\alpha r >> 1$. Then, if we take the far field asymptotic expansion of the spherical Bessel function h_2, we obtain for the scattered displacement field:

$$\vec{s}_\omega = \vec{a}_r P_2^m(\cos\theta)\begin{Bmatrix}\cos m\phi \\ \sin m\phi\end{Bmatrix}(-\varepsilon c_{2m}^\sigma)\frac{e^{ik_\alpha r}}{r}$$

$$+ \vec{a}_\theta \frac{\partial P_2^m(\cos\theta)}{\partial\theta}\begin{Bmatrix}\cos m\phi \\ \sin m\phi\end{Bmatrix}(-\varepsilon f_{2m}^\sigma)\frac{e^{ik_\beta r}}{r}$$

$$+\vec{a}_\phi \frac{P_2^m(\cos\theta)}{\sin\theta}\begin{Bmatrix}-m\sin m\phi \\ m\cos m\phi\end{Bmatrix}(-\varepsilon f_{2m}^\sigma)\frac{e^{ik_\beta r}}{r} \qquad (3.2.10)$$

We see that in the far field, the scattered compressional wave has motion only in the radial direction whereas the displacement contained in the shear potential is transverse to the direction of propagation.

Let us fix the polar axis along the vertical to the ground*. We remark that since the shot and the receivers

*Remark: The choice of the polar axis must be consistent with the system of axes used to evaluate the different harmonics of the parameters.

are at the same depth in the experiment of Fig. 4, we can set $\theta = \pi/2$ in our formula for the displacement field. Then, if we examine the value of the Legendre polynomials, we must conclude that the only scattered wave likely to produce the anomalous SH signal are related to the pair (2,2,1) and (2,2,2) of harmonics of the rigidity. Indeed, the pair (2,1,1) and (2,1,2) produces only vertical transverse motion whereas (2,0,0) produces no transverse motion at $\theta = \pi/2$.

It is extremely interesting to note that this $m = 2$ symmetry ($\sin 2\phi+\delta$) has been consistently observed for the radiation pattern of Love waves (constructive interference of SH waves in the crust) from underground nuclear explosions. (e.g. Brune and Pomeroy (1963), Aki (1964), Toksöz et al (1965)). But this does not permit us to conclude that scattering is the only process explaining the production of SH waves. Far from it, as a matter of fact, since the stress release processes discussed in Chapter I may also give the same radiation pattern. So, what we need then is an estimate of the efficiency of scattering. But let us reserve this work to Chapter IV where we will be able to include the influence of the fluid cavity in our discussion.

Observation of the displacement in the near field

It must be kept in mind that the preceding remarks apply only to far field measurement. Arrival time difference

in that case, permits us to distinguish between the shear and compressional wave. But this is not true in the near field where strong interference between shear and compressional wave exists. Since the production of very long waves make it practical to set the receiver in the near field, I would like to study the structure of the scattered wave there. It turns out to be very different from the far field results.

So let r, the distance of the receiver be such that

$$k_\alpha r_f < k_\alpha r << 1, \tag{3.2.11}$$

that is, the receiver is near the source but outside the inhomogeneities. In that case, we can use the near field asymptotic expansion of the spherical Bessel function involving the receiver position.

The motion in an arbitrary harmonic of the scattered wave is given by:

$$\vec{s}_\omega = \vec{a}_r P_n^m(\cos\theta)\begin{Bmatrix}\cos m\phi \\ \sin m\phi\end{Bmatrix}\left[\varepsilon c_{nm}^\sigma \frac{\partial h_n(k_\alpha r)}{\partial r} + \varepsilon(n)(n+1)\cdot f_{nm}^\sigma \frac{h_n(k_\alpha r)}{r}\right]$$

$$+\vec{a}_\theta \frac{\partial P_n^m(\cos\theta)}{\partial\theta}\begin{Bmatrix}\cos m\phi \\ \sin m\phi\end{Bmatrix}\left[\varepsilon c_{nm}^\sigma \frac{h_n(k_\alpha r)}{r} + \varepsilon \frac{f_{nm}^\sigma}{r}\cdot \frac{\partial r h_n(k_\beta r)}{\partial r}\right]$$

$$+\vec{a}_\phi \frac{P_n^m(\cos\theta)}{\sin\theta} \begin{Bmatrix} -m \sin m\phi \\ m \cos m\phi \end{Bmatrix} \left[\varepsilon c_{nm}^\sigma \frac{h_n(k_\alpha r)}{r} \right.$$

$$\left. + \varepsilon \frac{f_{nm}^\sigma}{r} \frac{\partial r h_n(k_\beta r)}{\partial r} \right] \qquad (3.2.12)$$

But, if we keep only the leading term in $h_n(kr)$ i.e.

$$h_n(kr) \to -i \frac{(2n)!}{2^n n!} k^{n+1} r^{n+1}$$

together with any pair $(c_{nm}^\sigma, f_{nm}^\sigma)$ for $n \geq 1$, as given in 3.2.4 and 3.2.6 then we find

$$\vec{s}_\omega = 0$$

In other words, the motion contained in the scattered compressional wave interferes strongly with the motion in the shear wave so as to cancel the displacement associated with the leading term of each potential.

In order to obtain the effective dominant term for the displacement field, we must keep more terms in the asymptotic expansion of the potential field. More precisely, we must keep the next lowest order term in $(c_{nm}^\sigma, f_{nm}^\sigma)$ and $h_n(kr)$ in their asymptotic expansion in power of kr_0 and kr respectively. But an equivalent and perhaps a more

convenient procedure in this case is to work out the static ($\omega \to 0$) approximation for our problem. This is detailed in Appendix VIII.

It is shown there that if P is the zero order pressure acting on the surface r = a, then the displacement field for $r > r_f$ can be expressed in the following way:

$$\vec{s} = \nabla\psi + \nabla\times\nabla\times r\vec{a}_r\psi_2 \tag{3.2.13}$$

where

$$\psi = -\frac{Pa^3}{4\mu_0 r} + \varepsilon c_0(-)\frac{Pa^3}{4\mu_0 r}$$

$$+ \sum_{n=1}^{\infty}\sum_{m=0}^{n}\left[\varepsilon\left(\frac{c^1_{nm}}{r^{n-1}} + \frac{d^1_{nm}}{r^{n+1}}\right)\cos m\phi\right.$$

$$\left.+\varepsilon\left(\frac{c^2_{nm}}{r^{n-1}} + \frac{d^2_{nm}}{r^{n+1}}\right)\sin m\phi\right]P^m_n(\cos\theta) \tag{3.2.14}$$

and

$$\psi_2 = \sum_{n=1}^{\infty}\sum_{m=0}^{n}\left[\varepsilon\left(\frac{f^1_{nm}}{r^{n-1}} + \frac{g^1_{nm}}{r^{n+1}}\right)\cos m\phi\right.$$

$$\left.+\varepsilon\left(\frac{f^2_{nm}}{r^{n-1}} + \frac{g^2_{nm}}{r^{n+1}}\right)\sin m\phi\right]P^m_n(\cos\theta) \tag{3.2.15}$$

where

$$c_{00} = 0 \quad \text{(in this case, we have to keep higher order term as given in 3.2.2)} \tag{3.2.16}$$

$$c_{nm}^{\sigma} = \frac{Pa^3}{4\mu_0} \frac{3n(n-1)}{(2n+1)(2n-1)(\lambda_0+2\mu_0)} \int_a^{r_f} \mu_{nm}^{\sigma} r_0^{n-3} dr_0 \tag{3.2.17}$$

$$d_{nm}^{\sigma} = -\frac{Pa^3}{4\mu_0} \frac{n(3n+5)}{(2n+1)(2n+3)(\lambda_0+2\mu_0)} \int_a^{r_f} \mu_{nm}^{\sigma} r_0^{n-1} dr_0 \tag{3.2.18}$$

$$f_{nm}^{\sigma} = + \frac{Pa^3}{4\mu_0} \frac{3(n-1)}{(2n+1)^2\mu_0} \int_a^{r_f} \mu_{nm}^{\sigma} r_0^{n-3} dr_0 \tag{3.2.19}$$

$$g_{nm}^{\sigma} = - \frac{Pa^3}{4\mu_0} \frac{3(n+1)}{(2n+1)(2n+3)\mu_0} \int_a^{r_f} \mu_{nm}^{\sigma} r_0^{n-1} dr_0 \tag{3.2.20}$$

If we try as before to find if some harmonic of the field has a dominant amplitude, we cannot be as conclusive as before. Indeed, one has to take into account the fact that as the position of the receiver approach the inhomogeneities, the harmonics with large n grow faster than the ones with small n. So, they more or less compensate for the fact that they weight less the inhomogeneities than the smaller n harmonics. In fact, one might expect that the different spherical harmonics of the displacement field have an amplitude somewhat in proportion to the corresponding

harmonic of the rigidity. Because of this, the displacement field near the source has a much more complicated structure than the one far from it.

Before closing this section, it is interesting to remark that the motion associated with the coefficients $(c_{2m}^{\sigma}, f_{2m}^{\sigma})$ is such that the shear displacement is wholly radial whereas the compressional displacement is radial and transverse.

We therefore see that we cannot interpret the displacement in the same way when we are dealing with near and far field data.

3.3 Scattering in a region situated many wavelengths from the source.

Let us now turn our attention to the high frequency end of the spectrum. Once more, we can simplify the evaluation of the coefficients of the scattered wave by expanding them in asymptotic series, but this time in terms of the large parameter* kr_0 where r_0 is a radius in the scatterer space. However, the situation is somewhat different than the low frequency case. Indeed, if we look at a spherical Bessel

---

*Remark: Here, k represents either k_α or k_β

function of order n, as given in Appendix II, eq. 32, we remark that we can neglect the second highest order term in kr_0 with respect to the first only when

$$kr_0 >> n^2 \tag{3.3.1}$$

This means that in practice, the harmonics representing the finer details of the medium, i.e. having a large value for n, cannot be adequately treated in this limit, within our formalism. Indeed, for large n, unless we are dealing with very high frequencies, the condition 3.3.1. constrain us to a consideration of the inhomogeneities very far from the source. But in that case, it is strongly suspected that plane wave analysis might provide a better synthesis of the result.

So let us restrict our consideration to the first p harmonics of the parameters (i.e. $n \leq p$). Furthermore, in order to meet 3.3.1, we will assume the medium to be inhomogeneous only within two sphere of radius r_{in} and r_f (see Fig. 5) where the inner radius, r_{in}, is such that

$$kr_{in} >> p^2 \tag{3.3.2}$$

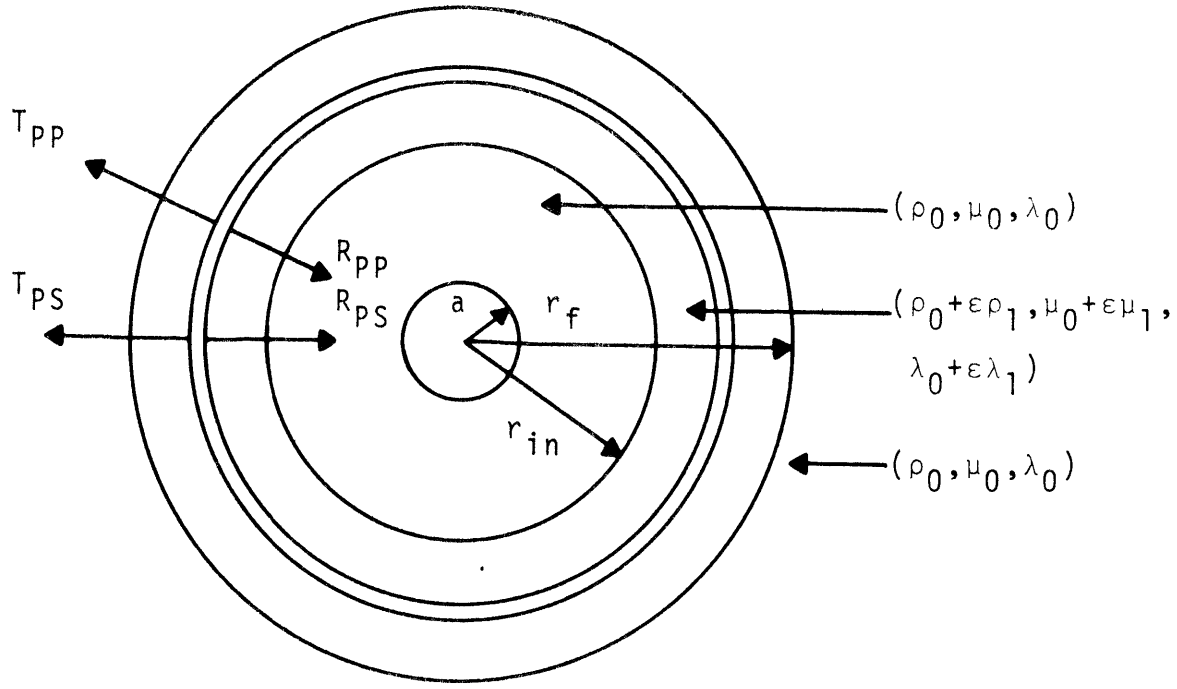

Figure 5. The heterogeneous region is bounded by two spheres of radius r_{in} and r_f where $k_\alpha r_{in} >> p^2$. The different types of scattered wave originating from an element of that zone are illustrated

Then, if the receiver radius is larger than r_f, we obtain the following results for the coefficients of the scattered wave (see Appendix IX).

$$c_{nm}^{\sigma} = \frac{G}{2}\frac{k_\alpha (i)^{-n}}{i(\lambda_0+2\mu_0)}\int_{r_{in}}^{r_f}\left[-\rho_{nm}^{\sigma}\left(\frac{\lambda_0+2\mu_0}{\rho_0}\right)+2\mu_{nm}^{\sigma}+\lambda_{nm}^{\sigma}\right]dr_0$$

$$+\frac{G}{2i}\frac{k_\alpha i^{-n}}{(\lambda_0+2\mu_0)}\int_{r_{in}}^{r_f}\left[-\rho_{nm}^{\sigma}\left(\frac{\lambda_0+2\mu_0}{\rho_0}\right)-2\mu_{nm}^{\sigma}-\lambda_{nm}^{\sigma}\right]e^{i2k_\alpha r_0}dr_0$$

all $n \leq p$ (3.3.3)

and

$$f_{nm}^{\sigma} = \frac{G}{2}\frac{(-i)^{-n}}{(\lambda_0+2\mu_0)}\int_{r_{in}}^{r_f}\left[-\rho_{nm}^{\sigma}\left(\frac{\lambda_0+2\mu_0}{\rho_0}\right)+2\mu_{nm}^{\sigma}\ \frac{\alpha}{\beta}\right]\frac{e^{i(k_\alpha-k_\beta)r_0}}{r_0}dr_0$$

$$+\frac{G}{2}\frac{i^{-n}}{(\lambda_0+2\mu_0)}\int_{r_{in}}^{r_f}\left[-\ \rho_{nm}^{\sigma}\left(\frac{\lambda_0+2\mu_0}{\rho_0}\right)+\ 2\mu_{nm\beta}^{\sigma\ \alpha}\right]\frac{e^{i(k_\alpha+k_\beta)r_0}}{r_0}\ dr_0$$

all $n \leq p$, $n > 0$ (3.3.4)

Arrival time consideration reveals that the first integral in each of these coefficients represents the transmitted compressional and shear wave respectively whereas the second integrals account for the reflected scattered waves.

The transmitted PP wave

Let us first consider a medium varying slowly over many wavelengths. Then, due to the oscillatory character of the exponential in three of the preceding integrals, they will not contribute much to the displacement field. So, let us neglect them here and consider only the transmitted PP wave.

Since the receiver position is in the far field, we can write the total displacment field, to the highest order in k r, as follows:

$$\vec{s}_\omega = \vec{a}_r G \frac{e^{ik_\alpha r}}{r} \cdot$$

$$\left\{1+\varepsilon\left[c_{00}+\sum_{n=1}^{p}\sum_{m=1}^{n}\left(c_{nm}^{1}(i)^n\cos m\phi+c_{nm}^{2}(-i)^n\sin m\phi\right)\cdot\right.\right.$$

$$\left.\left.P_m^n(\cos\theta)\right]\right\} \qquad (3.3.5)$$

Using the first integral in 3.3.3 we then obtain

$$\vec{s}_\omega = \vec{a}_r G\frac{e^{ik_\alpha r}}{r}\left\{1+\varepsilon ik_\alpha\phi\right\} \qquad (3.3.6)$$

where

$$\phi = \frac{1}{2(\lambda_0+2\mu_0)}\int_{r_{in}}^{r_f}\left[\rho_1\left(\frac{\lambda_0+2\mu_0}{\rho_0}\right)-2\mu_1-\lambda_1\right]dr_0 \qquad (3.3.7)$$

and where $\varepsilon(\rho_1,\mu_1,\lambda_1)$ is the total inhomogeneous part of each parameter contained in the spherical harmonics characterized by $n \leq p$.

We remark that the expression we have for the scattered wave cannot be uniformly valid for all frequencies. Indeed, since its amplitude grows in proportion to the wave number, eventually, for very high frequencies, the first order term will become as large as the zero order one even for slightly inhomogeneous medium. But, in that case, we can have recourse to the methods of geometrical optics in order to

to calculate the displacement field. This work is done in Appendix X and it is shown there that, to the highest order in $k_\alpha r$ and $k_\alpha r_0$, the displacement field can be expressed as follows:

$$\vec{s}_{g\ optics} = \vec{a}_r \frac{G}{r} e^{ik_\alpha r + i\varepsilon k_\alpha \phi} \qquad (3.3.8)$$

We remark that for

$$\varepsilon k_\alpha \phi << 1$$

we can expand the exponential in Taylor's series and thus recover the result we obtain by the method of small perturbation. In other words, when the above condition is fulfilled, there are two equivalent ways to represent the effect of the inhomogeneities on the main wave: we can add to it a scattered wave as in 3.3.6 or we can correct its phase as in 3.3.8. Eventually, for very high frequencies, only the second procedure will give an adequate result.

The other wave types

Let us assume that between r_{in} and r_f we have expanded in Fourier series the radial part of each harmonic of the parameters. The first term in this serie, that is

the one connected with the average properties of the parameters, is the only one controlling the transmitted PP wave recorded outside the inhomogeneities. We may therefore ask if the remaining part of the scattered wave contains some information on the other terms of the serie.

If we examine the second integral in 3.3.3, we remark that for a given frequency, the periodic part of the structure having wavenumber around k_1 where

$$k_1 = 2k_\alpha$$

is likely to be the most efficient scatterer of reflected P wave. In the same way, the shear component of the scattered wave will be mainly excited by the terms in the Fourier series having wave number around k_2 and k_3 where

$k_2 = k_\beta - k_\alpha$ for the transmitted PS wave

and

$k_3 = k_\beta + k_\alpha$ for the reflected PS wave

The above relations are known as the Bragg's conditions. In the case where a restricted number of terms in the Fourier series of the parameters give an adequate representation of the medium, we might expect peaks or lows in the spectral density of the scattered wave at frequencies connected to

the different wave number of the medium through these Bragg's conditions.

Though the occurence of such an event may be rather rare in nature, it might be interesting to investigate more thoroughly when a given part of the spectrum of the scattered wave is controlled mainly by the periodic part of the medium connect to this frequency range through the above condition. We will leave this work for future research.

3.4 Calculation of the scattered field for a particular model

In the preceding sections, we confined our attention to the contribution to the scattered wave coming from inhomogeneities near and far from the source in terms of wavelength. In practice, we have to take into account the effect of a part of the heterogeneous medium situated such that none of the above assumptions applied. In order to illustrate such a case, let us consider a model specified by the following properties

$$\rho = \rho_0 \quad \text{for all } r \tag{3.4.1}$$

$$\lambda = \lambda_0 \quad \text{for all } r$$

$$\mu = \mu_0 \quad \text{for } r < a$$

$$= \mu_0 + \frac{\partial \mu}{\partial Z} Z \equiv \mu_0 + \frac{\partial \mu}{\partial Z} \; r \; P_1^0 (\cos \theta)$$

$$\text{for } a \leq r \leq r_f$$

$$= \mu_0 + \frac{\partial \mu}{\partial Z} r_\ell \frac{(r-r_f)}{r_\ell - r_f} \; P_1^0(\cos \theta)$$

$$\text{for } r_\ell \leq r \leq r_f$$

$$= \mu_0 \quad \text{for } r > r_f \qquad (3.4.1)$$

That is, we have that the density ρ and the Lamé's constant λ are constant throughout space whereas the rigidity varies linearly along Z within a sphere of radius r_ℓ and trend continuously towards μ_0 between r_ℓ and r_f. (See Fig. 6).

In our preceding notation, we have that

$$\varepsilon\mu_{10} = \frac{\partial \mu}{\partial Z} r \qquad \text{for } a \leq r \leq r_\ell$$

$$= \frac{\partial \mu}{\partial Z} r_\ell \frac{(r-r_f)}{r_\ell - r_f} \quad \text{for } r_\ell \leq r \leq r_f \qquad (3.4.2)$$

So, the displacement field outside the inhomogeneities can be written as

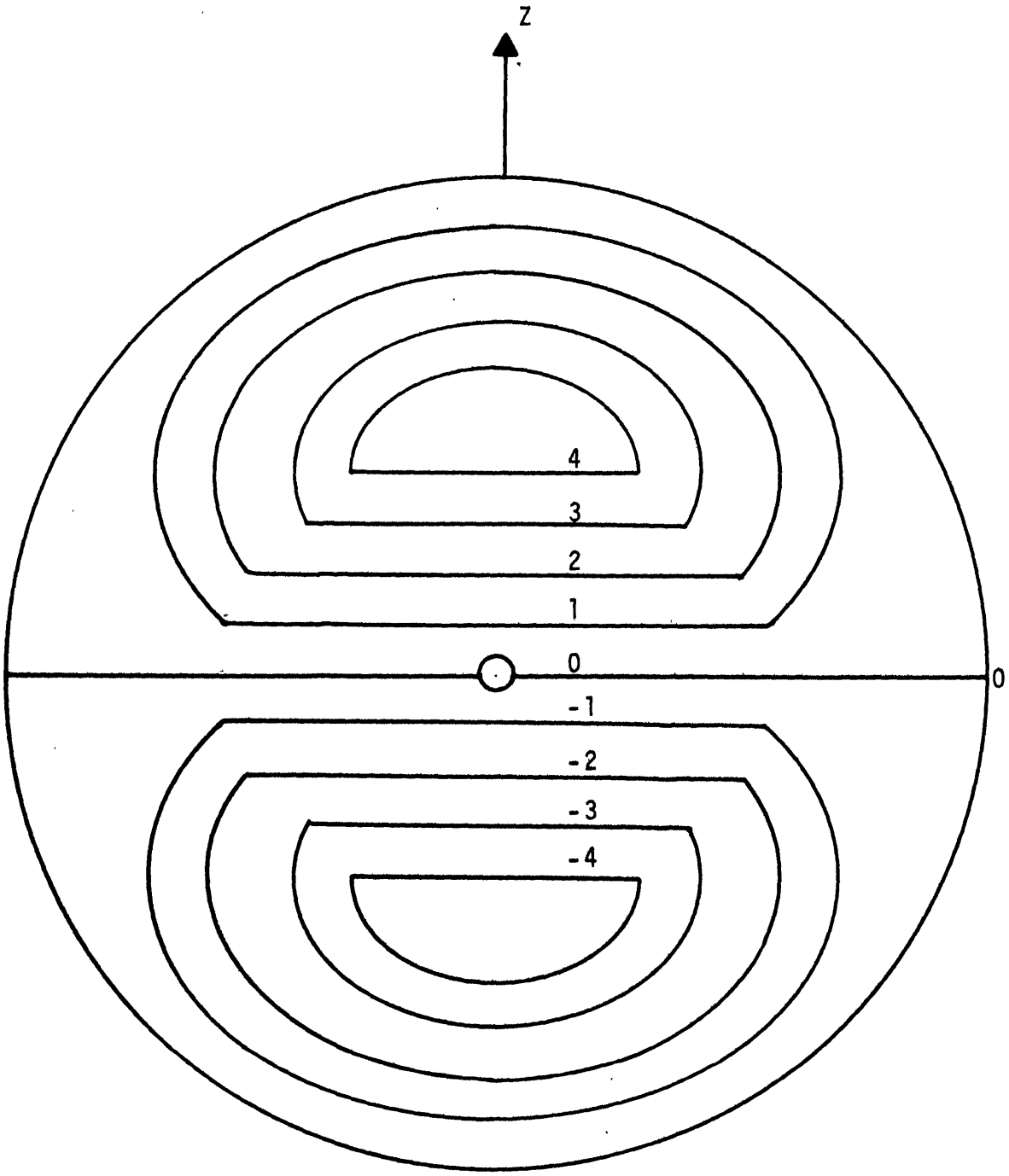

Figure 6. Contour of constant rigidity for the model specified above, in a plane cutting the polar axis. The drawing illustrates the case where $r_f = 2r_\ell$

$$\vec{s}_\omega = \nabla\psi + \nabla\times\nabla\times r\vec{a}_r\psi_2$$

$$= \vec{a}_r \frac{\partial\psi_0}{\partial r} + \vec{a}_r P_1(\cos\theta)\left[\varepsilon c_{10} \frac{\partial h_1(k r)}{\partial r} + 2\varepsilon f_{10}\frac{h_1(k_\beta r)}{r}\right]$$

$$+\vec{a}_\theta \frac{\partial P_1(\cos\theta)}{\partial\theta}\left[\varepsilon c_{10} \frac{h_1(k_\alpha r)}{r} + \frac{\varepsilon f_{10}}{r} \frac{\partial r h_1(k_\beta r)}{\partial r}\right] \tag{3.4.3}$$

where we have that

$$c_{10} = \frac{G}{i(\lambda_0+2\mu_0)}\int_a^{r_f}\mu_{10}k_\alpha\left(i + \frac{1}{k_\alpha r_0} + \frac{4}{(k_\alpha r_0)^3} + \frac{18}{(k_\alpha r_0)^5}\right)dr_0$$

$$+ \frac{G}{i(\lambda_0+2\mu_0)}\int_a^{r_f}\mu_{10}k_\alpha\left(i - \frac{5}{k_\alpha r_0} - \frac{16i}{(k_\alpha r_0)^2}\right.$$

$$\left. + \frac{32}{(k_\alpha r_0)^3} + \frac{36i}{(k_\alpha r_0)^4} - \frac{18}{(k_\alpha r_0)^5}\right)e^{2ik_\alpha r_0}\, dr_0 \tag{3.4.4}$$

and

$$f_{10} = \frac{G}{i\mu_0}\int_a^{r_f}\mu_{10}\left[-\frac{1}{r_0}\frac{k_\alpha}{k_\beta} + \frac{3i}{r_0^2}\left(\frac{k_\alpha - k_\beta}{k_\beta^2}\right) + \frac{1}{r_0^3}\cdot\right.$$

$$\left.\left(-\frac{9}{k_\beta^2} + \frac{3k_\alpha}{k_\beta^3} + \frac{3}{k_\alpha k_\beta}\right) + \frac{9i}{r_0^4}\left(\frac{k_\alpha - k_\beta}{k_\alpha k_\beta^3}\right) - \frac{9}{k_\alpha k_\beta^3 r_0^5}\right]$$

$$e^{i(k_\alpha - k_\beta)r_0} dr_0 \tag{3.4.5}$$

$$+ \frac{G}{i\mu_0}\int_a^{r_f} \mu_{10}\left[\frac{1}{r_0}\frac{k_\alpha}{k_\beta} + \frac{3i}{r_0^2}\left(\frac{k_\alpha+k_\beta}{k_\beta^2}\right) - \frac{1}{r_0^3}\cdot\right.$$

$$\left.\left(\frac{9}{k^2} + \frac{3k_\alpha}{k_\beta^3} + \frac{3}{k_\alpha k_\beta}\right) - \frac{9i}{r_0^4}\left(\frac{k_\alpha+k_\beta}{k_\alpha k_\beta^3}\right) + \frac{9}{k_\alpha k_\beta^3 r_0^5}\right]$$

$$e^{i(k_\alpha+k_\beta)r_0} dr_0 \qquad (3.4.5)$$

To obtain these coefficients, I have integrated by parts the terms involving the derivative of the rigidity in 2.7.3 and 2.7.4 and I have used the form of the spherical Bessel function given in Appendix II, eq. 32 and 33.

We remark that since the polar distribution of the inhomogeneities contains only the $P_1^0(\cos\theta)$ harmonic of the rigidity then, in the far field, the scattered compressional wave has the same polar distribution and its displacement field is purely radial. On the other hand, far from the source, the PS wave displacement is transverse to the direction of propagation and with a polar distribution specified by sin θ (see Fig. 7).

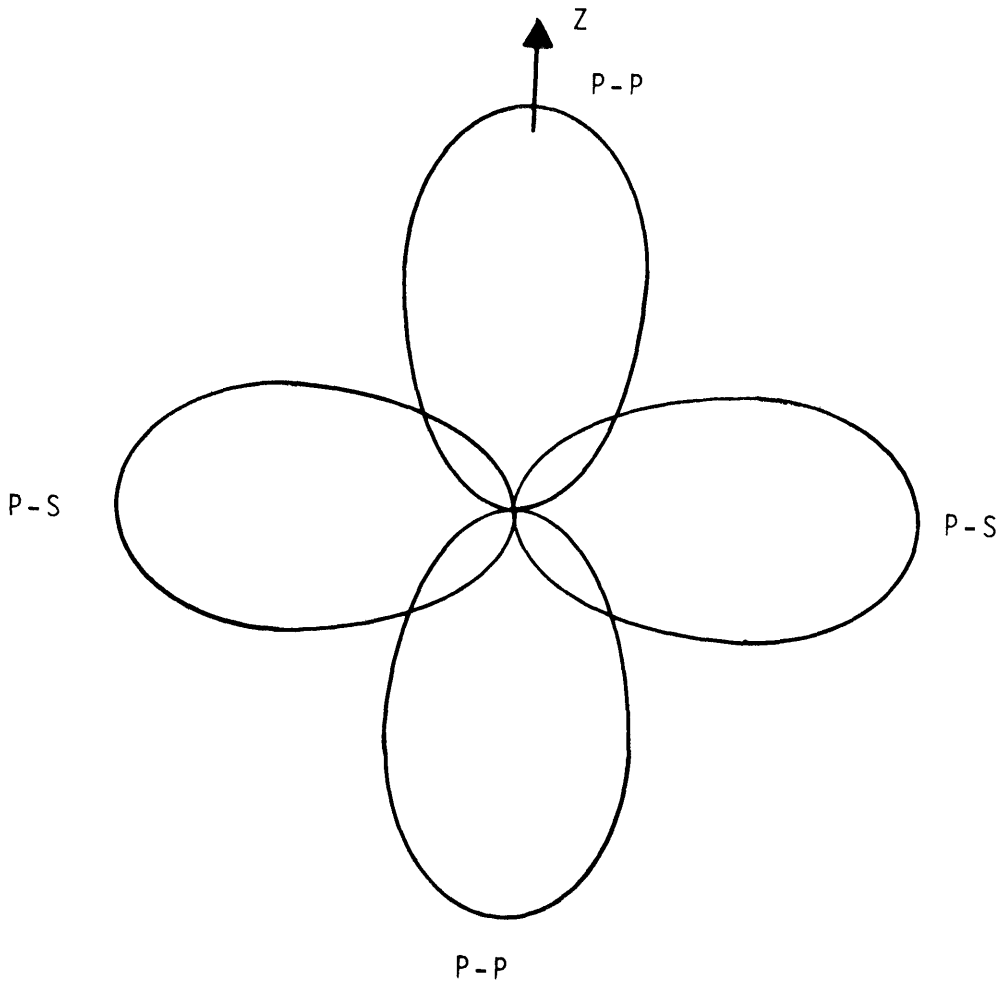

Figure 7. Polar distribution on the PP and PS wave in the far field

The coefficient of the PP wave

Let us calculate the scattered compressional wave. We remark that the first term in 3.4.4 is related to the transmitted PP wave whereas the second term is the contribution coming from the reflected PP wave. We see that in order to calculate the effect of the inhomogeneities far from the source, i.e., such that $k_\alpha r_0 >> 1$, we need only to take into account the first term in each integral. This is the result we obtain in 3.3.3.

On the other hand, though the form of 3.4.4 suggests to make a separate evaluation of the transmitted and reflected wave, such a process is far from being convenient when we have to take into account scattering near the source, i.e. such that $k_\alpha r_0 << 1$. Indeed, in such a case, each of these waves has a large amplitude almost exactly the same but opposite in sign. To see that more clearly, let us expand in Taylor's series the exponential term in the reflected wave. We then obtain

$$c_{10} = \frac{G}{i(\lambda_0+2\mu_0)}\int_a^{r_f} \mu_{10} k_\alpha \left(i + \frac{1}{k_\alpha r_0} + \frac{4}{(k_\alpha r_0)^3} + \frac{18}{(k_\alpha r_0)^5}\right) dr_0$$

$$+ \frac{G}{i(\lambda_0+2\mu_0)}\int_a^{r_f} \mu_{10} k_\alpha \left(R(r_0) - \frac{7i}{15} - \frac{1}{k_\alpha r_0} - \frac{4}{(k_\alpha r_0)^3}\right.$$

$$\left. - \frac{18}{(k_\alpha r_0)^5}\right) dr_0 \qquad (3.4.6)$$

where

$$R(r_0) = -\frac{66}{315} i(k_\alpha r_0)^2 + \frac{70}{315}(k_\alpha r_0)^3 + \frac{56i}{315}(k_\alpha r_0)^4$$

$$- \frac{22}{315}(k_\alpha r_0)^5 + \ldots$$

We remark that in order to calculate the effect of the inhomogeneities situated such that $k_\alpha r_0 \lesssim 1$ we can use

$$c_{10} = \frac{G}{\lambda_0+2\mu_0} \int_a^{1/k_\alpha} \mu_{10} \frac{8}{15} k_\alpha dr_0 \qquad (3.4.7)$$

This is the equation that we have obtained in 3.2.3 and, by inspection of $R(r_0)$, we see that a more exact calculation will reveal only a small correction to the above values, provided $k_\alpha r_0 \lesssim 1$. So, from a numerical point of view, it is better to evaluate the contribution to the scattered wave coming from the region $k_\alpha r_0 \lesssim 1$ by using 3.4.7 whereas we have to use 3.4.4 to calculate the effect of the heterogeneous medium outside that domain. In other words, to summarize, we can use the following formula to calculate c_{10}

$$\begin{aligned} c_{10} = {} & \frac{G}{\lambda_0+2\mu_0} \int_a^{1/k_\alpha} \mu_{10} \frac{8}{15} k_\alpha dr_0 \\ & + \frac{G}{i(\lambda_0+2\mu_0)} \int_{1/k_\alpha}^{r_f} \mu_{10} k_\alpha \left(i + \frac{1}{k_\alpha r_0} + \frac{4}{(k_\alpha r_0)^3} + \frac{18}{(k_\alpha r_0)^5} \right) \\ & \cdot dr_0 + \frac{G}{i(\lambda_0+2\mu_0)} \int_{1/k_\alpha}^{r_f} \mu_{10} k_\alpha \left(i - \frac{5}{k_\alpha r_0} - \frac{16i}{(k_\alpha r_0)^2} \right. \\ & \left. + \frac{32}{(k_\alpha r_0)^3} + \frac{36i}{(k_\alpha r_0)^4} - \frac{18}{(k_\alpha r_0)^5} \right) e^{2ik_\alpha r_0} dr_0 \end{aligned} \qquad (3.4.8)$$

This is the procedure I have followed to evaluate this coefficient for the model specified by 3.4.1 together with the relation

$$r_f = 2r_\ell \tag{3.4.9}$$

In order to describe the result, let us define Φ_c and η_c such that

$$\varepsilon^c{}_{10} = G\left(\frac{1}{\lambda_0+2\mu_0}\frac{\partial\mu}{\partial z}\, r_f\right)\Phi_c e^{-i\eta_c} \tag{3.4.10}$$

I will call Φ_c the normalized spectral density of the scattered P wave. Figure 8 is a plot of Φ_c against $k_\alpha r_f$.

The domain between zero and one i.e.

$$0 \leq k_\alpha r_f \leq 1$$

can be wholly evaluated by using only the first integral in 3.4.8. This is the low frequency limit that we have discussed before. It should be remarked that if we keep more terms in 3.4.7 the transition near $k_\alpha r_f = 1$ becomes smoother. At high frequency, i.e. for

$$k_\alpha r_f > 16$$

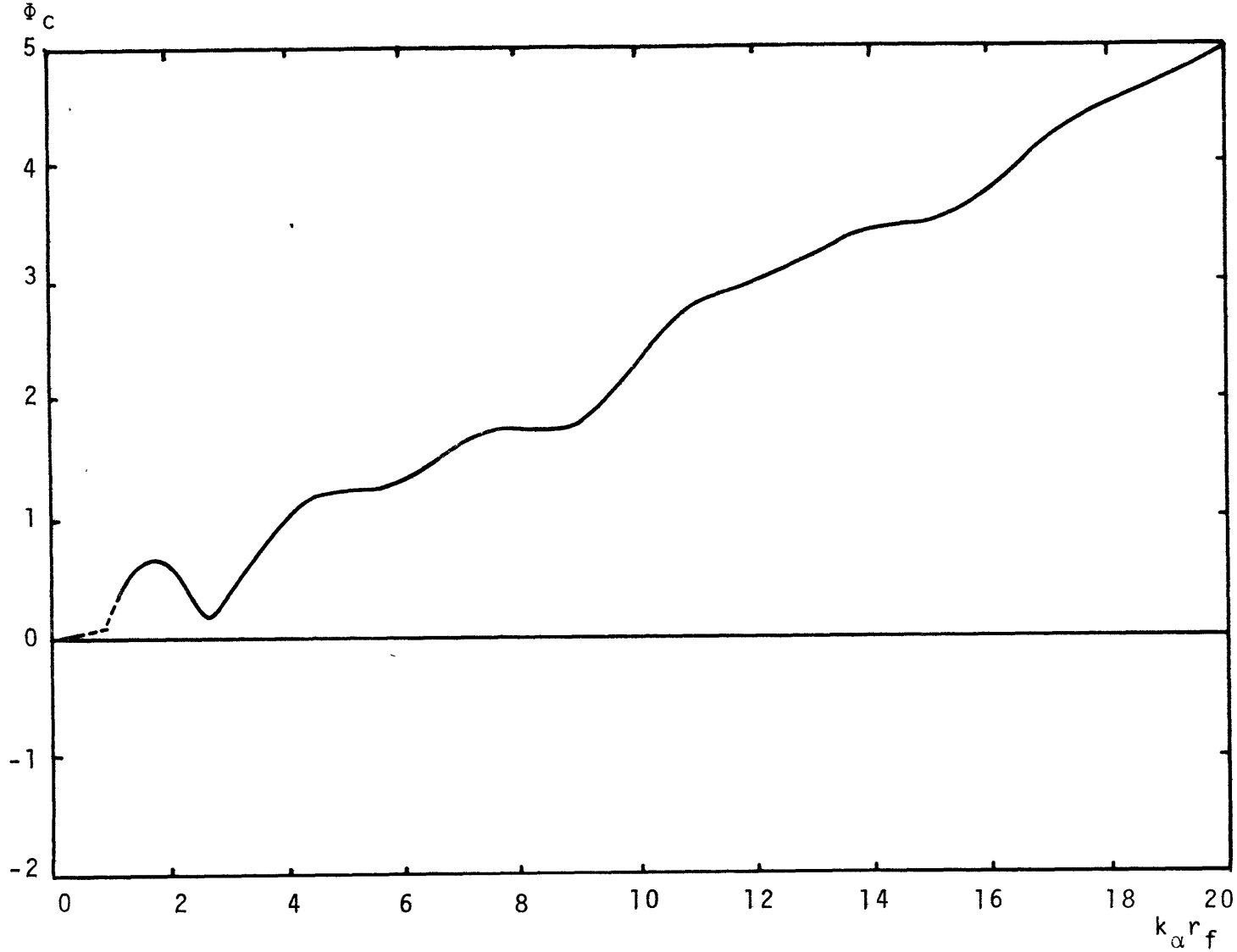

Figure 8. Normalized spectral density of the scattered P wave

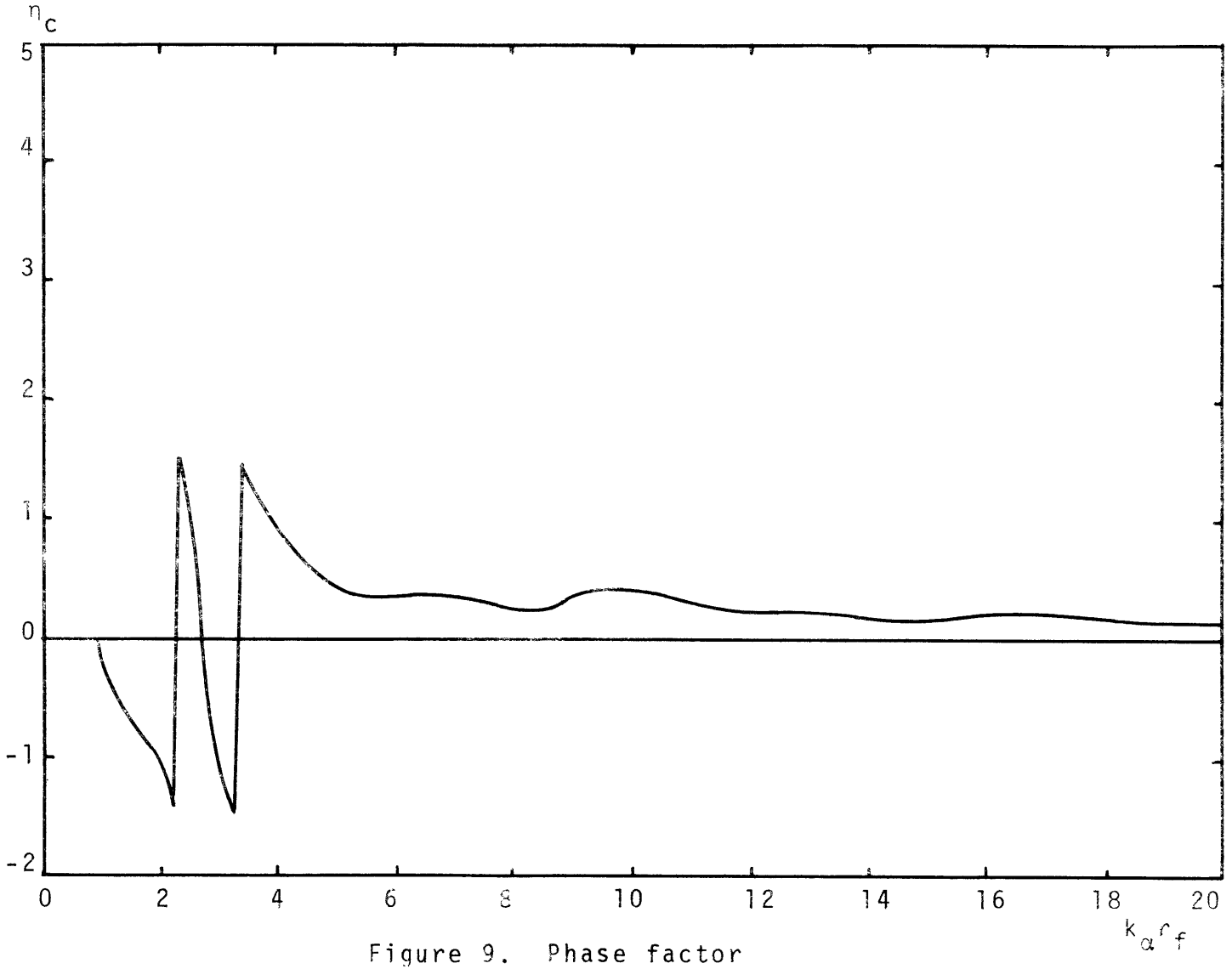

Figure 9. Phase factor

the behavior of Φ_c is dominated by the first two terms in the second integral of 3.4.8. As we have seen in section 3.3, the effect of the first term is to produce a phase shift of the main wave. On the other hand, the second term is equivalent to an amplitude correction to the zero order solution.

Between these two limits, we have a transition from one behavior to the other which depends on the details of the model studied. For example, in our case, the minimum at $k_\alpha r_f \simeq 2.8$ denotes the fact that the transmitted and reflected wave interferes strongly at such frequency so as to more or less cancel each other.

The phase factor η_c is plotted in Fig. 9. It should be noted that we have constrained the value of η_c between $\pi/2$ and $-\pi/2$ but we could have plotted an equivalent continous curve varying from zero around the origin to near -2π for large frequencies.

The coefficient of the PS wave

The coefficient of the scattered shear wave can be evaluated in the same way as the scattered PP wave. We remark in 3.4.5, that the first term represents the transmitted PS wave whereas the second integral is the contribution coming from the reflected shear wave. Again, it is inconvenient to evaluate these two integrals separately

when we have to take into account the effect of scattering within a wavelength from the source. Indeed, if we expand in each of these integrals, and sum the result, we obtain as shown in Appendix XII, the following result:

$$f_{10} \simeq \frac{G}{\mu_0} \int_a^{1/k_\alpha} \mu_0 \, \frac{2}{5} \, \frac{k_\beta^2}{k_\alpha} \, dr_0 \qquad (3.4.11)$$

This is the formula that we have obtained in 3.2.5 and, as shown in Appendix XII, we may expect that it will give an accurate representation of the effect of the inhomogeneities situated such that $k_\alpha r_0 \lesssim 1$.

In order to obtain the integrated effect of all the inhomogeneities we can then use the following formula for f_{10}

$$f_{10} = \frac{G}{\mu_0} \int_a^{r_f} \mu_{10} \, \frac{2}{5} \, \frac{k_\beta^2}{k_\alpha} \, dr_0$$

$$+ \frac{G}{i\mu_0} \int_{1/k_\alpha}^{r_f} \mu_{10} \left[- \frac{k_\alpha}{r_0 k_\alpha} + \frac{3i}{r_0^2} \left(\frac{k_\alpha - k_\beta}{k_\beta^2} \right) + \frac{1}{r_0^3} \cdot \right.$$

$$\left. \left(- \frac{9}{k_\beta^2} + \frac{3k_\alpha}{k_\beta^3} + \frac{3}{k_\alpha k_\beta} \right) + \frac{9i}{r_0^4} \left(\frac{k_\alpha - k_\beta}{k_\alpha k_\beta^3} \right) - \frac{9}{k_\alpha k_\beta^3 r_0^5} \right]$$

$$e^{i(k_\alpha - k_\beta) r_0} dr_0$$

$$+ \frac{G}{i\mu_0} \int_{1/k_\alpha}^{r_f} \mu_{10} \left[\frac{1}{r_0} \frac{k_\alpha}{k_\beta} + \frac{3i}{r_0} \left(\frac{k_\alpha + k_\beta}{k_\beta^2} \right) - \frac{1}{r_0^3} \right.$$

$$\left. \left(\frac{9}{k_\beta^2} + \frac{3k_\alpha}{k_\beta^3} + \frac{3}{k_\alpha k_\beta} \right) + \frac{9i}{r_0^4} \left(\frac{k_\alpha + k_\beta}{k_\alpha k_\beta} \right) + \frac{9}{k_\alpha k_\beta^3 r_0^5} \right]$$

$$e^{i(k_\alpha + k_\beta) r_0} \, dr_0 \qquad (3.4.12)$$

Again, to evaluate this expression, we will fix the relation between the two lengths scale in our model by 3.4.9. In order to calculate 3.4.12, we must also specify the relation between the shear and compressional phase velocity. This will be done here by imposing the relation $\mu_0 = \lambda_0$.

Following the compressional wave case let us define Φ_s and η_s such that

$$\varepsilon f_{10} = G \frac{1}{\lambda_0 + 2\mu_0} \frac{\partial \mu}{\partial Z} r_f \Phi_s e^{-i\eta_s} \qquad (3.4.13)$$

The normalized spectral density of the scattered shear wave, Φ_s, is plotted in Fig. 10 as a function of $k_\alpha r_f$. Again a smoother behavior around $k_\alpha r_f = 1$ is expected if more terms are kept in the expansion leading to eq. 3.4.13.

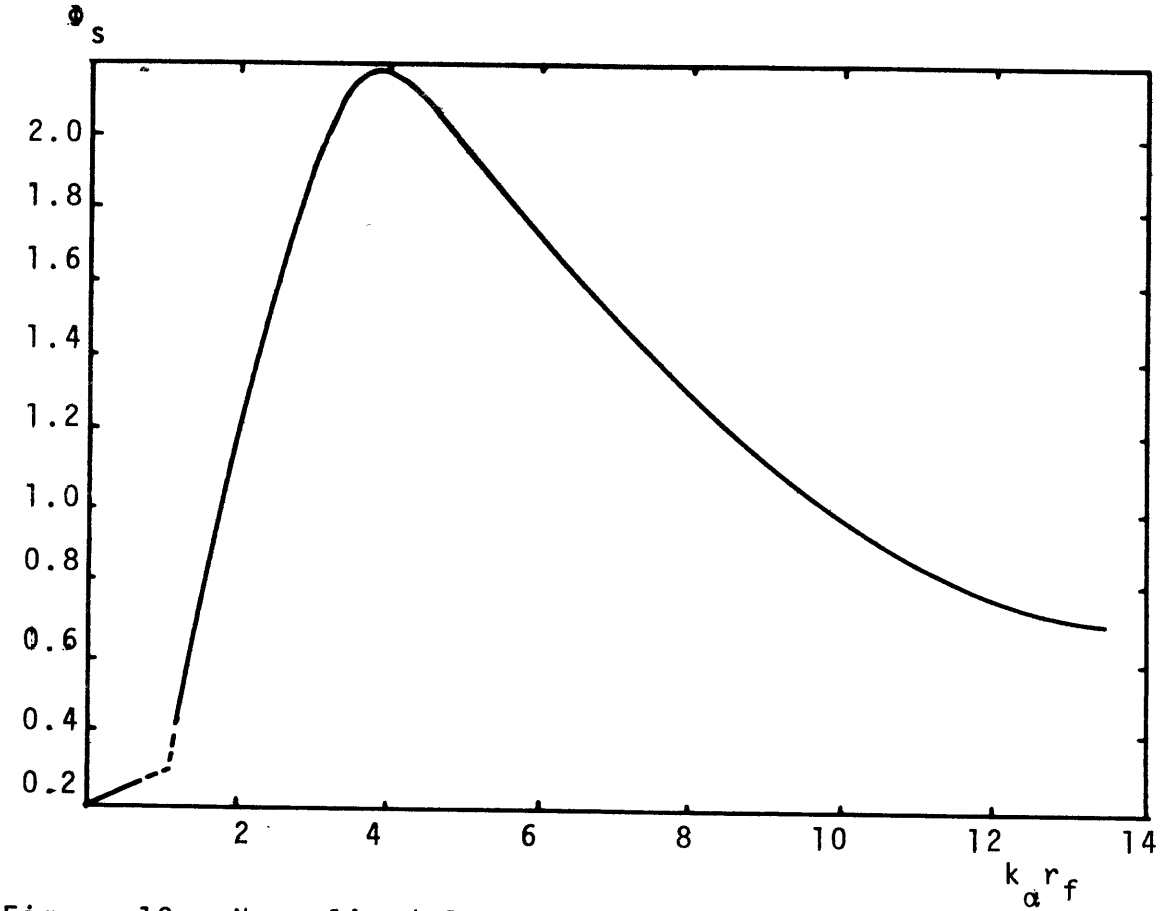

Figure 10. Normalized Spectral Density of the Scattered s wave

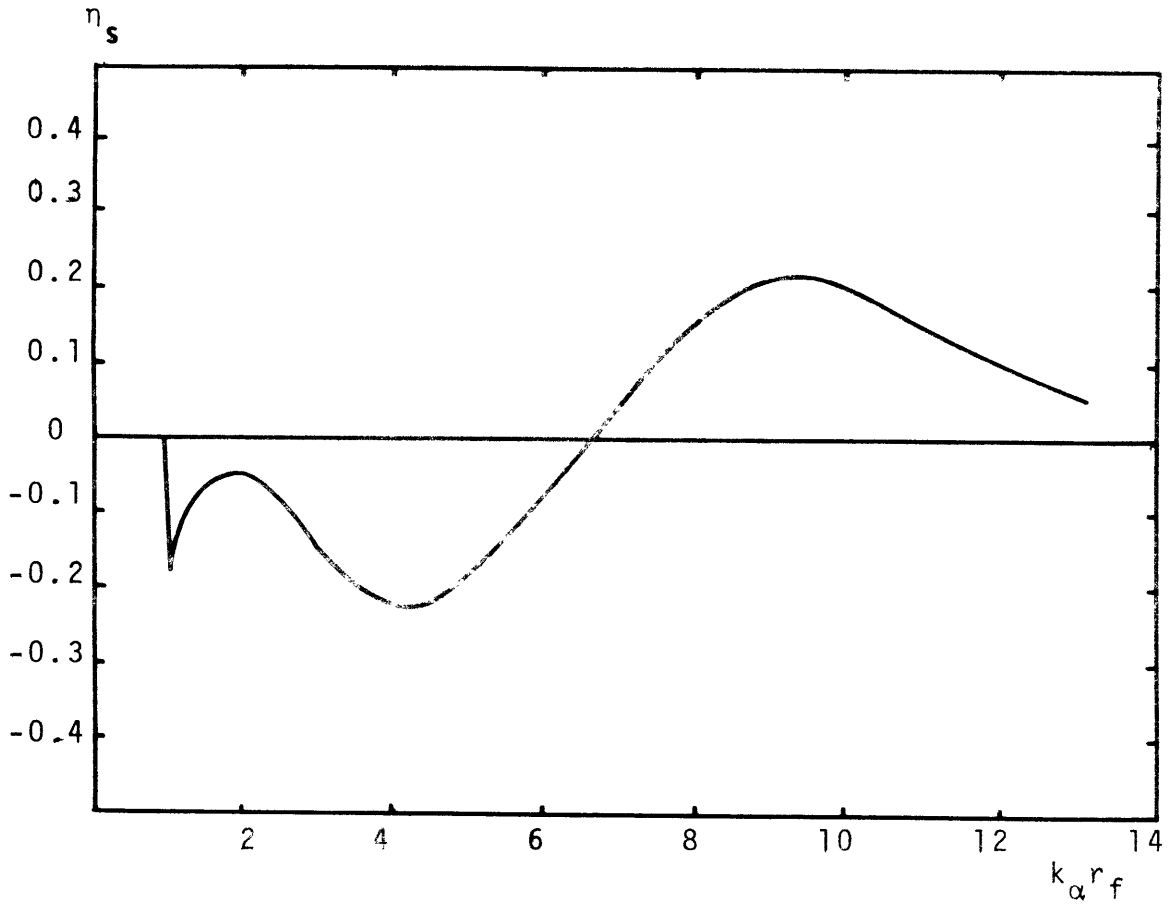

Figure 11. Phase factor

We remark that around $k_\alpha r_f = 3.8$, we have a maximum constructive interference between the transmitted and the reflected shear wave. At high frequencies, the shear wave spectrum decreases to zero as should be expected, since for this frequency range, the parameter is slowly varying over many wavelengths, and the transformation P to S becomes inefficient in such a case.

The phase factor η_s is plotted in Fig. 11. It should be remarked that, due to its very small value in $k_\alpha r_f \leq 2$, the error committed in obtaining 3.4.11 might alter the result substantially in that domain.

To summarize the preceding results, we note that there are basically two limits for which we might expect the first order scattered wave to be an inadequate representation of the scattering process. First, if the rigidity varies greatly within the inhomogeneous sphere, a measure of which is provided by the factor

$$\frac{1}{\lambda_0+2\mu_0} \frac{\partial \mu}{\partial Z} r_f$$

then the first order displacement field may become as large as the zero order one and more terms should be kept in our expansion in terms of ε. On the other hand, even if the properties of the medium are differing slightly from

the homogeneous values, the frequency may be large enough so that the first order compressional wave becomes of the same magnitude as the zero order one. In that case, we can apply the methods of geometrical optics to find the solution.

CHAPTER IV

A Fluid Cavity and the Point Forces Equivalent for SH Wave

4.1 The coefficients of the scattered wave when the medium inside the source is a fluid

One of the assumptions we made to deduce the preceding results was that the medium inside the source was an homogeneous solid. Now, we would like to investigate what modifications to these results must be introduced when we have a fluid specified by $(\rho^-, 0, \lambda^-)$ inside the cavity, $r < a$. In that case, we can still use the zero order solution of section 2.2 since to deduce it, we need only the average properties of the medium outside the source. Furthermore, since the wavelengths observed in practice are usually much larger than the radius of the cavity, we will confine our results to that part of the spectrum.

In order to calculate the first order scattered wave we can follow the general plan set-up in Chapter II. This is done in Appendix XII and some of the main results shown there are as follows. First, the three conclusions reached at the end of Chapter II still hold when we have a fluid inside the cavity. Furthermore, we can express the scattered wave in the same way as we have done in section

2.7 but here, to each coefficient found there, we must add some correction terms due to the presence of the fluid cavity. These new terms account for the interaction of the reflected wave with the source and are important only when the scattered wave is excited within a boundary layer around the source of radius less than ten times the radius of the cavity.

In relation to the amplitude of the scattered wave, it is shown that there are only two groups of spherical harmonics for which the correction terms depend on frequency only through the spectrum of the source, namely the groups specified by n = 0 and n = 2. The case n = 0, involving only compressional wave, is treated in Appendix XII so let us consider here the group n = 2. In that case, the coefficients of the scattered wave can be written as follows:

$$F_{c_{2m}^{\sigma}} = c_{2m}^{\sigma} + \frac{G}{\lambda_0+2\mu_0}\left(\frac{12\lambda_0+8\mu_0}{9\lambda_0+14\mu_0}\right)\int_a^{rf} \mu_{2m}^{\sigma} \frac{a^3}{r_0^4}\, dr_0 - \frac{G}{\lambda_0+2\mu_0}\left(\frac{144}{5}\,\frac{\lambda_0+\mu_0}{9\lambda_0+14\mu_0}\right)\int_a^{rf} \mu_{2m}^{\sigma} \frac{a^5}{r_0^6}\, dr_0 \qquad (4.1.1)$$

and

$$F_{f_{2m}^{\sigma}} = f_{2m}^{\sigma}$$

$$+ \frac{G}{\mu_0} \frac{k_\beta}{k_\alpha} \left(\frac{6\lambda_0+4\mu_0}{9\lambda_0+14\mu_0}\right) \int_a^{r_f} \mu_{2m}^{\sigma} \frac{a^3}{r_0^4} \, dr_0$$

$$- \frac{G}{\mu_0} \frac{k_\beta}{k_\alpha} \left(\frac{72}{5}\right) \left(\frac{\lambda_0+\mu_0}{9\lambda_0+14\mu_0}\right) \int_a^{r_f} \mu_{2m}^{\sigma} \frac{a^5}{r_0^6} \, dr_0 \qquad (4.1.2)$$

The coefficients $(c_{2m}^{\sigma}, f_{2m}^{\sigma})$ in the above expression are the same as the ones we have obtained in section 2.7 whereas the other terms are corrections due to the presence of the fluid cavity.

As we have seen in Chapter III, if the wave is scattered within a sphere centered at the origin and of radius much smaller than a wavelength then we can use the following asymptotic formulas for $(c_{2m}^{\sigma}, f_{2m}^{\sigma})$:

$$c_{2m}^{\sigma} = - \frac{4}{5} \frac{G}{\lambda_0+2\mu_0} \int_a^{r_f} \frac{\mu_{2m}^{\sigma}}{r_0} \, dr_0 \qquad (4.1.3)$$

$$f_{2m}^{\sigma} = - \frac{2}{5} \frac{G}{\mu_0} \frac{k_\beta}{k_\alpha} \int_a^{r_f} \frac{\mu_{2m}^{\sigma}}{r_0} \, dr_0 \qquad (4.1.4)$$

Thus we remark that provided the scattering occurs outside a sphere of radius more than a few times the one of the source, we can neglect the correction terms appearing

in 4.1.1 and 4.1.2 and recover the results previously obtained. On the other hand, it might be unwise to wholly neglect the influence of the fluid cavity since it is precisely the inhomogeneities very near the source that might produce the most significant contribution to the scattered wave.

Before applying the preceding results let us synthesize them a bit more.

4.2 Point forces equivalent and seismic moment for scattering of SH wave.

In order to discriminate between the different processes occuring near the source, it is often convenient to find a combination of point forces giving the same far field radiation pattern as each process. In this connection, we shall restrict our considerations to the pair of spherical harmonics of the potentials specified by (2,2,1) and (2,2,2) since they seem to give the dominant contribution to the SH wave scattered near the source. But first, let us consider the equivalent point force distribution for the explosion.

In order to obtain the far field radiation pattern of the main wave, we can use three mutually perpendicular identical, double point force without moment. If we define M_0 as the product of force with arm length of the component

double force, we find the relation

$$M_0(t) = \frac{\lambda_0 + 2\mu_0}{\mu_0} \pi a^3 P(t) \qquad (4.2.1)$$

where $P(t) = -T_{rr}(t)$ (see Sect. 2.2) is the pressure acting on the surface of the cavity. Here we have neglected terms of order $k_\alpha a$ since we are concerned only in wavelengths much longer than the radius of the cavity.

Let us now consider two force couples, each with moment M(t), combined such as to produce a double couple without moment and situated in the equatorial plane ($\theta = \pi/2$) as sketched in Figure 12.

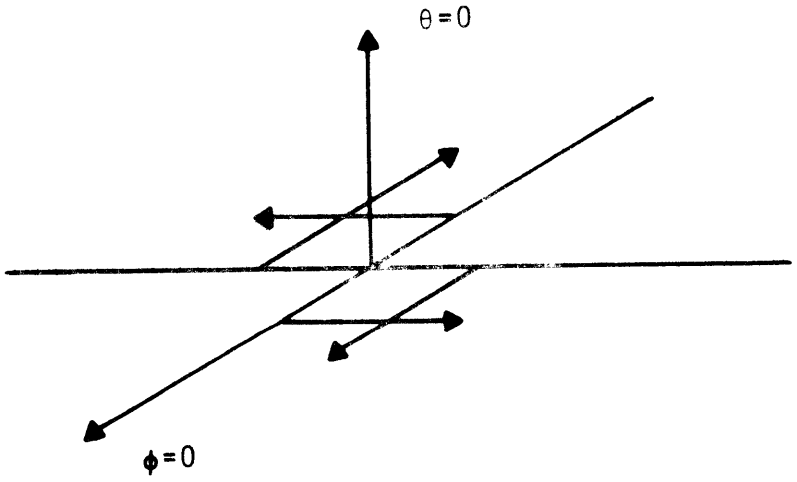

Figure 12. Double couple without moment

Then, we can show that the far field radiation pattern of this combination of point force can be expressed as follows (see e.g. White (1965))

$$\vec{s} = \vec{a}_r \frac{P_2^2(\cos\theta)\sin 2\phi}{\rho\,\alpha^3 r} \frac{1}{12\pi} \frac{\partial}{\partial t} M(t - \frac{r}{\alpha})$$

$$+\vec{a}_\theta \frac{\partial}{\partial\theta} \frac{P_2^2(\cos\theta)\sin 2\phi}{\rho\,\beta^3 r} \frac{1}{24\pi} \frac{\partial}{\partial t} M(t - \frac{r}{\beta})$$

$$+\vec{a}_\phi \frac{P_2^2(\cos\theta)}{\sin\theta\rho\beta^3 r} \frac{\partial}{\partial\phi} \sin 2\phi \frac{1}{24\pi} \frac{\partial}{\partial t} M(t - \frac{r}{\beta}) \qquad (4.2.2)$$

Let us now substitute in 3.2.10 the coefficients (c_{22}^2, f_{22}^2) by $({}^F c_{22}^2, {}^F f_{22}^2)$ and use the asymptotic form of the former coefficients as given in 4.13 and 4.1.4. Then we remark that, after Fourier transforming back in the time domain, we can express the (2,2,2) harmonic of the scattered waves in the same form as 4.2.2. provided we let:

$$M(t) = M_0(t)\eta_2 \qquad (4.2.3)$$

where

$$\eta_2 = \frac{3\varepsilon}{\lambda_0+2\mu_0}\left[\frac{4}{5}\int_a^{r_f} \frac{\mu_{22}^2}{r_0}\,dr_0 - \frac{12\lambda_0+8\mu_0}{9\lambda_0+14\mu_0}\int_a^{r_f} \mu_{22}^2 \frac{a^3}{r_0^3}\,dr_0\right.$$

$$\left. + \frac{144}{5}\left(\frac{\lambda_0+\mu_0}{9\lambda_0+14\mu_0}\right)\int_a^{r_f} \mu_{22}^2 \frac{a^5}{r_0^6}\,dr_0\right] \qquad (4.2.4)$$

We can now combine the harmonics of the potential specified by (2,2,2) and (2,2,1) in the following way:

First we define η_1 by replacing μ_{22}^2 in η_2 by μ_{22}^1. Secondly, we consider a coordinate system, (r,θ,ϕ^1) related to the one we used to calculate η_1 and η_2, (r,θ,ϕ), by the relation

$$\phi^1 = \phi + \tan^{-1} \frac{\eta_1}{\eta_2} \tag{4.2.5}$$

Then, in this new coordinate system, the sum of the displacements associated with these potentials can be expressed as 4.2.2 provided we let

$$M(t) = M_0(t) \sqrt{\eta_1^2+\eta_2^2} \tag{4.2.6}$$

In order to see how we can apply these results, let us consider a particular example.

4.3 Scattering of SH wave around the Boxcar nuclear explosion

In order to illustrate the preceding results, we need the detailed distribution of rigidity within wavelength from the source. Since this information can be more easily obtained near a source of long wavelengths, let us consider an explosion produced on the Nevada Test Site. In particular,

we shall choose Boxcar since the displacement field generated by this event is well documented in the literature. Moreover, we shall restrict our consideration to waves with period longer than 10 secs. So we may presumably use the asymptotic formulas of the preceding section in order to calculate the scattered wave excited within the first 10-20 kms around the source.

Let us first briefly describe the structure of the medium around this explosion. For this, we will follow a paper by Orkild et al in the Memoir 110 of the Geological Society of Ameria, which details the geological setting of the Nevada Test Site.

Structure and rigidity distribution around the source

Boxcar was located in the Silent Canyon Caldera, a late tertiary volcanic center, in eastern Pahute Mesa. The wall of the buried Silent Canyon Caldera was approximately located by a steepening of gravity contours into a 20 milligals gravity low (see Fig. 13).

Figure 14 shows an east-west cross section of Pahute Mesa and the major rock types of the caldera. The basement rocks are older volcanic rocks than the ones in Silent Canyon caldera. Within the caldera, drilling and gravity data indicate two basins: a shallow broad basin in the eastern part and a deep basin elongated along a N20°E trend

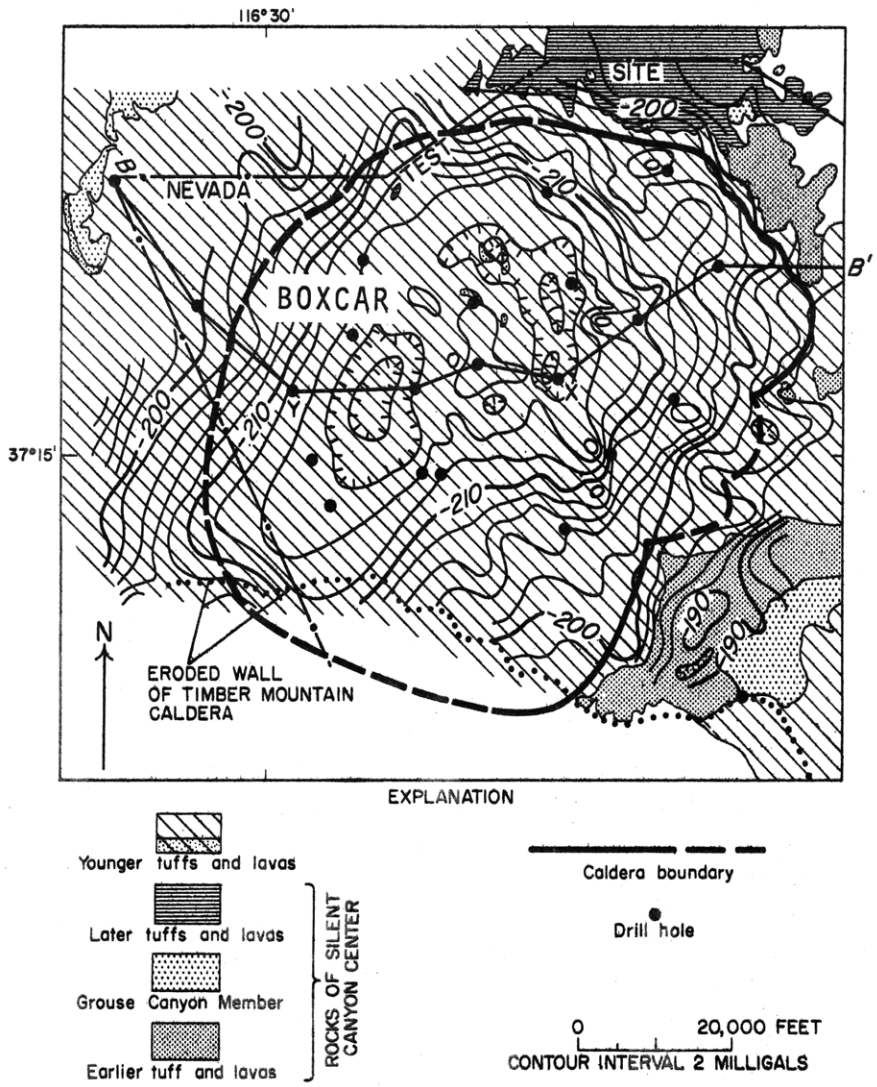

Figure 13. Residual gravity map of Silent Canyon Caldera, showing outline of caldera, location of drill holes and Boxcar, and major geologic units. Gravity data by D.L. Healy and C.H. Miller

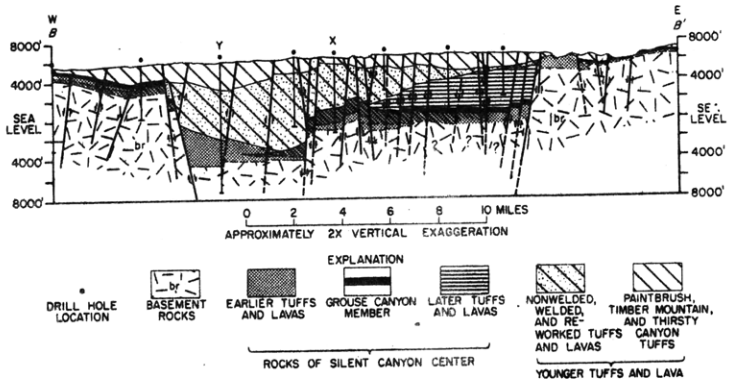

Figure 14. Generalized east-west cross section of Pahute Mesa showing Silent Canyon Caldera and major rock types. Cross-hatch shows Tub Spring Member of Belted Range Tuff.

in the western part. Boxcar was situated 1.17 km deep in this latter basin, approximately 3.5 kms from the west wall and 10 kms from the north wall of the caldera.

If we examine Fig. 14, we remark that it is difficult to infer something on lateral variation of the rigidity within this deep basin. On the other hand, it is precisely very near the source that we might expect the scattering of SH waves to be the most efficient. So this lack of information might cause a substantial error in our results. But nevertheless, let us obtain a rough estimate of the scattered SH wave likely to have been generated by the lateral rigidity contrast between the material inside the caldera and the surrounding older volcanic rocks. In order to obtain an estimate of this contrast let us follow the data of Stauder (1971)(see table I), which were obtained by averaging the measurement of rigidity through the 4.1 kms deep exploration drill hole Y on Fig. 13 and 14.

TABLE I

Rigidity model based on data from drill hole Y and obtained by Carroll (1966)

Depth to layer, km	μ dyne/cm^2
0.0	5.12×10^{10}
0.96	8.15×10^{10}
1.33	1.01×10^{11}
2.14	1.50×10^{11}
5.00	3.25×10^{11}

We remark that the average value of the rigidity over the first 2.5 kms is

$$\mu_1 = 0.8\times10^{11} \text{ dyne/cm}^2 \qquad (4.3.1)$$

In the following, this is the rigidity we will take to represent the medium inside the caldera. On the other hand, the older volcanic rocks under the caldera have rigidity approximately equal to

$$\mu_2 = 1.7\times10^{11} \text{ dyne/cm}^2 \qquad (4.3.2)$$

This is the value we will take to represent the rigidity of the material on the west side of the western wall of the caldera.

In our preceding analysis, we have assumed that we were dealing with an infinite solid which obviously is not the case here. But, in order to apply our preceding results we will assume that above the ground lies a homogeneous solid characterized by (ρ_2,μ_2,λ_2). These values will also be taken to represent the average properties of the medium around Boxcar.

Model of the structure and of the distribution of rigidity around Boxcar

Sketched in Figure 15 and 16 are the models we will use to calculate the scattered SH wave around Boxcar.

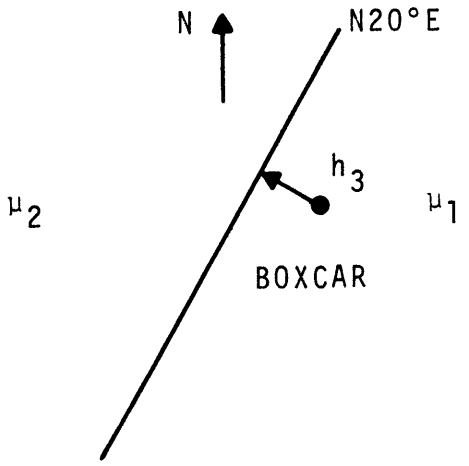

Figure 15. Model of the geological map around Boxcar

Fig. 15 is a model of the geological map detailed in Fig. 13. The line trending N20°E represents the west wall of the Silent Canyon caldera. Boxcar was approximately at a distance of h_3 = 3.5 kms from this boundary.

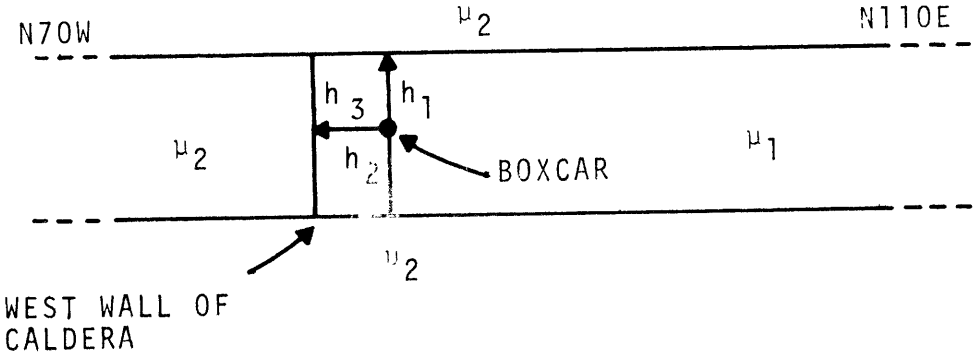

Figure 16. Model of the cross-section through Boxcar trending N70W

Figure 16 is a model of the cross-section shown in Fig. 14. The model inside the caldera is modelled by a semi-infinite layer of thickness h_1+h_2 = 2.5 km and rigidity μ_1. We will assume that this layer is embedded in a medium of rigidity μ_2.

For simplicity, let us choose our coordinate system such that the polar axis is vertical to the ground whereas the axis specified by $\theta = \pi/2$ and $\phi = 0$ is parallel to the west wall of the caldera, i.e. along a N20°E direction, and pointing towards the south. Then the spherical harmonics of the rigidity characterized by (2,2,1) and (2,2,2) can be written as follows

$$\varepsilon\mu_1 = \varepsilon\mu_{22}^1 P_2^2(\cos\theta)\cos 2\phi + \varepsilon\mu_{22}^2 P_2^2(\cos\theta)\sin 2\phi \quad (4.3.3)$$

where, in our case

$$\varepsilon\mu_{21}^1 = 0 \qquad \text{for } r \leq h_3 \quad (4.3.4)$$

$$\simeq \frac{5}{48\pi}(\mu_2-\mu_1)\left[3\frac{(h_2+h_1)}{r} - \frac{(h_2^3+h_1^3)}{r^3}\right]\left[\frac{2h_3\sqrt{r^2-h_3^2}}{r^2}\right]$$

$$\text{for } r \geq h_3$$

and

$$\varepsilon\mu_{22}^2 = 0 \text{ for all } r$$

We have assumed the western wall to be somewhat curved in order to facilitate the evaluation of the spherical harmonics but this introduces negligible error when h_1, h_2 and h_3 are as specified above.

Location of the nodes in the scattered SH and Love wave

With the above data, let us investigate the direction of the nodes in the scattered SH wave and its resulting Love waves. In the chosen coordinate system the s_ϕ motion is proportional to sin 2ϕ for the rigidity specified above so we are expecting nodes at the azimuthal angles 0°, 90°, 180° and 270°. The node at 180° corresponds to a node in the N20°E direction.

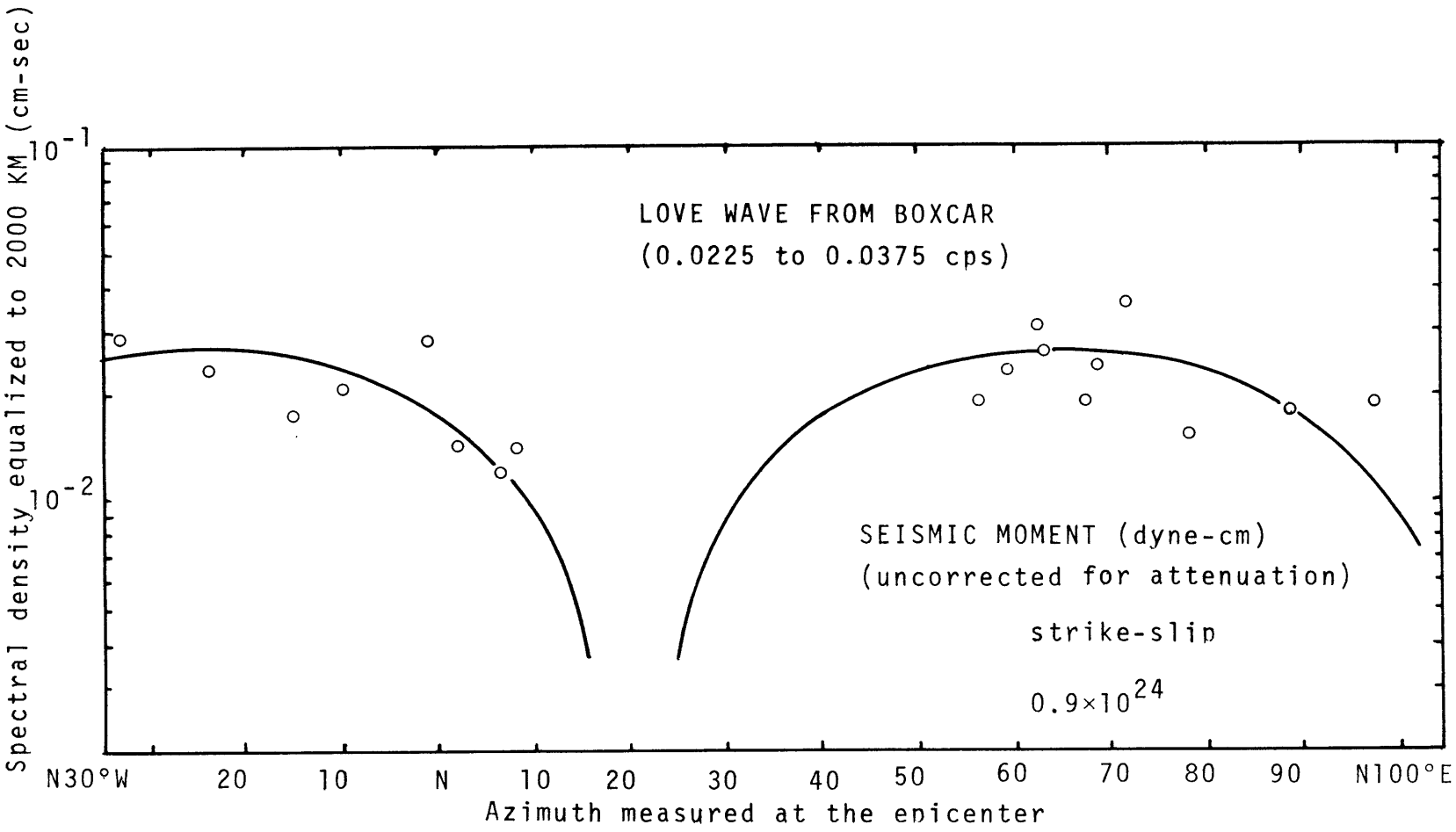
Spectral density equalized to 2000 KM (cm-sec)
10^{-1}
10^{-2}
LOVE WAVE FROM BOXCAR
(0.0225 to 0.0375 cps)
SEISMIC MOMENT (dyne-cm)
(uncorrected for attenuation)
strike-slip
0.9×10^{24}
N30°W 20 10 N 10 20 30 40 50 60 70 80 90 N100°E
Azimuth measured at the epicenter

Figure 17.

Figure 17 shows the spectral density of Love wave generated from Boxcar, plotted against the azimuthal angle These data, averaged over the frequency band from 0.0225 to 0.0375 cps were recorded at the WWSS and Canadian stations and equalized to an epicentral distance 2000 kms for geometrical spreading. (Aki and Tsai (1971).)

Surprisingly enough, we remark that the node at N20°E coincides exactly with one of the node predicted above.

Let us now investigate if the seismic moments agree well with observation.

Seismic moments

Let us evaluate the quantity η_1 defined in the preceding section. For a radius of the source of 700 meters, which seems adequate in the case of Boxcar (Aki and Tsai (1970)), the correction terms due to the presence of the fluid cavity give negligible contribution to the seismic moment. This is mainly due to the small ratio ($a/h_3 \simeq 0.2$) between the radius of the cavity (a) and the distance of Boxcar to the western wall of the caldera (h_3).

So, in that case we obtain

$$\eta_1 = \frac{12}{5(\lambda_2+2\mu_2)} \int_a^{r_f} \frac{\mu_{22}^1}{r_0} dr_0$$

$$\simeq 0.05 \left[\frac{\mu_2-\mu_1}{\mu_2}\right]\left[\frac{h_2+h_1}{h_3}\right] \qquad (4.3.5)$$

Here we have assumed that r_f is much larger than h_3 and that $\mu_2 = \lambda_2$. Then we obtain for the model specified above:

$$\eta_1 \simeq 0.02 \qquad (4.3.6)$$

Aki and Tsai (1971) have estimated the seismic moments of the Boxcar explosion and the SH wave generated around it. They have restricted their consideration to long period wave (T > 10 sec.) and, modelling the seismic moments by a step function in time, H(t), they have obtained a good fit with observation in the cases where they chose.

$$M_0 \simeq (2.5\text{-}3.0)\times 10^{24} H(t) \text{ dyne-cm}$$

and

$$M(t) \simeq (0.9\text{-}1.2)\times 10^{24} H(t) \text{ dyne-cm}$$

In our preceding notation, this means that the observed value for η_1 is

$$\eta_1 \simeq 0.3 \text{ to } 0.4 \qquad (4.3.7)$$

So we remark that the observed ratio of seismic moments is about an order of magnitude higher than the one we calculate. Does this mean that our model of the rigidity distribution was not accurate enough to calculate the scattered SH wave? Or does it imply that more efficient processes than scattering, for example release of preexisting stress around Boxcar, have produced the observed Love wave signal? Hopefully, future research will permit us to find the answer.

CHAPTER V

Conclusions

5.1 Summary with suggestions for future work

In order to obtain a good zero order analysis of the displacement field, the seismologist finds it often convenient to model the medium by a homogeneous solid characterized by some average properties of the real earth. The aim of this paper was to complete the above picture by calculating the first order displacement field generated by an arbitrary distribution of parameters around a compressional source. But, in order to do so, we have not taken into account the effect of the surface of the earth on the displacement field. Thus, a more complete investigation would include this boundary in the calculation of the zero and first order displacement field.

If this was done, the chief question that would remain would be to determine the accuracy of the first order scattered wave obtained by the method of small perturbation. In that respect there are mainly two directions that one can follow in order to improve the preceding analysis.

First, as we have seen in Chapter III, the first order scattered wave calculated by the method of small perturbation is not valid for all frequencies. Indeed, for frequencies high enough, the medium is slowly varying over

many wavelengths and the scattered wave grows in proportion to the frequency. This is due, as we have shown by using the method of geometrical optics, to a phase correction of the zero order solution. So, this suggests that one should try to combine the two preceding methods in order to obtain a uniformly valid first order scattered field over the whole range of frequencies.

Secondly, one should investigate the class of structure for which multiple scattering, i.e. higher order terms in our expansion in terms of ε, can be neglected in the calculation of the displacement field. In this connection, it might be worthwhile to study simple structure, for example layered media, for which exact solutions are known and compare these solutions with the ones obtained by the method of small perturbation.

In this respect, though we have found it convenient in this study to analyze the displacement field through a spherical coordinate system, this choice might prove to be a poor competitor to other systems of coordinates when we try to synthesize the scattered field generated by some particular model. But, more generally, if a given structure can be expressed as the sum of two substructures, i.e.

$$(\rho_1,\mu_1,\lambda_1) = (\rho_a,\mu_a,\lambda_a) + (\rho_b,\mu_b,\lambda_b) ,$$

then, as can be verified in Chapter II, the first order scattered wave is just the sum of the waves generated by each of these substructures. Therefore, we may find it convenient to analyze part of the scattered wave in one coordinate system and to calculate the remaining part in another system. For example, if we are expecting that some of the main features in the distribution of parameters can be described by a layered structure, then it might prove convenient to analyze its contribution to the scattered wave through a cylindrical coordinate system whereas we can use the formulas we have developed to calculate the wave excited by the remaining inhomogeneities. This choice to a large extent will be guided by the nature of the data we have obtained.

In this connection, since clearly we cannot deduce from a finite set of measurements the complete structure of the medium, it might prove rewarding to analyze part of the medium through the methods we have developed but obtain only statistical information about the remaining part. Such attempts have already appeared in the literature (e.g. Dunkin (1969), Karal et al (1964), Knopoff et al (1964)) and it should be interesting to connect their analysis with the preceding one. On the other hand, it might prove a worthwhile endeavor to examine more closely the contribution

to the scattered wave coming from the periodic parts of a given structure connected to a given frequency through Bragg's conditions. Of course, if it can be shown that for a wide class of realistic models, the scattered wave generated through Bragg's effect gives the main contribution to the scattered displacement field, then the inverse problem would be considerably simplified.

Perhaps an important application of the preceding analysis will be to provide better modelling techniques for the medium near the source. But, in that respect, we are facing some experimental difficulties. Indeed, at least part of the anomalous field which seems to originate near the source is caused by the relaxation of preexisting stress around the explosion site and part of it is due to the scattering of elastic waves occuring say within a sphere of radius much smaller than a wavelength. Since both of these waves are intimately mixed-up, it is difficult to distinguish between the two processes. Furthermore, since in the theories of stress relaxation, the preexisting stress is the unknown parameter that we try to determine through the observation of the anomalous field, we cannot remove its effect in order to model the distributions of parameters. So it seems that in order to determine the importance of scattering near the source, one would have to make an independant measurement of the

distribution of medium parameters around the source. An attempt in that direction was made in Chapter IV, in the case of Boxcar. It did not appear there that scattering would be enough to explain the amplitude of Love wave generated around this nuclear event. But, because of lack of information, we have not considered the inhomogeneities very near the source, which might be more important than the broad structure we have considered. Hopefully, this will be done in the near future.

APPENDIX I

The Sharpe's Problem

Since the stress is given on the surface of the cavity we do not need the continuity of displacement in this case.

We have to solve

$$\rho_0 \frac{\partial^2 \vec{s}_0}{\partial t^2} - 2\mu_0 \nabla\cdot\tilde{\tilde{S}}_0 - \lambda_0 \nabla\cdot|\tilde{\tilde{S}}_0|\tilde{\tilde{I}} = 0 \qquad (I.1)$$

subject to the boundary condition

$$2\mu_0 \vec{a}_r\cdot\cdot\tilde{\tilde{S}}_0 + \lambda_0 \vec{a}_r\cdot\cdot|\tilde{\tilde{S}}_0|\tilde{\tilde{I}}\Big|_{r=a} = T_{rr}(t)\vec{a}_r \qquad (I.2)$$

Since the motion will be purely radial, we then have to solve

$$\rho_0 \frac{\partial^2 \vec{s}_r^0}{\partial t^2} - (\lambda_0+2\mu_0) \frac{\partial}{\partial r} \frac{1}{r^2} \frac{\partial r^2 s_r^0}{\partial r} = 0 \qquad (I.3)$$

Let

$$s_r^0 = \frac{\partial \psi_0}{\partial r} \qquad (I.4)$$

then we find

$$\frac{\partial^2 \psi_0}{\partial t^2} - \frac{\lambda_0+2\mu_0}{\rho_0} \frac{1}{r^2} \frac{\partial r^2}{\partial r} \frac{\partial \psi_0}{\partial r} = 0 \qquad (I.5)$$

subject to the boundary condition

$$(\lambda_0+2\mu_0)\left.\frac{\partial s_r^0}{\partial r}+\frac{2\lambda_0 s_r^0}{r}\right|_{r=a}=(\lambda_0+2\mu_0)\left.\frac{\partial^2\psi_0}{\partial r^2}+\frac{2\lambda_0}{r}\frac{\partial\psi_0}{\partial r}\right|_{r=a}$$

$$=T_{rr}(t) \qquad (I.6)$$

The general outgoing solution of eq. 5 is given by

$$\psi_0=\frac{F(t-\frac{(r-a)}{\alpha})}{r} \qquad (I.7)$$

where

$$\alpha=\left(\frac{\lambda_0+2\mu_0}{\rho_0}\right)^{\frac{1}{2}}$$

Using the fact that

$$\frac{\partial^n F}{\partial r^n}=\frac{(-1)^n}{\alpha^n}\frac{\partial^n F}{\partial t^n} \qquad (n=1,2) \qquad (I.8)$$

the boundary condition becomes

$$(\lambda_0+2\mu_0)\frac{1}{\alpha^2 a}\frac{d^2F(t)}{dt^2}+\frac{4\mu_0}{\alpha a^2}\frac{dF(t)}{dt}+\frac{4\mu_0 F(t)}{a^3}=T_{rr}(t)$$

$$(I.9)$$

which we recognize as the equation of a damped harmonic oscillator. If we let

$$\frac{Q}{4} = \frac{\mu_0}{\lambda_0+2\mu_0}$$

$$x = \frac{\alpha Q}{2a}\sqrt{\frac{4}{Q} - 1}$$

and

$$v = \frac{\alpha Q}{2a}$$

then we can write the solution for F(t) as follows

$$F(t) = \int_{-\infty}^{t} \frac{a}{x} T_{rr}(t')e^{-v(t-t')}\sin x(t-t')dt' \qquad (I.10)$$

and

$$\psi_0 = \frac{1}{r}\int_{-\infty}^{t-(\frac{r-a}{\alpha})} \frac{a}{x} T_{rr}(t')e^{-v(t-(\frac{r-a}{\alpha})-t')} \sin x(t-(\frac{r-a}{\alpha})-t')dt'$$

In our calculation, what we need is the Fourier transform with respect to time of the displacement. So let

$$(\psi_{0\omega}, F_\omega, T_{rr\omega}) \leftrightarrow (\psi_0(t-(\frac{r-a}{\alpha})), F(t), T_{rr}(t))$$

then

$$\psi_0 = \frac{F_\omega e^{i\omega(\frac{r-a}{\alpha})}}{r}$$

$$= Gh_0(k_\alpha r) \qquad \text{(I.11)}$$

where

$$G = iF_\omega k_\alpha e^{-ik_\alpha a}$$

$$h_0(k_\alpha r) = \frac{-ie^{ik_\alpha r}}{k_\alpha r}$$

and F_ω can be found by Fourier transforming Eq. 9.

$$F_\omega = \frac{T_{rr\omega}\, a^3}{(\lambda_0+2\mu_0)(-k_\alpha^2 a^2 - ik_\alpha aQ+Q)}$$

where

$$k_\alpha = \frac{\omega}{\alpha}$$

APPENDIX II

Green's Functions

We would like to find the solution to the following equation:

$$-\rho_0\omega^2\vec{s}^{g}_{11\omega} - 2\mu_0\nabla\cdot\tilde{\tilde{S}}^{g}_{11\omega} - \lambda_0\nabla\cdot|\tilde{\tilde{S}}^{g}_{11\omega}|\tilde{\tilde{I}}$$

$$= P_n^m(\cos\theta)\cos m\phi\, A\delta(r-r_0)\vec{a}_r$$

$$+ \frac{\partial}{\partial\theta} P_n^m(\cos\theta)\cos m\phi B\delta(r-r_0)\vec{a}_\theta$$

$$+ \frac{P_n^m(\cos\theta)}{\sin\theta} \frac{\partial}{\partial\phi}\cos m\phi\, B\delta(r-r_0)\vec{a}_\phi$$

$$\equiv \vec{F} \qquad \text{(II.1)}$$

Potential representation

Let us represent $\vec{F}$ in the following form

$$\vec{F} = \nabla\Psi + \nabla\times\vec{a}_r r\Psi_1 + \nabla\times\nabla\times\vec{a}_r r\Psi_2 \qquad \text{(II.2)}$$

i.e.

$$AP_n^m(\cos\theta)\cos m\phi\delta(r-r_0) =$$

$$= \frac{\partial\Psi}{\partial r} + \frac{1}{r\sin\theta}\left[-\frac{\partial}{\partial\theta}\sin\theta\frac{\partial\Psi_2}{\partial\theta} - \frac{1}{\sin\theta}\frac{\partial^2\Psi_2}{\partial\phi^2}\right] \qquad \text{(II.3)}$$

$$B \frac{\partial}{\partial \theta} P_n^m(\cos\theta)\cos m\phi\,\delta(r-r_0) =$$

$$\frac{1}{r}\frac{\partial \Psi}{\partial \theta} + \frac{1}{r}\left[\frac{1}{\sin\theta}\frac{\partial r\Psi_1}{\partial \phi} + \frac{\partial r}{\partial r}\frac{\partial \Psi_2}{\partial \theta}\right] \qquad \text{(II.4)}$$

$$B \frac{P_n^m(\cos\theta)}{\sin\theta}\frac{\partial}{\partial \phi}\cos m\phi\,\delta(r-r_0) = \frac{1}{r\sin\theta}\frac{\partial \Psi}{\partial \phi} +$$

$$+ \frac{1}{r}\left[\frac{\partial}{\partial r}\frac{r}{\sin\theta}\frac{\partial \Psi_2}{\partial \phi} - \frac{\partial r\Psi_1}{\partial \theta}\right] \qquad \text{(II.5)}$$

If we operate eq. 5 with $\frac{\partial \sin\theta}{\partial \theta}$ and eq. 4 with $\frac{\partial \cdot}{\partial \phi}$ and substract the results we obtain

$$\frac{1}{r\sin\theta}\frac{\partial^2 r\Psi_1}{\partial \phi^2} + \frac{1}{r}\frac{\partial}{\partial \theta}\sin\theta\frac{\partial r}{\partial \theta}\Psi_1 = 0 \qquad \text{(II.6)}$$

so we must conclude that

$$\Psi_1 = 0$$

Let

$$\Psi = P_n^m(\cos\theta)\cos m\phi\,\ell(r)$$

$$\Psi_2 = P_n^m(\cos\theta)\cos m\phi\,p(r)$$

and using Legendre's equation i.e.

$$\frac{1}{\sin\theta}\frac{d}{d\theta}\sin\theta\frac{d}{d\theta}P_n^m(\cos\theta)+\left[(n)(n+1)-\frac{m^2}{\sin^2\theta}\right]\cdot$$

$$P_n^m(\cos\theta) = 0 \qquad \text{(II.7)}$$

we obtain

$$AP_n^m(\cos\theta)\cos m\phi\,\delta(r-r_0) = P_n^m(\cos\theta)\cos m\phi\left[\frac{\partial \ell}{\partial r}+\frac{(n)(n+1)p}{r}\right] \qquad \text{(II.8)}$$

$$B\frac{\partial}{\partial\theta}P_n^m(\cos\theta)\cos m\phi\,\delta(r-r_0)$$

$$= \frac{\partial}{\partial\theta}P_n^m(\cos\theta)\cos m\phi\left[\frac{\ell}{r}+\frac{1}{r}\frac{\partial rp}{\partial r}\right] \qquad \text{(II.9)}$$

$$B\frac{P_n^m(\cos\theta)}{\sin\theta}\frac{\partial\cos m\phi}{\partial\phi}\delta(r-r_0) = \frac{P_n^m(\cos\theta)}{\sin\theta}$$

$$\frac{\partial\cos m\phi}{\partial\phi}\left[\frac{\ell}{r}+\frac{1}{r}\frac{\partial rp}{\partial r}\right] \qquad \text{(II.10)}$$

We see that it is sufficient to solve

$$A\delta(r-r_0) = \frac{\partial\ell}{\partial r}+(n)(n+1)\frac{p}{r} \qquad \text{(II.11)}$$

$$B\delta(r-r_0) = \frac{\ell}{r}+\frac{1}{r}\frac{\partial rp}{\partial r} \qquad \text{(II.12)}$$

Solving these equations we obtain with the condition that the representation is finite at r = 0 and ∞,

$$\ell = -\frac{A(n+1)r^n}{(2n+1)r_0^n} + \frac{n(n+1)Br^n}{(2n+1)r_0^n} \quad \text{for } r < r_0 \tag{II.13}$$

$$= \frac{A\, nr_0^{n+1}}{(2n+1)r^{n+1}} + \frac{n(n+1)Br_0^{n+1}}{(2n+1)r^{n+1}} \quad \text{for } r > r_0 \tag{II.14}$$

$$p = \frac{Ar^n}{(2n+1)r_0^n} - \frac{nBr^n}{(2n+1)r_0^n} \quad \text{for } r < r_0 \tag{II.15}$$

$$= \frac{Ar_0^{n+1}}{(2n+1)r^{n+1}} + \frac{(n+1)Br_0^{n+1}}{(2n+1)r^{n+1}} \quad \text{for } r > r_0 \tag{II.16}$$

So we have the representation

$$\vec{F} = \nabla P_n^m(\cos\theta)\cos m\phi\,\ell + \nabla\times\nabla\times\vec{a}_r r P_n^m(\cos\theta)\cos m\phi\, p \tag{II.17}$$

Solution of equation 1.

Let

$$\vec{s}^{g}_{11\omega} = \nabla\Phi + \nabla\times\vec{a}_r r\phi_1 + \nabla\times\nabla\times\vec{a}_r r\phi_2 \tag{II.18}$$

and

$$\vec{F} = \nabla\Psi + \nabla\times\vec{a}_r r\Psi_1 + \nabla\times\nabla\times\vec{a}_r r\Psi_2 \tag{II.19}$$

then we can rewrite eq. 1 in the form

$$-\rho_0\omega^2\vec{s}^g_{11\omega} - (\lambda_0+2\mu_0)\nabla\ \nabla\cdot\vec{s}^g_{11\omega}+\mu_0\nabla\times\nabla\times\vec{s}^g_{11\omega} = \vec{F} \qquad \text{(II.20)}$$

or

$$\nabla(-\rho_0\omega^2\Phi-(\lambda_0+2\mu_0)\nabla^2\Phi-\Psi)$$

$$+\left[\frac{1}{\sin\theta}\frac{\partial}{\partial\phi}(-\rho_0\omega^2\phi_1-\mu_0\nabla^2\phi_1-\Psi_1)\right]\vec{a}_\theta$$

$$+\left[-\frac{\partial}{\partial\theta}(-\rho_0\omega^2\phi_1-\mu_0\nabla^2\phi_1-\Psi_1)\right]\vec{a}_\phi$$

$$+\nabla\times\left\{\left[\frac{1}{\sin\theta}\frac{\partial}{\partial\phi}(-\rho_0\omega^2\phi_2-\mu_0\nabla^2\phi_2-\Psi_2)\right]\vec{a}_\theta\right.$$

$$\left.+\left[-\frac{\partial}{\partial\theta}(-\rho_0\omega^2\phi_2-\mu_0\nabla^2\phi_2-\Psi_2)\right]\vec{a}_\phi\right\}$$

$$= 0 \qquad \text{(II.21)}$$

So we see that it is sufficient to solve for

$$-\rho_0\omega^2\Phi-(\lambda_0+2\mu_0)\nabla^2\Phi = \Psi \qquad \text{(II.22)}$$

$$-\rho_0\omega^2\phi_1-\mu_0\nabla^2\phi_1 = \Psi_1 \qquad \text{(II.23)}$$

$$-\rho_0\omega^2\phi_2 - \mu_0\nabla^2\phi_2 = \Psi_2 \qquad \text{(II.24)}$$

In the case we are studying we have

$$\Psi = P_n^m(\cos\theta)\cos m\phi\,\ell(r)$$

$$\Psi_1 = 0$$

$$\Psi_2 = P_n^m(\cos\theta)\cos m\phi\, p(r)$$

So we must conclude that

$$\phi_1 = 0 \tag{II.25}$$

that is, no torsional waves are generated. If we let

$$\Phi = P_n^m(\cos\theta)\cos m\phi\, g(r)$$

$$\phi_2 = P_n^m(\cos\theta)\cos m\phi\, g_2(r)$$

and use eq. 7 we obtain

$$P_n^m(\cos\theta)\cos m\phi\left[\frac{1}{r^2}\frac{\partial}{\partial r}r^2\frac{\partial g}{\partial r} + \left[k_\alpha^2 - \frac{n(n+1)}{r^2}\right]g\right]$$

$$= -P_m^n(\cos\theta)\,\frac{\cos m\phi\,\ell(r)}{\lambda_0+2\mu_0} \tag{II.26}$$

and

$$P_n^m(\cos\theta)\cos m\phi\left[\frac{1}{r^2}\frac{\partial}{\partial r}r^2\frac{\partial}{\partial r}g_2+\left[k_\beta^2-\frac{(n)(n+1)}{r^2}\right]g_2\right]$$

$$= - P_n^m(\cos\theta)\frac{\cos m\phi}{\mu_0}\, p(r) \qquad \text{(II.27)}$$

which reduces to

$$\frac{1}{r^2}\frac{\partial}{\partial r}r^2\frac{\partial}{\partial r}g+\left[k_\alpha^2-\frac{n(n+1)}{r^2}\right]g = -\frac{\ell(r)}{\lambda_0+2\mu_0} \qquad \text{(II.28)}$$

and

$$\frac{1}{r^2}\frac{\partial}{\partial r}r^2\frac{\partial}{\partial r}g_2+\left[k_\beta^2-\frac{n(n+1)}{r^2}\right]g_2=-\frac{p(r)}{\mu_0} \qquad \text{(II.29)}$$

These two equations can be solved by the same procedure. Indeed let N be such that

$$\frac{1}{r^2}\frac{\partial}{\partial r}r^2\frac{\partial N}{\partial r}+\left[k_\alpha^2-\frac{(n)(n+1)}{r^2}\right]N = -\delta(r-b_0) \qquad \text{(II.30)}$$

Then we obtain, under the conditions that the solution be finite at r = 0 and radiating at $r \to \infty$

$$N(r,b_0) = -\frac{k_\alpha b_0^2}{i} j_n(k_\alpha b_0) h_n(k_\alpha r) \qquad \text{for } r > b_0$$

$$= -\frac{k_\alpha b_0^2}{i} h_n(k_\alpha b_0) j_n(k_\alpha r) \qquad \text{for } r < b_0 \tag{II.31}$$

where j_n, k_n are the spherical Bessel functions defined by

$$h_n(kr) = \frac{e^{ikr}}{ikr} i^{-n} \sum_{m=0}^{n} \frac{(n+m)!}{m!(n-m)!} \left(\frac{i}{2kr}\right)^m \tag{II.32}$$

and

$$j_n(kr) = \frac{h_n(kr) + \overline{h_n(kr)}}{2} \tag{II.33}$$

where the bar indicates the complex conjugate. The solution to equation 28 is then given by

$$g(r,r_0) = \int_0^\infty N(r,b_0) \frac{\ell(b_0,r_0)}{\lambda_0+2\mu_0} db_0 \tag{II.34}$$

In the same way if we let

$$M(r,b_0) = -\frac{k_\beta b_0^2}{i} j_n(k_\beta b_0) h_n(k_\beta r) \qquad \text{for } r > b_0$$

$$= -\frac{k_\beta b_0^2}{i} h_n(k_\beta b_0) j_n(k_\beta r) \qquad \text{for } r < b_0 \tag{II.35}$$

then

$$g_2(r,r_0) = \int_0^\infty M(r,b_0)\ \frac{p(b_0,r_0)}{\mu_0}\, db_0 \qquad \text{(II.36)}$$

If we perform these integrations by making liberal use of spherical Bessel function identities as they appear for example in Morse and Feshbach (1953) then we obtain

$$g = -\frac{Ar_0^2}{i(\lambda_0+2\mu_0)}\ \frac{dj_n(k_\alpha r_0)}{dk_\alpha r_0}\ h_n(k_\alpha r) - \frac{An}{(2n+1)}\ \frac{r_0^{n+1}}{\omega^2\rho_0 r^{n+1}}$$

$$- \frac{B(n)(n+1)r_0^2 h_n(k_\alpha r)}{i(\lambda_0+2\mu_0)}\ \frac{j_n(k_\alpha r_0)}{k_\beta r_0} + \frac{n(n+1)Br_0^{n+1}}{(2n+1)\omega^2\rho_0 r^{n+1}}$$

$$\text{for } r > r_0 \qquad \text{(II.37)}$$

$$= -\frac{Ar_0^2 j_n(k_\alpha r)}{i(\lambda_0+2\mu_0)}\ \frac{dh_n(k_\alpha r_0)}{dk_\alpha r_0} + \frac{A(n+1)r^n}{(2n+1)r_0^n\omega^2\rho_0}$$

$$- \frac{B(n)(n+1)}{i(\lambda_0+2\mu_0)}\ r_0^2 j_n(k_\alpha r)\ \frac{h_n(k_\alpha b_0)}{k_\alpha b_0} - \frac{B(n)(n+1)r^n}{(2n+1)r_0^n\omega^2\rho_0}$$

$$\text{for } r < r_0 \qquad \text{(II.38)}$$

and

$$g_2 = -Ar_0^2 \frac{h_n(k_\beta r)}{i\mu_0} \frac{j_n(k_\beta r_0)}{k_\beta r_0} - \frac{Ar_0^{n+1}}{(2n+1)r^{n+1}\omega^2\rho_0}$$

$$- \frac{Br_0^2}{i\mu_0} h_n(k_\beta r)\left(\frac{j_n(k_\beta r_0)}{k_\beta r_0} + \frac{dj_n(k_\beta r_0)}{dk_\beta r_0}\right)$$

$$+ \frac{(n+1)Br_0^{n+1}}{(2n+1)\omega^2\rho_0 r^{n+1}} \quad \text{for } r > r_0 \qquad \text{(II.39)}$$

$$= - Ar_0 \frac{j_n(k_\beta r)}{i\mu_0} \frac{h_n(k_\beta r_0)}{k_\beta r_0} - \frac{Ar^n}{(2n+1)r_0^n\omega^2\rho_0}$$

$$- \frac{Br_0^2}{i\mu_0} j_n(k_\beta r)\left[\frac{h_n(k_\beta r_0)}{k_\beta r_0} + \frac{dh_n(k_\beta r_0)}{dk_\beta r_0}\right]$$

$$+ \frac{n}{(2n+1)} \frac{Br^n}{r_0^n\omega^2\rho_0} \quad \text{for } r < r_0 \qquad \text{(II.40)}$$

The displacement field contained in these potentials is given by

$$\vec{s}_{11\omega} = \nabla\Phi + \nabla\times\nabla\times\vec{a}_r r\phi_2$$

$$= \vec{a}_r\left[P_n^m(\cos\theta)\cos m\phi\left[\frac{\partial g}{\partial r} + \frac{n(n+1)g_2}{r}\right]\right]$$

$$+\vec{a}_\theta\left[\frac{\partial}{\partial\theta}P_n^m(\cos\theta)\cos m\phi\left[\frac{g}{r} + \frac{1}{r}\frac{\partial r}{\partial r}g_2\right]\right]$$

$$+\vec{a}_\phi\left[\frac{P_n^m(\cos\theta)}{\sin\theta}\frac{\partial\cos m\phi}{\partial\phi}\left[\frac{g}{r} + \frac{1}{r}\frac{\partial r g_2}{\partial r}\right]\right] \qquad \text{(II.41)}$$

By substituting g and g_2 in the expression for the displacement, the reader may verify that no contribution to the motion comes from the underlined terms in g and g_2.

We can therefore neglect these terms in the expression of the potential and we finally obtain that the displacement solution of eq. 1 can be written as

$$\vec{s}_{1\omega} = \nabla K + \nabla\times\nabla\times\vec{a}_r rH$$

where K and H are given in 2.46 and 2.47.

APPENDIX III

Transformation of Ψ_2^B

We can recast the shear potential coming from the body perturbation in a more convenient form. Indeed we have

$$\psi_2^B = \frac{P_n^m(\cos\theta)}{i\mu_0} \cos m\phi \; h_n(k_\beta r)\cdot$$

$$\int_a^{r_f} -\Big\{\Big[-\rho^1_{nm}\Big(\frac{\lambda_0+2\mu_0}{\rho_0}\Big)+2\mu^1_{nm}+\lambda^1_{nm}\Big]\frac{\partial}{\partial r_0}\,\frac{1}{r_0^2}\,\frac{\partial r_0^2 s^0_{r_0\omega}}{\partial r_0}$$

$$+\,\frac{2\partial\mu^1_{nm}}{\partial r_0}\,\frac{\partial s^0_{r_0\omega}}{\partial r_0}+\frac{\partial\lambda^1_{nm}}{\partial r_0}\,\frac{1}{r_0^2}\,\frac{\partial r_0^2 s^0_{r_0\omega}}{\partial r_0}\Big\} r_0^2\,\frac{j_n(k_\beta r_0)}{k_\beta r_0}$$

$$-\Big[\underline{\frac{2\mu^1_{nm}}{r_0^2}\,s^0_{r_0\omega}}+\underline{\frac{\lambda^1_{nm}}{r_0^2}}\,\frac{\partial r_0^2 s^0_{r_0\omega}}{\partial r_0}\Big] r_0^2\Big(\frac{j_n(k_\beta r_0)}{k_\beta r_0}$$

$$+\,\underline{\frac{dj_n(k_\beta r_0)}{dk_\beta r_0}}\Big)\,dr_0$$

If we integrate by parts the underlined terms in the integral we obtain

$$\psi_2^B = \frac{-P_n^m(\cos\theta)\cos m\phi}{i\mu_0} h_n(k_\beta r)$$

$$\left\{\left[\frac{2\mu_{nm}^1 s_{r_0\omega}^0}{r_0^2} + \frac{\lambda_{nm}^1}{r_0^2}\frac{\partial r_0^2 s_{r_0\omega}^0}{\partial r_0}\right]_{r_0} \frac{j_n(k_\beta r_0)}{k_\beta}\right\}\Bigg|_a^{r_f}$$

$$+ \frac{P_n^m(\cos\theta)\cos m\phi}{i\mu_0} h_n(k_\beta r)$$

$$\int_a^{r_f} \Big\{ -\left[-\rho_{nm}^1\left(\frac{\lambda_0+2\mu_0}{\rho_0}\right)+2\mu_{nm}^1\right]\frac{\partial}{\partial r_0}\left(\frac{\partial r_0^2 s_{r_0\omega}^0}{\partial r_0}\right)$$

$$-2r_0^2\left[\frac{\partial}{\partial r_0}\left(\frac{s_{r_0\omega}^0}{r_0}\right)\right]\left[\frac{\partial}{\partial r_0}\left(\frac{\mu_{nm}^1}{r_0}\right)\right]\Big\}\frac{r_0^2 j_n(k_\beta r_0)}{k_\beta r_0}\, dr_0$$

APPENDIX IV

The Body Perturbation for n = 0

We would like to find the displacement field $\vec{s}_{11}$ in the special case where the parameters distributions vary only with r, i.e.

$$(\rho_1,\mu_1,\lambda_1) = (\rho_{00}(r),\mu_{00}(r),\lambda_{00}(r)).$$

Let

$$(\vec{s}_{11},\tilde{\tilde{S}}_{11},s^0_r) \leftrightarrow (\vec{s}_{11\omega},\tilde{\tilde{S}}_{11\omega},s^0_{r\omega})$$

then we have to solve

$$-\rho_0\omega^2\vec{s}_{11\omega}-2\mu_0\nabla\cdot\tilde{\tilde{S}}_{11\omega}-\lambda_0\nabla\cdot|\tilde{\tilde{S}}_{11\omega}|\tilde{\tilde{I}}$$

$$= \left[-\rho^1_{00}\left(\frac{\lambda_0+2\mu_0}{\rho_0}\right)+ 2\mu_{00}+\lambda_{00}\right]\frac{\partial}{\partial r}\frac{1}{r^2}\frac{\partial r^2 s^0_{r\omega}}{\partial r}\vec{a}_r$$

$$+ 2\frac{\partial\mu_{00}}{\partial r}\frac{\partial s^0_{r\omega}}{\partial r}\vec{a}_r + \frac{\partial\lambda_{00}}{\partial r}\frac{1}{r^2}\frac{\partial r^2 s^0_{r\omega}}{\partial r}\vec{a}_r \qquad \text{(IV.1)}$$

First, let us find the Green function $\vec{s}^g_{11\omega}$ solution of

$$-\rho_0\omega^2\vec{s}^g_{11\omega}- 2\mu_0\nabla\cdot\tilde{\tilde{S}}^g_{11} -\lambda_0\nabla\cdot|\tilde{\tilde{S}}^g_{11\omega}|\tilde{\tilde{I}}$$

$$= A\delta(r-r_0)\vec{a}_r \equiv \vec{F} \qquad \text{(IV.2)}$$

Potential representation

Since $\nabla\times\vec{F} = 0$ we can represent the body force as the gradient of a scalar, i.e.

$$A\delta(r-r_0)\vec{a}_r = \nabla\Psi \tag{IV.3}$$

$$= \frac{\partial}{\partial r}\Psi \tag{IV.4}$$

this last equation being obtained because of the spherical symmetry of the body force.

The solution is

$$\Psi = C_1 \text{ (constant)} \quad \text{for } r < r_0 \tag{IV.5}$$

$$= C_2 \text{ (constant)} \quad \text{for } r > r_0 \tag{IV.6}$$

and we obtain

$$C_2 - C_1 = A$$

by integrating the equation around r_0. So we find

$$\Psi = C_2 - A \quad \text{for } r < r_0 \tag{IV.7}$$

$$= C_2 \quad \text{for } r > r_0 \tag{IV.8}$$

Green's function

We can write eq. 2 as

$$-\rho_0\omega^2 s^g_{r11\omega} - (\lambda_0+2\mu_0)\ \frac{\partial}{\partial r}\ \frac{1}{r^2}\ \frac{\partial r^2 s^g_{r11\omega}}{\partial r} = \frac{\partial \Psi}{\partial r} \qquad \text{(IV.9)}$$

Let

$$s^g_{r11\omega} = \frac{\partial \phi}{\partial r}$$

and integrate eq. 9 with respect to r. We obtain

$$-\rho_0\omega^2\phi - (\lambda_0+2\mu_0)\ \frac{1}{r^2}\ \frac{\partial r^2}{\partial r}\ \frac{\partial \phi}{\partial r} = \Psi + C_3 \qquad \text{(IV.10)}$$

where C_3 is an arbitrary constant. The solution to

$$\frac{1}{r^2}\ \frac{\partial}{\partial r}\ r^2\ \frac{\partial N}{\partial r} + k_\alpha^2 N = -\ \frac{B}{\lambda_0+2\mu_0}\ \delta(r-b_0) \qquad \text{(IV.11)}$$

subject to the radiation condition at infinity and finiteness of the field at r = 0 is

$$N(b_0,r) = -\ \frac{Bk_\alpha b_0^2}{i(\lambda_0+2\mu_0)} j_0(k_\alpha b_0) h_0(k_\alpha r) \quad \text{for } r > b_0$$

$$= -\ \frac{Bk_\alpha b_0^2}{i(\lambda_0+2\mu_0)}\ h_0(k_\alpha b_0) j_0(k_\alpha r) \quad \text{for } r < b_0$$

(IV.12)

where k_0, j_0 are the spherical Bessel function of order zero as defined in Appendix II. So we have

$$\phi = \int_0^r -(\Psi+C_3)\ \frac{k_\alpha b_0^2}{i(\lambda_0+2\mu_0)}\ j_0(k_\alpha b_0)h_0(k_\alpha r)db_0$$

$$+\int_r^\infty -(\Psi+C_3)\ \frac{k_\alpha b_0^2}{i(\lambda_0+2\mu_0)} h_0(k_\alpha b_0)j_0(k_\alpha r)db_0 \qquad ((V.13)$$

Making use of the spherical Bessel function identities we obtain

$$\phi = \frac{Ar_0^2}{i(\lambda_0+2\mu_0)}\ j_1(k_\alpha r_0)h_0(k_\alpha r)\ -\ \frac{(C_2+C_3)}{\omega^2\rho_0}$$

$$\text{for } r > r_0 \qquad (IV.14)$$

$$= \frac{Ar_0^2}{i(\lambda_0+2\mu_0)}\ h_1(k_\alpha r_0)j_1(k_\alpha r)\ +\ \frac{A}{\omega^2\rho_0}\ -\ \frac{(C_2+C_3)}{\omega^2\rho_0}$$

$$(IV.15)$$

but since

$$s^g_{r11\omega} = \frac{\partial\phi}{\partial r}$$

all the constant terms in the expression of the potential do not contribute to the motion. So we can write.

$$\vec{s}^{g}_{11} = \nabla K \tag{IV.16}$$

where

$$K = \frac{Ar_0^2}{i(\lambda_0+2\mu_0)} j_1(k_\alpha r_0) h_0(k_\alpha r) \quad \text{for } r > r_0 \tag{IV.17}$$

$$= \frac{Ar_0^2}{i(\lambda_0+2\mu_0)} h_1(k_\alpha r_0) j_0(k_\alpha r) \quad \text{for } r < r_0 \tag{IV.18}$$

The reader may verify these formulae by the checking process outlined in Chapter II. Making use of this Green's function, we can therefore write that the solution of eq. 1 for a point outside the inhomogeneity ($r > r_f$) is

$$\vec{s}_{11\omega} = \nabla \psi^B \tag{IV.19}$$

where

$$\psi^B = \frac{h_0(k_\alpha r)}{i(\lambda_0+2\mu_0)} \int_a^{r_f} \left\{ \left[-\rho_{00} \left(\frac{\lambda_0+2\mu_0}{\rho_0} \right) + 2\mu_{00} + \lambda_{00} \right] \cdot \right.$$

$$\frac{\partial}{\partial r_0} \frac{1}{r_0^2} \frac{\partial r_0^2 s^0_{r_0\omega}}{\partial r_0} + 2\frac{\partial \mu_{00}}{\partial r_0} \frac{\partial s^0_{r_0\omega}}{\partial r_0}$$

$$\left. + \frac{\partial \lambda_{00}}{\partial r_0} \frac{1}{r_0^2} \frac{\partial r_0^2 s^0_{r_0\omega}}{\partial r_0} \right\} r_0^2 j_1(k_\alpha r_0) dr_0 \tag{IV.20}$$

APPENDIX V

The Surface Perturbation

We have to find the scattered wave caused by the inhomogeneous value of the parameters around the source, i.e. we have to solve for r > a

$$-\rho_0\omega^2\vec{s}_{12\omega} - 2\mu_0\nabla\cdot\tilde{\tilde{S}}_{12} - \lambda_0\nabla\cdot|\tilde{\tilde{S}}_{12\omega}|\tilde{\tilde{I}} = 0 \qquad (V.1)$$

and for r < a

$$-\rho_0\omega^2\vec{s}_{12\omega} - 2\mu_0\nabla\cdot\tilde{\tilde{S}}_{12} - \lambda_0\nabla\cdot|\tilde{\tilde{S}}_{12\omega}|\tilde{\tilde{I}} = 0 \qquad (V.2)$$

subject to the boundary conditions at r = a

$$2\mu_0\vec{a}_r\cdot\cdot\tilde{\tilde{S}}_{12\omega} + \lambda_0\vec{a}_r\cdot\cdot|\tilde{\tilde{S}}_{12\omega}|\tilde{\tilde{I}}\Big|_{r=a^-}$$

$$= 2\mu_0\vec{a}_r\cdot\cdot\tilde{\tilde{S}}_{12\omega} + \lambda_0\vec{a}_r\cdot\cdot|\tilde{\tilde{S}}_{12\omega}|\tilde{\tilde{I}}$$

$$+ 2\mu_1\vec{a}_r\cdot\cdot\tilde{\tilde{S}}_{0\omega} + \lambda_1\vec{a}_r\cdot\cdot|\tilde{\tilde{S}}_{0\omega}|\tilde{\tilde{I}}\Big|_{r=a^+} \qquad (V.3)$$

$$\vec{s}_{12}\Big|_{r=a^-} = \vec{s}_{12}\Big|_{r=a^+} \qquad (V.4)$$

where we have set

$$(\vec{s}_{12}, \tilde{\tilde{S}}_{12}, \vec{s}^{-}_{12}, \tilde{\tilde{S}}^{-}_{12}, \tilde{\tilde{S}}_{0}) \leftrightarrow (\vec{s}_{12\omega}, \tilde{\tilde{S}}_{12\omega}, \vec{s}^{-}_{12\omega}, \tilde{\tilde{S}}_{12\omega}, \tilde{\tilde{S}}_{0\omega})$$

as the Fourier transform pairs. As shown in Appendix II, the general solution of eq. 1 and 2 can be expressed as

$$\vec{s}_{12\omega} = \nabla\psi^{+} + \nabla\times\vec{a}_r r\psi_1^{+} + \nabla\times\nabla\times\vec{a}_r r\psi_2^{+} \tag{V.5}$$

and

$$\vec{s}^{-}_{12} = \nabla\psi^{-} + \nabla\times\vec{a}_r r\psi_1^{-} + \nabla\times\nabla\times\vec{a}_r r\psi_2^{-} \tag{V.6}$$

where the potential are solutions of

$$-\rho_0\omega^2(\psi^{+},\psi^{-}) - (\lambda_0+2\mu_0)\nabla^2(\psi^{+},\psi^{-}) = 0 \tag{V.7}$$

and

$$-\rho_0\omega^2(\psi_1^{+},\psi_2^{+},\psi_1^{-},\psi_2^{-}) - \mu_0\nabla^2(\psi_1^{+},\psi_2^{+},\psi_1^{-},\psi_2^{-}) = 0 \tag{V.8}$$

We can write our boundary conditions as follows

$$2\mu_0\frac{\partial s^{-}_{r12\omega}}{\partial r} + \lambda_0\nabla\cdot\vec{s}^{-}_{12\omega}\Big|_{r=a^{-}} = 2\mu_0\frac{\partial s_{r12\omega}}{\partial r} + \lambda_0\nabla\cdot\vec{s}_{12\omega} + 2\mu_1\frac{\partial s^{0}_{r\omega}}{\partial r} + \lambda_1\nabla\cdot\vec{s}^{0}_{\omega}\Big|_{r=a^{+}} \tag{V.9}$$

$$\left[\frac{1}{r}\frac{\partial s^{-}_{r12\omega}}{\partial\theta} + r\frac{\partial s^{-}_{\theta 12\omega}}{\partial r}\right]_{r=a^{-}} = \left[\frac{1}{r}\frac{\partial s_{r12\omega}}{\partial\theta} + r\frac{\partial s_{\theta 12\omega}}{\partial r}\right]_{r=a^{+}} \tag{V.10}$$

$$\left[\frac{1}{r \sin\theta}\frac{\partial s^{-}_{r12\omega}}{\partial\phi} + r\frac{\partial}{\partial r}\frac{s^{-}_{\phi 12\omega}}{r}\right|_{r=a^{-}}$$

$$= \left[\frac{1}{r \sin\theta}\frac{\partial s_{r12\omega}}{\partial\phi} + r\frac{\partial}{\partial r}\frac{s_{\phi 12\omega}}{r}\right|_{r=a^{+}} \qquad (V.11)$$

and

$$\vec{s}^{-}_{12\omega}\Big|_{r=a^{-}} = \vec{s}_{12\omega}\Big|_{r=a^{+}} \qquad (V.12)$$

or, if we use the potential representation, the stress conditions are

$$2\mu_0\frac{\partial}{\partial r}\left(\frac{\partial\psi^{-}}{\partial r} + \frac{1}{r\sin\theta}\left[-\frac{\partial}{\partial\theta}\sin\theta\frac{\partial\psi^{-}_2}{\partial\theta} - \frac{1}{\sin\theta}\frac{\partial^2\psi_2}{\partial\phi^2}\right]\right)$$

$$+\lambda_0\nabla\cdot\nabla\psi^{-}\Big|_{r=a^{-}} = 2\mu_0\frac{\partial}{\partial r}\left(\frac{\partial\psi^{+}}{\partial r} + \frac{1}{r\sin\theta}\cdot\right.$$

$$\left.\left[\frac{\partial}{\partial\theta}\sin\theta\frac{\partial\psi^{+}_2}{\partial\theta} - \frac{1}{\sin\theta}\frac{\partial^2\psi^{+}_2}{\partial\phi^2}\right]\right) + \lambda_0\nabla^2\psi^{+}$$

$$+2\mu_1\frac{\partial s^{}_{r\omega}}{\partial r} + \frac{\lambda_1}{r^2}\frac{\partial r^2\vec{s}^{0}_{\omega}}{\partial r}\Big|_{r=a^{+}} \qquad (V.13)$$

$$\frac{1}{r}\frac{\partial}{\partial\theta}\left(\frac{\partial\psi^-}{\partial r}+\frac{1}{r\sin\theta}\left[-\frac{\partial}{\partial\theta}\sin\theta\frac{\partial\psi_2^-}{\partial\theta}-\frac{1}{\sin\theta}\frac{\partial^2\psi_2^-}{\partial\phi^2}\right]\right)$$

$$+r\frac{\partial}{\partial r}\frac{1}{r}\left(\frac{1}{r}\frac{\partial\psi^-}{\partial\theta}+\frac{1}{r}\left[\frac{1}{\sin\theta}\frac{\partial r\psi_1^-}{\partial\phi}+\frac{\partial}{\partial r}r\frac{\partial\psi_2^-}{\partial\theta}\right]\right)\Bigg|_{r=a^-}$$

$$=\frac{1}{r}\frac{\partial}{\partial\theta}\left(\frac{\partial\psi^+}{\partial r}+\frac{1}{r\sin\theta}\left[-\frac{\partial}{\partial\theta}\sin\theta\frac{\partial\psi_2^+}{\partial\theta}-\frac{1}{\sin\theta}\frac{\partial^2\psi_2^+}{\partial\phi^2}\right]\right)$$

$$+r\frac{\partial}{\partial r}\frac{1}{r}\left(\frac{1}{r}\frac{\partial\psi^+}{\partial\theta}+\frac{1}{r}\left[\frac{1}{\sin\theta}\frac{\partial r\psi_1^+}{\partial\phi}+\frac{\partial}{\partial r}r\frac{\partial\psi_2^+}{\partial\theta}\right]\right)\Bigg|_{r=a^+}$$

(IV.14)

$$\frac{1}{r\sin\theta}\frac{\partial}{\partial\phi}\left(\frac{\partial\psi^-}{\partial r}+\frac{1}{r\sin\theta}\left[-\frac{\partial}{\partial\theta}\sin\theta\frac{\partial\psi_2^-}{\partial\theta}-\frac{1}{\sin\theta}\frac{\partial^2\psi_2^-}{\partial\phi^2}\right]\right)$$

$$+r\frac{\partial}{\partial r}\frac{1}{r}\left(\frac{1}{r\sin\theta}\frac{\partial\psi^-}{\partial\phi}+\frac{1}{r}\left[\frac{\partial}{\partial r}\frac{r}{\sin\theta}\frac{\partial\psi_2^-}{\partial\phi}-\frac{\partial}{\partial\theta}r\psi_1^-\right]\right)\Bigg|_{r=a^-}$$

$$=\frac{1}{r\sin\theta}\frac{\partial}{\partial\phi}\left(\frac{\partial\psi^+}{\partial r}+\frac{1}{r\sin\theta}\left[-\frac{\partial}{\partial\theta}\sin\theta\frac{\partial\psi_2^+}{\partial\theta}-\frac{1}{\sin\theta}\frac{\partial^2\psi_2^+}{\partial\phi^2}\right]\right)$$

$$+r\frac{\partial}{\partial r}\frac{1}{r}\left(\frac{1}{r\sin\theta}\frac{\partial\psi^+}{\partial\phi}+\frac{1}{r}\left[\frac{\partial}{\partial r}\frac{r}{\sin\theta}\frac{\partial\psi_2^+}{\partial\phi}-\frac{\partial r}{\partial\theta}\psi_1^+\right]\right)\Bigg|_{r=a^+}$$

(V.15)

and the continuity of displacement reads

$$\frac{\partial \psi^-}{\partial r} + \frac{1}{r \sin\theta}\left[-\frac{\partial}{\partial\theta}\sin\theta\,\frac{\partial \psi_2^-}{\partial\theta} - \frac{1}{\sin\theta}\,\frac{\partial^2 \psi_2^-}{\partial\phi^2}\right]\Bigg|_{r=a^-}$$

$$= \frac{\partial \psi^+}{\partial r} + \frac{1}{r \sin\theta}\left[-\frac{\partial}{\partial\theta}\sin\theta\,\frac{\partial \psi_2^+}{\partial\theta} - \frac{1}{\sin\theta}\,\frac{\partial^2 \psi_2^+}{\partial\phi^2}\right]\Bigg|_{r=a^+} \tag{V.16}$$

$$\frac{1}{r}\frac{\partial \psi^-}{\partial\theta} + \frac{1}{r}\left[\frac{1}{\sin\theta}\,\frac{\partial r\psi_1^-}{\partial\phi} + \frac{\partial}{\partial r}\,r\,\frac{\partial \psi_2^-}{\partial\theta}\right]\Bigg|_{r=a^-}$$

$$= \frac{1}{r}\frac{\partial \psi^+}{\partial\theta} + \frac{1}{r}\left[\frac{1}{\sin\theta}\,\frac{\partial r\psi_1^+}{\partial\phi} + \frac{\partial}{\partial r}r\,\frac{\partial \psi_2^+}{\partial\theta}\right]\Bigg|_{r=a^+} \tag{V.17}$$

$$\frac{1}{r \sin\theta}\,\frac{\partial \psi^-}{\partial\phi} + \frac{1}{r}\left[\frac{\partial}{\partial r}\,\frac{r}{\sin\theta}\,\frac{\partial \psi_2^-}{\partial\phi} - \frac{\partial}{\partial\theta}\,r\psi_1^-\right]\Bigg|_{r=a^-}$$

$$= \frac{1}{r \sin\theta}\,\frac{\partial \psi^+}{\partial\phi} + \frac{1}{r}\left[\frac{\partial}{\partial r}\,\frac{r}{\sin\theta}\,\frac{\partial \psi_2^+}{\partial\phi} - \frac{\partial r}{\partial\theta}\,\psi_1^+\right]\Bigg|_{r=a^+}$$

(V.18)

First, I would like to show that no torsional waves are generated at the boundary r = a.

We remark that since the above conditions hold all along the surface r = a, we can take the derivative of them with

respect to θ and ϕ. If we operate on eq. 15 with $\frac{\partial}{\partial\theta}\sin\theta$ and on eq. 14 with $\frac{\partial}{\partial\phi}$ and subtract the results, we obtain

$$\frac{\partial}{\partial\theta}\sin\theta\,\frac{\partial}{\partial\theta}\,r\,\frac{\partial}{\partial r}\,\frac{\psi_1^-}{r}+\frac{1}{\sin\theta}\,\frac{\partial^2}{\partial\phi^2}\,r\,\frac{\partial}{\partial r}\,\frac{\psi_1^-}{r}\Bigg|_{r=a^-}$$

$$=\frac{\partial}{\partial\theta}\sin\theta\,\frac{\partial}{\partial\theta}\,r\,\frac{\partial}{\partial r}\,\frac{\psi_1^+}{r}+\frac{1}{\sin\theta}\,\frac{\partial^2}{\partial\phi^2}\,r\,\frac{\partial}{\partial r}\,\frac{\psi_1^+}{r}\Bigg|_{r=a^+} \tag{V.19}$$

Performing the same operation on eq. 7 and 6 respectively, we obtain

$$\frac{\partial}{\partial\theta}\sin\theta\,\frac{\partial}{\partial\theta}\,\psi_1^-+\frac{1}{\sin\theta}\,\frac{\partial^2\psi_1^-}{\partial\phi^2}\Bigg|_{r=a^-}$$

$$=\frac{\partial}{\partial\theta}\sin\theta\frac{\partial\psi_1^+}{\partial\theta}-\frac{1}{\sin\theta}\,\frac{\partial^2\psi_1^+}{\partial\phi^2}\Bigg|_{r=a^+} \tag{V.20}$$

Let us consider an arbitrary harmonic of (ψ_1^-,ψ_1^+) solution of eq. 8, i.e.

$$\psi_1^- = a_{n_-,m_-}P_{n^-}^{m^-}(\cos\theta)\cos m_-\phi j_{n_-}(k_\beta r)$$

$$\psi_1^+ = b_{nm}P_n^m(\cos\theta)\cos m\phi k_n(k_\beta r)$$

where the radial functions are chosen so as to satisfy the radiation condition at ∞, and the finiteness of the field at the origin.

If we employ Legendre's equation (see Appendix II, eq. 7) and the orthogonality of the Legendre's polynomials in eq. 19, 20 we obtain that

$$(n_-, m_-) = (n, m)$$

and

$$a_{nm} \frac{\partial}{\partial r} j_n(k_\beta r)\Big|_{r=a^-} = b_{nm} \frac{\partial}{\partial r} h_n(k_\beta r)\Big|_{r=a^+} \qquad \text{(V.21)}$$

$$a_{nm} j_n(k_\beta r)\Big|_{r=a^-} = b_{nm} h_n(k_\beta r)\Big|_{r=a^+} \qquad \text{(V.22)}$$

The only solution of the two last equations being

$$a_{nm} = b_{nm} = 0$$

we see that the surface perturbation does not provide any source of torsional wave. In fact, the only source terms in our equation are contained in eq. 13.

At this point, let us consider a general term in the expansion of our parameters, i.e.

$$(\rho_1(a),\mu_1(a),\lambda_1(a)) = (\rho^1_{nm},\mu^1_{nm},\lambda^1_{nm})P^m_n(\cos\theta)\cos m\phi$$

for $n > 0$

The case $n = 0$ will be treated later. Then eq. 13 can be written as

$$2\mu_0 \frac{\partial}{\partial r}\left(\frac{\partial}{\partial r}\psi^- + \frac{1}{r\sin\theta}\left[-\frac{\partial}{\partial\theta}\sin\theta\frac{\partial\psi_2^-}{\partial\theta} - \frac{1}{\sin\theta}\frac{\partial^2\psi_2^-}{\partial\phi^2}\right]\right.$$

$$\left. +\lambda_0\nabla^2\psi^-\right|_{r=a^-} = 2\mu_0 \frac{\partial}{\partial r}\left(\frac{\partial\psi^+}{\partial r} + \frac{1}{r\sin\theta}\left[-\frac{\partial}{\partial\theta}\sin\theta\frac{\partial\psi_2^+}{\partial\theta}\right.\right.$$

$$\left.\left. -\frac{1}{\sin\theta}\frac{\partial^2\psi_2^+}{\partial\phi^2}\right]\right) +\lambda_0\nabla^2\psi^+ + 2\mu^1_{nm}P^m_n(\cos\theta)\cos m\phi\frac{\partial s^0_{r\omega}}{\partial r}$$

$$+\lambda^1_{nm}P^m_n(\cos\theta)\cos m\phi\nabla\cdot\vec{s}^0_\omega \qquad (V.23)$$

The reader may verify that the source terms are orthogonal to all the spheroidal waves $(\psi^-,\psi_2,\psi^+,\psi_2^+)$ except the one which can be expressed as

$$\psi^+ = P^m_n(\cos\theta)\cos m\phi\, Ah_n(k_\alpha r)$$

$$\psi_2^+ = P^m_n(\cos\theta)\cos m\phi\, Bh_n(k_\beta r)$$

$$\psi^{-} = P_n^m(\cos\theta)\cos m\phi \; Cj_n(k_\alpha r)$$

$$\psi_2^{-} = P_n^m(\cos\theta)\cos m\phi \; Dj_n(k_\beta r)$$

The choice of the radial function is guided by the condition that the wave should be outgoing at infinity and finite at the origin.

By replacing these functions in equations 13 to 18, and using Legendre's equation and several spherical Bessel function identities we finally obtain that

$$\vec{s}_{12\omega} = \nabla\psi^s + \nabla\times\nabla\times\vec{a}_r r\psi_2^s \qquad \text{(V.24)}$$

where

$$(\psi^s, \psi_2^s) \equiv (\psi^+, \psi_2^+)$$

and

$$\psi^s = \frac{-P_n^m(\cos\theta)\cos m\phi \; h_n(k_\alpha r)}{i(\mu_0+2\lambda_0)} \left(2\mu_{nm}^1 \frac{\partial s_{a\omega}^0}{\partial a} + \frac{\lambda_{nm}^1}{a^2} \frac{\partial a^2 s_{a\omega}^0}{\partial a}\right) \cdot$$

$$a^2 \frac{dj_n(k_\alpha a)}{dk_\alpha a} \qquad \text{(V.25)}$$

$$\psi_2^s = \frac{-P_n^m(\cos\theta)\cos m\phi \; h_n(k_\beta r)}{i\mu_0} \left(2\mu_{nm}^1 \frac{\partial s_{a\omega}^0}{a} + \frac{\lambda_{nm}^1}{a^2} \frac{\partial a^2 s_{a\omega}^0}{\partial a}\right) \cdot$$

$$a^2 \frac{j_n(k_\beta a)}{k_\beta a} \qquad \text{(V.26)}$$

We still have to consider the special case where the distributions of the parameters vary only with r at the boundary r = a, i.e.

$$(\rho_1(a),\mu_1(a),\lambda_1(a)) = (\rho_{00}(a),\mu_{00}(a),\lambda_{00}(a))$$

In that case no shear waves are generated and we need to consider only the compressional potential.

Following the same argument as before, let

$$\vec{s}^{+}_{12\omega} = \nabla\psi^{s} \qquad \vec{s}^{-}_{12\omega} = \nabla\psi^{-} \tag{V.27}$$

with

$$\psi^{s} = Ak_0(k_\alpha r)$$

$$\psi^{-} = Bj_0(k_\alpha r)$$

subject to the boundary conditions

$$2\mu_0 \frac{\partial^2 B}{\partial r^2} j_0(k_\alpha r) + \lambda_0 \nabla^2 B j_0(k_\alpha r)\Big|_{r=a^-}$$

$$= 2\mu_0 \frac{\partial^2 A}{\partial r^2} h_0(k_\alpha r) + \lambda_0 \nabla^2 A h_0(k_\alpha r)$$

$$+ 2\mu_{00} \frac{\partial s^0_{r\omega}}{\partial r} + \lambda_{00} \frac{1}{r^2} \frac{\partial r^2}{\partial r} s^0_{r\omega}\Big|_{r=a^+} \tag{V.28}$$

and

$$\frac{\partial B j_0(k_\alpha r)}{\partial r} = \frac{\partial}{\partial r} A h_0(k_\alpha r) \tag{V.29}$$

Solving these equations we obtain that

$$\psi_s = \frac{h_0(k_\alpha r)}{i(\lambda_0+2\mu_0)} \left(2\mu_{00} \frac{\partial s^0_{a\omega}}{\partial a} + \lambda_{00} \frac{1}{a^2} \frac{\partial a^2 s^0_{a\omega}}{\partial a}\right) a^2 j_1(k_\alpha a) \tag{V.30}$$

APPENDIX VI

The Scattered Wave when the Receiver is within the Inhomogeneities

When the receiver position, r, is within the inhomogeneous region, i.e. $r < r_f$, we must take into account the wave reflected in $r > r_f$ which reach the seismometer. In that case, we must make full use of the Green's function found in Sect. 2.4.

The displacement field at r, can then be given as

$$\vec{s}_\omega = \nabla\psi + \nabla\times\nabla\times r\vec{a}_r\psi_2$$

where

$$\psi = Gh_0(k_\alpha r) + \varepsilon c_{00}h_0(k_\alpha r) + \varepsilon d_{00}j_0(k_\alpha r)$$

$$+ \sum_{n=1}^{\infty}\sum_{m=0}^{n}(\varepsilon c^1_{nm}\cos m\phi+\varepsilon c^2_{nm}\sin m\phi)h_n(k_\alpha r)P^m_n(\cos\theta)$$

$$+ \sum_{n=1}^{\infty}\sum_{m=0}^{n}(\varepsilon d^1_{nm}\cos m\phi+\varepsilon d^2_{nm}\sin m\phi)j_n(k_\alpha r)P^m_n(\cos\theta)$$

and

$$\psi_2 = \sum_{n=1}^{\infty}\sum_{m=0}^{n}(\varepsilon f^1_{nm}\cos m\phi+\varepsilon f^2_{nm}\sin m\phi)h_n(k_\beta r)P^m_n(\cos\theta)$$

$$+ \sum_{n=1}^{\infty}\sum_{m=0}^{n}(\varepsilon g^1_{nm}\cos m\phi+\varepsilon g^2_{nm}\sin m\phi)j_n(k_\beta r)P^m_n(\cos\theta)$$

where

$Gh_0(k_\alpha r)$ is the zero order solution (VI.1)

$$c_{00} = \frac{1}{i(\lambda_0+2\mu_0)} \left(2\mu_{00}(a) \frac{\partial s^0_{a\omega}}{\partial a} + \frac{\lambda_{00}(a)}{a^2} \frac{\partial a^2 s^0_{a\omega}}{\partial a}\right) a^2 j_1(k_\alpha a)$$

$$+ \frac{1}{i(\lambda_0+2\mu_0)} \int_a^r \left\{ \left[-\rho_{00}\left(\frac{\lambda_0+2\mu_0}{\rho_0}\right) + 2\mu_{00} + \lambda_{00} \right] \frac{\partial}{\partial r_0} \frac{1}{r_0^2} \cdot \right.$$

$$\left. \frac{\partial r_0^2 s^0_{r_0\omega}}{\partial r_0} + 2 \frac{\partial \mu_{00}}{\partial r_0} \frac{\partial s^0_{r_0\omega}}{\partial r_0} + \frac{\partial \lambda_{00}}{\partial r_0} \frac{1}{r_0^2} \frac{\partial r_0^2 s^0_{r_0\omega}}{\partial r_0} \right\} \cdot$$

$$r_0^2 j_1(k_\alpha r_0) dr_0 \qquad \text{(VI.2)}$$

$$d_{00} = \frac{1}{i(\lambda_0+2\mu_0)} \int_r^{r_f} \left\{ \left[-\rho_{00}\left(\frac{\lambda_0+2\mu_0}{\rho_0}\right) + 2\mu_{00} + \lambda_{00} \right] \frac{\partial}{\partial r_0} \frac{1}{r_0^2} \cdot \right.$$

$$\left. \frac{\partial r_0^2 s^0_{r_0\omega}}{\partial r_0} + 2 \frac{\partial \mu_{00}}{\partial r_0} \frac{\partial s^0_{r_0\omega}}{\partial r_0} + \frac{\partial \lambda_{00}}{\partial r_0} \frac{1}{r_0^2} \frac{\partial r_0^2 s^0_{r_0\omega}}{\partial r_0} \right\}$$

$$r_0^2 h_1(k_\alpha r_0) dr_0 \qquad \text{(VI.3)}$$

$$c^{\sigma}_{nm} = -\left(2\mu^{\sigma}_{nm}(a) \frac{\partial s^{0}_{a\omega}}{\partial a} + \frac{\lambda^{\sigma}_{nm}(a)}{a^2} \frac{\partial a^2 s^{0}_{a\omega}}{\partial a} \right) \frac{a^2}{i(\lambda_0+2\mu_0)} \cdot$$

$$\frac{dj_n(k_\alpha a)}{dk_\alpha a} + \frac{1}{i(\lambda_0+2\mu_0)} \int_a^r -\left\{ \left[-\rho^{\sigma}_{nm} \left(\frac{\lambda_0+2\mu_0}{\rho_0} \right) \right.\right.$$

$$\left. + 2\mu^{\sigma}_{nm} + \lambda^{\sigma}_{nm} \right] \frac{\partial}{\partial r_0} \frac{1}{r_0^2} \frac{\partial r_0^2 s^{0}_{r_0\omega}}{\partial r_0} + 2 \frac{\partial \mu^{\sigma}_{nm}}{\partial r_0} \frac{\partial s^{0}_{r_0\omega}}{\partial r_0}$$

$$\left. + \frac{\partial \lambda^{\sigma}_{nm}}{\partial r_0} \frac{1}{r_0^2} \frac{\partial r_0^2 s^{0}_{r_0\omega}}{\partial r_0} \right\} r_0^2 \frac{dj_n(k_\alpha r_0)}{dk_\alpha r_0}$$

$$- \left[\frac{2\mu^{\sigma}_{nm}}{r_0^2} s^{0}_{r_0\omega} + \frac{\lambda^{\sigma}_{nm}}{r_0^3} \frac{\partial r_0^2 s^{0}_{r_0\omega}}{\partial r_0} \right] (n)(n+1) r_0^2 \cdot$$

$$\frac{j_n(k_\alpha r_0)}{k_\alpha r_0} \, dr_0 \qquad \text{(VI.4)}$$

$$d^{\sigma}_{nm} = \frac{1}{i(\lambda_0+2\mu_0)} \int_r^f -\left\{ \left[-\rho_{nm} \left(\frac{\lambda_0+2\mu_0}{\rho_0} \right) + 2\mu^{\sigma}_{nm} + \lambda^{\sigma}_{nm} \right] \frac{\partial}{\partial r_0} \frac{1}{r_0^2} \cdot \right.$$

$$\left. \frac{\partial r_0^2 s^{0}_{r_0\omega}}{\partial r_0} + 2 \frac{\partial \mu^{\sigma}_{nm}}{\partial r_0} \frac{\partial s^{0}_{r_0\omega}}{\partial r_0} + \frac{\partial \lambda^{\sigma}_{nm}}{\partial r_0} \frac{1}{r_0^2} \frac{\partial r_0^2 s^{0}_{r_0\omega}}{\partial r_0} \right\} r_0^2 \frac{dh_n(k_\alpha r_0)}{dk_\alpha r_0}$$

$$- \left[\frac{2\mu^{\sigma}_{nm}}{r_0^2} s^{0}_{r_0\omega} + \frac{\lambda^{\sigma}_{nm}}{r_0^3} \frac{\partial r_0^2 s^{0}_{r_0\omega}}{\partial r_0} \right] (n)(n+1) r_0^2 \frac{h_n(k_\alpha r_0)}{k_\alpha r_0} \, dr_0$$

$$\text{(VI.5)}$$

$$f^{\sigma}_{nm} = -\left(2\mu^{\sigma}_{nm}(a)\ \frac{\partial s^{0}_{a\omega}}{\partial a} - 2\mu^{\sigma}_{nm}(a)\ \frac{s^{0}_{a\omega}}{a}\right)\frac{a^2}{i\mu_0}\ \frac{j_n(k_\beta a)}{k_\beta a}$$

$$+ \frac{1}{i\mu_0}\int_a^r \left\{-\left[-\rho^{\sigma}_{nm}\left(\frac{\lambda_0+2\mu_0}{\rho_0}\right) + 2\mu^{\sigma}_{nm}\right]\frac{\partial}{\partial r_0}\ \frac{1}{r_0^2}\ \frac{\partial r_0^2 s^{0}_{r_0\omega}}{\partial r_0}\right.$$

$$\left. - 2r_0^2\left[\frac{\partial}{\partial r_0}\ \frac{s^{0}_{r_0\omega}}{r_0}\right]\left[\frac{\partial}{\partial r_0}\ \frac{\mu^{\sigma}_{nm}}{r_0}\right]\right\} r_0^2\ \frac{j_n(k_\beta r_0)}{k_\beta r_0}\ dr_0 \qquad \text{(VI.6)}$$

$$f^{\sigma}_{nm} = \frac{1}{i\mu_0}\int_r^{r_f} \left\{-\left[-\rho^{\sigma}_{nm}\left(\frac{\lambda_0+2\mu_0}{\rho_0}\right) + 2\mu^{\sigma}_{nm}\right]\frac{\partial}{\partial r_0}\ \frac{1}{r_0^2}\ \frac{\partial r_0^2 s^{0}_{r_0\omega}}{\partial r_0}\right.$$

$$\left. - 2r_0^2\left[\frac{\partial}{\partial r_0}\ \frac{s^{0}_{r_0\omega}}{r_0}\right]\left[\frac{\partial}{\partial r_0}\ \frac{\mu^{\sigma}_{nm}}{r_0}\right]\right\} r_0^2\ \frac{h_n(k_\beta r_0)}{k_\beta r_0}\ dr_0 \qquad \text{(VI.7)}$$

APPENDIX VII

Evaluation of the Coefficients of the Scattered Wave when the Inhomogeneities are near the Source

We have to evaluate the coefficient $c_{nm}^{\sigma}, f_{nm}^{\sigma}$ as given in Sect. 2.7, eq. 2,3,4, for the case where all the inhomogeneities are near the source .

Using some spherical Bessel function identities we have that

$$\psi_0 = Gh_0(k_\alpha r) \tag{VII.1}$$

$$s^0_{r\omega} = \frac{\partial \psi_0}{\partial r} = -k_\alpha G h_1(k_\alpha r) \tag{VII.2}$$

$$\frac{\partial s^0_{r_0\omega}}{\partial r} = -k_\alpha^2 G \frac{dh_1(k_\alpha r)}{dk_\alpha r} \tag{VII.3}$$

$$\frac{1}{r^2}\frac{\partial r^2 s^0_{r\omega}}{\partial r} = -k_\alpha^2 G h_0(k_\alpha r) \tag{VII.4}$$

$$\frac{\partial}{\partial r}\frac{s^0_{r\omega}}{r} = -k_\alpha^2 \frac{G}{r}\frac{dh_1(k_\alpha r)}{dk_\alpha r} + \frac{k^2 G h_1(k_\alpha r)}{r\, k_\alpha r} \tag{VII.5}$$

$$\frac{\partial}{\partial r}\frac{1}{r^2}\frac{\partial r^2 s^0_{r\omega}}{\partial r} = k_\alpha^3 G h_1(k_\alpha r) \tag{VII.6}$$

so we can recast our coefficient in the following form

$$c_{00} = \frac{G}{i(\lambda_0+2\mu_0)} \left(-2\mu_{00}(a) \frac{dh_1(k_\alpha a)}{dk_\alpha a} - \lambda_{00}(a)h_0(k_\alpha a)\right)$$

$$\cdot k_\alpha^2 a^2 j_1(k_\alpha a) + \frac{G}{i(\lambda_0+2\mu_0)} \int_a^{r_f} \left[\left\{-\rho_{00}\left(\frac{\lambda_0+2\mu_0}{\rho_0}\right)+2\mu_{00}+\lambda_{00}\right\}\right.$$

$$\cdot k_\alpha h_1(k_\alpha r_0) - 2\left(\frac{\partial \mu_{00}}{\partial r_0}\right) \frac{dh_1(k_\alpha r_0)}{dk_\alpha r_0} - \left(\frac{\partial \lambda_{00}}{\partial r_0}\right) h_0(k_\alpha r_0) \Big]$$

$$\cdot k_\alpha^2 r_0^2 j_1(k_\alpha r_0) dr_0 \qquad \text{(VII.7)}$$

$$c_{nm}^{\sigma} = \frac{G}{i(\lambda_0+2\mu_0)} \left(2\mu_{nm}^{\sigma}(a) \frac{dh_1(k_\alpha a)}{dk_\alpha a} + \lambda_{nm}^{\sigma}(a)h_0(k_\alpha a)\right)$$

$$\cdot k_\alpha^2 a^2 \frac{dj_n(k_\alpha a)}{dk_\alpha a} + \frac{G}{i(\lambda_0+2\mu_0)} \int_a^{r_f} \left\{ - \left[-\rho_{nm}^{\sigma}\left(\frac{\lambda_0+2\mu_0}{\rho_0}\right)+2\mu_{nm}^{\sigma}\right.\right.$$

$$\left.\left. +\lambda_{nm}^{\sigma}\right] k_\alpha h_1(k_\alpha r_0) + 2\left(\frac{\partial \mu_{nm}^{\sigma}}{\partial r_0}\right) \frac{dh_1(k_\alpha r_0)}{dk_\alpha r_0} + \left(\frac{\partial \lambda_{nm}^{\sigma}}{\partial r_0}\right) h_0(k_\alpha r_0) \right\}$$

$$\cdot k_\alpha^2 r_0^2 \frac{dj_n(k_\alpha r_0)}{dk_\alpha r_0} + \left[\frac{2\mu_{nm}^{\sigma} h_1(k_\alpha r_0)}{k_\alpha r_0^2} + \lambda_{nm}^{\sigma} \frac{h_0(k_\alpha r_0)}{r_0} \right]$$

$$\cdot (n)(n+1) k_\alpha^2 r_0^2 \frac{j_n(k_\alpha r_0)}{k_\alpha r_0} dr_0 \qquad \text{(VII.8)}$$

$$f_{nm}^{\sigma} = \frac{G}{i\mu_0}\left(2\mu_{nm}^{\sigma}\frac{dh_1(k_\alpha a)}{dk_\alpha a} - 2\mu_{nm}^{\sigma}\frac{h_1(k_\alpha a)}{k_\alpha a}\right)k_\alpha^2 a^2\frac{j_n(k_\beta a)}{k_\beta a}$$

$$+\frac{G}{i\mu_0}\int_a^{r_f}\left\{-\left[-\rho_{nm}^{\sigma}\left(\frac{\lambda_0+2\mu_0}{\rho_0}\right)+2\mu_{nm}^{\sigma}\right]k_\alpha h_1(k_\alpha r_0)\right.$$

$$\left.-2r_0\left[-\frac{dh_1(k_\alpha r_0)}{dk_\alpha r_0}+\frac{h_1(k_\alpha r_0)}{k_\alpha r_0}\right]\left[\frac{\partial}{\partial r_0}\frac{\mu_{nm}^{\sigma}}{r_0}\right]\right\}$$

$$k_\alpha^2 r_0^2\frac{j_n(k_\beta r_0)}{k_\beta r_0}\,dr_0 \qquad \text{(VII.9)}$$

Since, in our case, we are examining the effect of the inhomogeneity wholly distributed within a sphere centered at the origin and of radius r_f such that

$$k_\alpha r_f << 1$$

we can use the following near field asymptotic expansions of the spherical Bessel functions

$$h_0(kr) \to -\frac{i}{kr}(1+ikr) \qquad \text{(VII.10)}$$

$$h_1(kr) \to -\frac{i}{k^2r^2}\left(1+\frac{k^2r^2}{2}\right) \qquad \text{(VII.11)}$$

$$\frac{dh_1(kr)}{dkr} \rightarrow \frac{2i}{k^2r^3} + \text{term of order 1} \qquad \text{(VII.12)}$$

$$\frac{j_n(kr)}{kr} \rightarrow \frac{2^n n!}{(2n+1)!}\, k^{n-1}r^{n-1}\left(1 - \frac{k^2r^2}{2(2n+3)}\right) \qquad \text{(VII.13)}$$

$$\frac{dj_n(kr)}{dkr} \rightarrow \frac{2^n n!}{(2n+1)!}\, k^{n-1}r^{n-1}\left(n - \frac{(n+2)k^2r^2)}{2(2n+3)}\right) \qquad \text{(VII.14)}$$

If we substitute these expressions in VII.7, 8, 9, and if we keep only the lowest order term in kr, we find the formulas detailed in 3.2.2 - 3.2.6 for the coefficients of the scattered wave.

APPENDIX VIII

The Static Approximation

When the inhomogeneities are near the source and the receivers are located near them, i.e.

$$k_\alpha r_f < k_\alpha r << 1$$

then we can use the static approximation to calculate the displacement field.

So we have to solve.

$$\nabla \cdot \tilde{\tilde{T}} = 0 \tag{VIII.1}$$

where

$$\tilde{\tilde{T}} = 2(\mu_0+\varepsilon\mu_1)(\tilde{\tilde{S}}_0+\varepsilon\tilde{\tilde{S}}_1+\ldots)+(\lambda_0+\varepsilon\lambda_1)(|\tilde{\tilde{S}}_0|+\varepsilon|\tilde{\tilde{S}}_1|+\ldots)\tilde{\tilde{I}} \tag{VIII.2}$$

Substituting eq. 2 in eq. 1 and collecting the order, we obtain

$$\nabla \cdot (2\mu_0\tilde{\tilde{S}}_0+\lambda_0|\tilde{\tilde{S}}_0|\tilde{\tilde{I}}) = 0 \tag{VIII.3}$$

$$-\nabla \cdot (2\mu_0\tilde{\tilde{S}}_1+\lambda_0|\tilde{\tilde{S}}_1|\tilde{\tilde{I}}) = 2\nabla\mu_1 \cdot\cdot \tilde{\tilde{S}}_0+\nabla\lambda_1 \cdot\cdot |\tilde{\tilde{S}}_0|\tilde{\tilde{I}}$$

$$+2\mu_1\nabla \cdot \tilde{\tilde{S}}_0+\lambda_1\nabla \cdot |\tilde{\tilde{S}}_0|\tilde{\tilde{I}} \tag{VIII.4}$$

We will assume that there is a small homogeneous layer around the surface of the cavity so that, as shown in Chap. II, the perturbed field is wholly contained in the body perturbations. Let P be the pressure acting on the surface r = a, then the boundary condition is

$$(\lambda_0+2\mu_0)\frac{\partial s_r^0}{\partial r}+2\lambda_0\frac{s_r^0}{r}\bigg|_{r=a} = -P$$

It should be noted here that, due to the different sign conventions we use when dealing with stress and pressure, the radial stress T_{rr} used in Appendix 1 is related to the above pressure by the relation

$$T_{rr} = -P$$

The solution to eq. 3 subject to eq. 5 is

$$s_r^0 = \frac{Pa^3}{4\mu_0 r^2} \qquad \text{(VIII.6)}$$

If we substitute that solution in eq. 4, we find

$$-\nabla\cdot(2\mu_0\tilde{\tilde{S}}_1+\lambda_0|\tilde{\tilde{S}}_1|\tilde{\tilde{I}}) = 2\nabla\mu_1\cdot\cdot\tilde{\tilde{S}}_0$$

The other terms vanish due to the form of the main field.

Let us consider again an arbitrary harmonic of the rigidity distributions, i.e.

$$\mu_1 = \mu^1_{nm}(r)P^m_n(\cos\theta)\cos m\phi \quad \text{with } n > 0 \tag{VIII.8}$$

Then, we can write eq. 7 in the form

$$-\nabla\cdot(2\mu_0\tilde{\tilde{S}}^1_1+\lambda_0|\tilde{\tilde{S}}^1_1|\tilde{\tilde{I}}) = \vec{a}_r 2\,\frac{\partial\mu^1_{nm}}{\partial r}\,\frac{\partial s^0_r}{\partial r}\,P^m_n(\cos\theta)\cos m\phi$$

$$+\vec{a}_\theta 2\mu^1_{nm}\,\frac{s^0_r}{r^2}\,\frac{\partial}{\partial\theta}\,P^m_n(\cos\theta)\cos m\phi$$

$$+\vec{a}_\phi 2\mu^1_{nm}\,\frac{s^0_r}{r^2}\,\frac{P^m_n(\cos\theta)\partial\cos m\phi}{\sin\theta\,\partial\phi} \tag{VIII.9}$$

Green's functions

In order to solve eq. 9 we would like to find the Green's function solution of

$$-\nabla\cdot(2\mu_0\tilde{\tilde{S}}^g_1+\lambda_0|\tilde{\tilde{S}}^g_1|\tilde{\tilde{I}}) = A\delta(r-r_0)P^m_n(\cos\theta)\cos m\phi\vec{a}_r$$

$$+B\delta(r-r_0)\,\frac{\partial}{\partial\theta}\,P^m_n(\cos\theta)\cos m\phi\,\vec{a}_\theta$$

$$+B\delta(r-r_0)\,\frac{P^m_n(\cos\theta)}{\sin\theta}\,\frac{\partial}{\partial\phi}\cos m\phi\,\vec{a}_\phi \tag{VIII.10}$$

By following the step of the derivation in Appendix II, we can see that the Green's function solution of eq. 10 is given by the limit $\omega \to 0$ of eq. 37, 38, 39, 40, Appendix II, i.e. we can express the displacement field in the following way

$$\vec{s}_1^{\,g} = \nabla g_1 + \nabla\times\nabla\times\vec{a}_r r g_2 \qquad \text{(VIII.11)}$$

where

$$g_1 = \left\{ \frac{A r_0^{n+1}}{(2n+1)(\lambda_0+2\mu_0) r^{n+1}} \left[\frac{n r^2}{2(2n-1)} - \frac{(n+2) r_0^2}{2(2n+3)} \right] \right.$$

$$\left. + \frac{B(n)(n+1)}{(2n+1)(\lambda_0+2\mu_0)} \frac{r_0^{n+1}}{r^{n+1}} \left[\frac{r^2}{2(2n-1)} - \frac{r_0^2}{2(2n+3)} \right] \right\} \cdot$$

$$P_n^m(\cos\theta)\cos m\phi \quad \text{for } r > r_0$$

$$= \left\{ - \frac{A}{(\lambda_0+2\mu_0)(2n+1)} \frac{r^n}{r_0^n} \left[- \frac{(n+1) r^2}{2(2n+3)} + \frac{(n-1) r_0^2}{2(2n-1)} \right] \right.$$

$$\left. + \frac{B(n)(n+1)}{(\lambda_0+2\mu_0)(2n+1)} \frac{r^n}{r_0^n} \left[- \frac{r^2}{2(2n+3)} + \frac{r_0^2}{2(2n-1)} \right] \right\} \cdot$$

$$P_n^m(\cos\theta)\cos m\phi \quad \text{for } r < r_0 \qquad \text{(VIII.12)}$$

and

$$g_2 = \left\{ \frac{A}{(2n+1)\mu_0} \frac{r_0^{n+1}}{r^{n+1}} \left[\frac{r^2}{2(2n-1)} - \frac{r_0^2}{2(2n+3)} \right] \right.$$

$$\left. + \frac{B}{(2n+1)\mu_0} \frac{r_0^{n+1}}{r^{n+1}} \left[\frac{(n+1)r^2}{2(2n-1)} - \frac{(n+3)r_0^2}{2(2n+3)} \right] \right\} P_n^m(\cos\theta)\cos m\phi$$

$$\text{for } r > r_0$$

$$= \left\{ \frac{A}{\mu_0(2n+1)} \frac{r^n}{r_0^n} \left[- \frac{r^2}{2(2n+3)} + \frac{r_0^2}{2(2n-1)} \right] \right.$$

$$\left. - \frac{B}{\mu_0(2n+1)} \frac{r^n}{r_0^n} \left[- \frac{nr^2}{2(2n+3)} + \frac{(n-2)r_0^2}{2(2n-1)} \right] \right\} P_n^m(\cos\theta)\cos m\phi$$

(VIII.13)

The reader might verify these formulas by applying the procedure outlined in Sect. 1.4, Chap. II.

Using these Green's functions, if we perform the integration of the source terms in eq. 9 we obtain that

$$\vec{s}_1 = \nabla\psi + \nabla\times\nabla\times\vec{a}_r r\psi_2 \quad \text{for } r > r_f \tag{VIII.14}$$

where for $r < r_f$

$$\psi = \sum_{n=1}^{\infty} \sum_{m=0}^{n} \left[\left(\frac{c_{nm}^{1}}{r^{n-1}} + \frac{d_{nm}^{1}}{r^{n+1}} \right) \cos m\phi \right.$$

$$\left. + \left(\frac{c_{nm}^{2}}{r^{n-1}} + \frac{d_{nm}^{2}}{r^{n+1}} \right) \sin m\phi \right] P_n^m(\cos \theta) \qquad \text{(VIII.15)}$$

and

$$\psi_2 = \sum_{n=1}^{\infty} \sum_{m=0}^{n} \left[\left(\frac{f_{nm}^{1}}{r^{n-1}} + \frac{g_{nm}^{1}}{r^{n+1}} \right) \cos m\phi \right.$$

$$\left. + \left(\frac{f_{nm}^{2}}{r^{n-1}} + \frac{g_{nm}^{2}}{r^{n+1}} \right) \sin m\phi \right] P_n^m(\cos \theta) \qquad \text{(VIII.16)}$$

where

$$c_{nm}^{\sigma} = + \frac{Pa^3}{4\mu_0} \frac{3n(n-1)}{(2n+1)(2n-1)(\lambda_0+2\mu_0)} \int_a^{r_f} \mu_{nm}^{\sigma} r_0^{n-3} \, dr_0 \qquad \text{(VIII.17)}$$

$$d_{nm}^{\sigma} = - \frac{Pa^3}{4\mu_0} \frac{n(3n+5)}{(2n+1)(2n+3)(\lambda_0+2\mu_0)} \int_a^{r_f} \mu_{nm}^{\sigma} r_0^{n-1} dr_0 \qquad \text{(VIII.18)}$$

$$f_{nm}^{\sigma} = + \frac{Pa^3}{4\mu_0} \frac{3(n-1)}{(2n+1)^2\mu_0} \int_a^{r_f} \mu_{nm}^{\sigma} r_0^{n-3} dr_0 \qquad \text{(VIII.19)}$$

$$g_{nm}^{\sigma} = - \frac{Pa^3}{4\mu_0} \frac{3(n-1)}{(2n+1)(2n+3)\mu_0} \int_a^{r_f} \mu_{nm}^{\sigma} r_0^{n-1} \, dr_0 \qquad \text{(VIII.20)}$$

It should be remarked that

$$c_{1m}^{\sigma} = f_{1m}^{\sigma} = 0$$

so that it is still the $P_n^m(\cos\theta)$ harmonic of the potential that gives the maximum weighting of the inhomogeneities near the source. Indeed we have in that case

$$c_{2m}^{\sigma} = + \frac{Pa^3}{4\mu_0} \frac{2}{5} (\lambda_0+2\mu_0) \int_a^{r_f} \frac{\mu_{2m}^{\sigma}}{r_0} dr_0 \qquad \text{(VIII.21)}$$

and

$$f_{2m}^{\sigma} = + \frac{Pa^3}{4\mu_0} \frac{3}{25} \int_a^{r_f} \frac{\mu_{2m}^{\sigma}}{r_0} dr_0 \qquad \text{(VIII.22)}$$

The case n = 0

We still have to deal with the case where the inhomogeneities have a pure radial variation i.e.

$$\mu_1 = \mu_{00}(r) \qquad \text{(VIII.23)}$$

In that case eq. 7 reads

$$-\nabla\cdot(2\mu_0\tilde{\tilde{S}}_1+\lambda_0|\tilde{\tilde{S}}_1|\tilde{\tilde{I}}) = \vec{a}_r \frac{\partial\mu_{00}}{\partial r} \frac{\partial s_r^0}{\partial r} \qquad \text{(VIII.24)}$$

Green's function

By following the same steps as Appendix IV, we find that the Green's function solution of

$$-\nabla\cdot(2\mu_0\tilde{\tilde{S}}_1^g + \lambda_0|\tilde{\tilde{S}}_1^g|\tilde{\tilde{I}}) = \vec{a}_r A\delta(r-r_0) \qquad \text{(VIII.25)}$$

is given by

$$\vec{s}_1^g = \nabla g_1 \qquad \text{(VIII.26)}$$

where

$$g_1 = -\frac{Ar_0^3}{(\lambda_0+2\mu_0)3r} \qquad \text{for } r > r_0$$

$$= \frac{A}{(\lambda_0+2\mu_0)}\,\frac{r^2}{6} \qquad \text{for } r < r_0$$

so that the solution of eq. 24 is given by

$$\vec{s}_1 = \nabla\psi$$

where for $r > r_f$

$$\psi_1 = - \frac{1}{\lambda_0+2\mu_0} \frac{1}{3r}\int_a^{r_f} 2 \frac{\partial \mu_{00}}{\partial r_0} \frac{\partial s^0_{r_0}}{\partial r_0} r_0^3 \, dr_0$$

$$= + \frac{Pa^3}{4\mu_0} \frac{1}{(\lambda_0+2\mu_0)} \frac{1}{3r} \int_a^{r_f} 4 \frac{\partial \mu_{00}}{\partial r_0} \, dr_0$$

$$= + \frac{Pa^3}{4\mu_0} \frac{1}{(\lambda_0+2\mu_0)} \frac{4}{3r} (\mu_{00}(r_f)-\mu_{00}(a))$$

$$= 0$$

since we have assumed $\mu_{00}(r_f) = \mu_{00}(a) = 0$.

So we see that to the order considered, no scattered field is generated by the radial variation of the parameter in $r > r_f$.

APPENDIX IX

Evaluation of the Coefficients of the Scattered wave when the Inhomogeneities are far from the Source

We consider a model composed of the spherical harmonics of the medium parameters specified by $n \leq p$. Furthermore, we restrict their radial variation to the interior of two spheres of radius r_{in} and r_f such that

$$k_\alpha r_f > k_\alpha r_{in} >> p^2$$

In this case, we can use the far field asymptotic expansion of the spherical Bessel functions appearing in VII 7, 8, 9, i.e.

$$k_n(kr) \to \frac{e^{ikr}(i)^{-n}}{ikr}$$

$$j_n(kr) \to \frac{e^{ikr}(i)^{-n}}{2ikr} + \frac{e^{ikr}(-i)^{-n}}{2(-ikr)}$$

Then, keeping the highest order terms in kr in VII 7, 8, 9, we obtain the formulas detailed in 3.3.1 and 3.3.2 for the coefficients of the scattered wave.

APPENDIX X

Geometrical Optics Approximation

Following Karal and Keller (1959), if we substitute in 2.1.3 a displacement field of the form

$$\vec{s} = \vec{A} e^{i\omega(\phi - t)} \tag{X.1}$$

where

$$\vec{A} = \sum_{n=0}^{\infty} (i\omega)^{-n} A_n$$

and ϕ is independent of ω, we then find that, for a compressional source, the phase ϕ must satisfy the eikonal equation

$$\nabla\phi \cdot \nabla\phi = \frac{\rho}{\lambda + 2\mu} = \frac{\rho_0 + \varepsilon\rho_1}{\lambda_0 + 2\mu_0 + \varepsilon\lambda_1 + \varepsilon 2\mu_1}$$

If we use the method of small perturbation to solve that equation, i.e. we assume that

$$\phi = \phi_0 + \varepsilon\phi_1 + \ldots$$

then collecting the order, we have to solve

$$\nabla\phi_0 \cdot \nabla\phi_0 = \frac{\rho_0}{\lambda_0 + 2\mu_0} \tag{X.2}$$

$$2\nabla\phi_0\cdot\nabla\phi_1 = \frac{\varepsilon\rho_1}{\lambda_0+2\mu_0} - \varepsilon\rho_0 \frac{(\lambda_1+2\mu_1)}{(\lambda_0+2\mu_0)^2} \tag{X.3}$$

We will assume that the phase is zero at the boundary r = a, then because of the spherical symmetry

$$\nabla\phi_0\cdot\nabla\phi_0 = \left(\frac{\partial\phi_0}{\partial r}\right)^2 = \frac{\rho_0}{\lambda_0+2\mu_0} \tag{X.4}$$

so

$$\phi_0 = \left(\frac{\rho_0}{\lambda_0+2\mu_0}\right)^{\frac{1}{2}}(r-a) \tag{X.5}$$

Eq. 3 then reads

$$2\left(\frac{\rho_0}{\lambda_0+2\mu_0}\right)^{1/2} \frac{\partial\phi_1}{\partial r} = \frac{\varepsilon\rho_1}{\lambda_0+2\mu_0} - \varepsilon\rho_0 \frac{(\lambda_1+2\mu_1)}{(\lambda_0+2\mu_0)^2}$$

so

$$\phi_1 = \frac{1}{2} \frac{\rho_0^{1/2}}{(\lambda_0+2\mu_0)^{3/2}} \int_{r_{in}}^{r_f} \rho_1\left(\frac{\lambda_0+2\mu_0}{\rho_0}\right) - (2\mu_1+\lambda_1)dr_0 \tag{X.6}$$

To determine the amplitude, if we let

$$A_n = A_n^1 + \varepsilon A_n^2 + \ldots$$

then, since for $r < r_{in}$

$$\sum (i\omega)^{-n} A_n^1 = \vec{a}_r \frac{G}{r} e^{ik_\alpha a}$$

we therefore have

$$\vec{s}_{g\cdot optics} = \vec{a}_r \left(\frac{G}{r} + \text{terms order } \varepsilon\omega^0 + \ldots\right) \cdot$$

$$e^{ik_\alpha r + i\varepsilon\omega\phi_1 + \ldots - i\omega t} \qquad (X.7)$$

APPENDIX XI

The f_{10} Coefficient for Inhomogeneities near the Source

If we expand in Taylor's series the exponential terms in each of the integrals in 3.4.5 we obtain

$$f_{10} = \frac{G}{i\mu_0}\int_a^{r_f}\mu_{10}\left(R_1(r_0) + \frac{i}{10}\left(-2\frac{k_\alpha^4}{k_\beta^3} + 2\frac{k_\beta^2}{k_\alpha}\right) + \frac{3}{8r_0}\cdot\right.$$

$$\left(-\frac{2}{3}\frac{k_\alpha}{k_\beta} - \frac{k_\beta}{k_\alpha} - \frac{k_\alpha^3}{k_\beta^2}\right) + \frac{1}{r_0^3}\left(-\frac{3}{2}\frac{k_\alpha}{k_\beta^2} - \frac{3}{2}k_\alpha k_\beta\right)$$

$$\left.-\frac{9}{k_\alpha k_\beta^3 r^2}\right)dr_0$$

$$+\frac{G}{i\mu_0}\int_a^{r_f}\mu_{10}\left(R_2(r_0) + \frac{i}{10}\left(2\frac{k_\alpha^4}{k_\beta^3} + 2\frac{k_\beta^2}{k_\alpha}\right) + \frac{3}{8r_0}\cdot\right.$$

$$\left(\frac{2}{3}\frac{k_\alpha}{k_\beta} + \frac{k_\beta}{k_\alpha} + \frac{k_\alpha^2}{k_\beta^2}\right) + \frac{1}{r_0^3}\left(\frac{3}{2}\frac{k_\alpha}{k_\beta^2} + \frac{3}{2}k_\alpha k_\beta\right) + \left.\frac{9}{k_\alpha k_\beta^3 r_0^5}\right)dr_0$$

(XII.1)

where

$$R_1+R_2 = ir^2\left[k_\alpha^3\left(\frac{88}{280} - \frac{66}{210}\right) + k_\beta^2 k_\alpha\left(\frac{48}{280} - \frac{11}{210}\right) - \frac{8}{280}\frac{k_\beta^4}{k_\alpha}\right]$$

$$+ \text{terms of order } k_\alpha^4 r^3 + \ldots.$$

If we examine the case where

$$\lambda_0 = \mu_0$$

we obtain that

$$R_1+R_2 = ir^2 k_\alpha^3 (0.03) + \ldots$$

So, if $k_\alpha r_0 \leq 1$, we can evaluate the effect of the inhomogeneities by using

$$f_{10} = \frac{G}{\mu_0}\int_a^{1/k_\alpha} \mu_{10}\,\frac{2}{5}\,\frac{k_\beta^2}{k_\alpha}\,dr_0$$

since the contribution from the other terms is likely to be small.

APPENDIX XII

The Coefficients of the Scattered wave When We Have a Fluid Inside the Source Cavity

In order to investigate the influence of a fluid cavity on the zero order solution, we can follow the procedure outlined in Chapter II. As shown there, we can first evaluate the surface and body perturbation and then synthesize these results by calculating the coefficients of the scattered wave.

The surface perturbation

In order to find the scattered wave generated by the inhomogeneous distribution of parameters on the surface of the source, we can solve the equations detailed in Section 2.3. In the case where the medium inside the source is a fluid specified by $(\rho^-,0,\lambda^-)$ we can write the first order boundary conditions as follows:

1) Continuity of stresses

$$\lambda^- \nabla\cdot\vec{s}^-_{12}\Big|_{r=a^-} = 2\mu_1 \frac{\partial s^0_{r\omega}}{\partial r} + \lambda_1 \nabla\cdot\vec{s}^0_{\omega} + 2\mu_0 \frac{\partial s_{r\omega}}{\partial r} + \lambda_0 \nabla\cdot\vec{s}_{12}\Big|_{r=a^+}$$

$$0 = \frac{1}{r}\frac{\partial s_{r12}}{\partial\theta} + r\frac{\partial}{\partial r}\left(\frac{\partial s_{\theta 12}}{r}\right)\Bigg|_{r=a^+}$$

and

$$0 = \frac{1}{r \sin\theta} \frac{\partial s_{r12}}{\partial \phi} + r \frac{\partial}{\partial r}\left(\frac{s_{\phi 12}}{r}\right)\Bigg|_{r=a^+}$$

2) Continuity of the normal component of the displacement

$$s^-_{r12}\Big|_{r=a^-} = s_{r12}\Big|_{r=a^+}$$

In the region r > a, we can still express the displacement field in terms of potentials by the following relation:

$$\vec{s}_{12\omega} = \nabla\psi^s + \nabla\times\vec{a}_r r\psi_1^s + \nabla\times\nabla\times\vec{a}_r r\psi_2^s$$

where $(\psi^+, \psi_1^+, \psi_2^+)$ obey the wave equation with phase velocity α for ψ^+ and β for ψ_1^+ and ψ_2^+.

In the region r < a we can express the displacement field as follows:

$$\vec{s}^-_{12\omega} = \nabla\psi^-$$

where ψ^- obeys the wave equation with phase velocity

$$\left(\frac{\lambda^-}{\rho^-}\right)^{1/2} \equiv \alpha^-$$

Let us consider an arbitrary term in the decomposition of the parameters at the boundary r = a, i.e.

$$(\rho_1(a),\mu_1(a),\lambda_1(a)) = (\rho^1_{nm},\mu^1_{nm},\lambda^1_{nm})P^m_n(\cos\theta)\cos m\phi$$

Then following an argument similar to the one given in Appendix IV, we can express the potential field as follows:

$$\psi^s = Ah_n(k_\alpha r)P^m_n(\cos\theta)\cos m\phi$$

$$\psi^s_1 = 0 \text{ (no torsional waves are generated)}$$

$$\psi^s_2 = Bh_n(k_\beta r)\ P^m_n(\cos\theta)\cos m\phi$$

$$\psi^- = Cj_n(k_{\alpha^-} r)P^m_n(\cos\theta)\cos m\phi$$

We can calculate the coefficients A, B, C with the boundary conditions and, since we are interested only in the part of the spectrum where the wavelength is much larger than the radius of the cavity i.e. ka << 1, we can retain only the lowest order in ka in the result. These operations give the following results:

$$A = -\left(2\mu_{nm}^{1}\,\frac{\partial s_{a\omega}^{0}}{\partial a} + \frac{\lambda_{nm}^{1}}{a^{2}}\,\frac{\partial a^{2}s_{a\omega}^{0}}{\partial a}\right)\frac{2^{n}n!}{(2n+1)!}\,\frac{k_{\alpha}^{n-1}a^{n+1}}{i(\lambda_{0}+2\mu_{0})}\cdot$$

$$f(\lambda_{0},\mu_{0},n)$$

$$B = -\left(2\mu_{nm}^{1}\,\frac{\partial s_{a\omega}^{0}}{\partial a} + \frac{\lambda_{nm}^{1}}{a^{2}}\,\frac{\partial a^{2}s_{a\omega}^{0}}{\partial a}\right)\frac{2^{n}n!}{(2n+1)!}\,\frac{k_{\beta}^{n-1}a^{n+1}}{i\mu_{0}}\cdot$$

$$g(\lambda_{0},\mu_{0},n)$$

where

$$f(\lambda_{0},\mu_{0},n) = \frac{n(4n^{2}-1)(\lambda_{0}+2\mu_{0})}{\lambda_{0}(2n^{2}+1)+\mu_{0}(2n^{2}+2n+2)}$$

and

$$g(\lambda_{0},\mu_{0},n) = \frac{n(4n^{2}-1)(\lambda_{0}+2\mu_{0})}{\lambda_{0}(2n^{2}+1)+\mu_{0}(2n^{2}+2n+2)}$$

The case n = 0 can be treated in a similar way and the result is the following

$$\psi^{s} = Ah_{0}(k_{\alpha}r)$$

where

$$A = \left(2\mu_{00}\,\frac{\partial s_{a\omega}}{\partial a} + \frac{\lambda_{00}}{a^{2}}\,\frac{\partial a^{2}s_{a\omega}^{0}}{\partial a}\right)\frac{k_{\alpha}a^{3}}{i(3)(\lambda_{0}+2\mu_{0})}\,q(\lambda^{-},\mu_{0},\lambda_{0})$$

and

$$q(\lambda^-,\mu_0,\lambda_0) = \frac{\lambda_0+2\mu_0}{\lambda^-+\frac{4}{3}\mu_0}$$

It is interesting at this point to compare these results with the ones we obtained in Section 2.5. If we calculate the asymptotic expansion of these potentials for $ka << 1$, and if we keep the lowest order in ka, we then obtain the same result as above but with

$$f(\lambda,\mu,n) = g(\lambda_0,\mu_0,n) = q(\lambda^-,\lambda_0,\mu_0) = 1$$

So we see that the difference between these two models lies within the f, g, q factors. If we examine these factors, we remark that, except for the case $n = 1$, the scattered wave generated at $r = a$, will have a larger amplitude when there is a fluid inside the cavity. In order to investigate the extent of the region for which the difference between the two models persists let us evaluate the body perturbation.

Green's function for the body perturbation.

In order to find the Green's function solution of eq. 2.4.4 when there is a fluid inside the cavity, let us first consider the Green's function K found in 2.4.6 and

rewrite it in the following form

$$K = \left[-\frac{A}{2} \frac{dh_n(k_\alpha r_0)}{dk_\alpha r_0} - \frac{B(n)(n+1)}{2} \frac{h_n(k_\alpha r_0)}{k_\alpha r_0} \right] \frac{r_0^2}{i(\lambda_0+2\mu_0)}$$

$$\cdot h_n(k_\alpha r) P_n^m(\cos\theta)\cos m\phi$$

$$+ \left[-\frac{A}{2} \frac{\overline{dh(k_\alpha r_0)}}{dk_\alpha r_0} - \frac{B(n)(n+1)}{2} \frac{\overline{h_n(k_\alpha r_0)}}{k_\alpha r_0} \right] \frac{r_0^2}{i(\lambda_0+2\mu_0)}$$

$$\cdot h_n(k_\alpha r) P_n^m(\cos\theta)\cos m\phi \quad \text{for } r > r_0$$

$$= \left[-\frac{A}{2} \frac{dh_n(k_\alpha r_0)}{dk_\alpha r_0} - B(n)(n+1) \frac{h_n(k_\alpha r_0)}{k_\alpha r_0} \right] \frac{r_0^2}{i(\lambda_0+2\mu_0)}$$

$$\cdot \frac{h_n(k_\alpha r)}{2} P_n^m(\cos\theta)\cos m\phi$$

$$+ \left[-\frac{A}{2} \frac{dh_n(k_\alpha r_0)}{dk_\alpha r_0} - B(n)(n+1) \frac{h_n(k_\alpha r_0)}{k_\alpha r_0} \right] \frac{r_0^2}{i(\lambda_0+2\mu_0)}$$

$$\cdot \frac{\overline{h_n(k_\alpha r)}}{2} P_n^m(\cos\theta)\cos m\phi \quad \text{for } r < r_0$$

Arrival time considerations reveal that for each domain of observation, we can distinguish two waves reaching the receiver: one of them travels directly from the scatterer

position to the receiver whereas the other must pass through the origin before reaching the receiver. Now, when we have a fluid inside the cavity, the incoming wave towards the origin is transformed at the surface of the cavity such as to meet the continuity of stresses and normal displacement there. So, at that surface, the incoming energy is partitioned into a compressional wave penetrating inside the source and a compressional and shear wave reflected towards infinity.

We therefore see that in order to find the Green's function when the medium inside the source is a fluid we can perform the following operations:

1) Separate the Green's function found in Chapter II into the two parts specified above
2) Use the incoming wave towards the origin to find the partition of wave at the surface of the cavity. This result will give us an outgoing shear and compressional wave for each of the two incoming wave types.
3) For $r > r_0$ we can take the sum of the outgoing compressional waves just found and add to it the compressional wave reaching directly the receiver. We can do the same process with the shear wave.
4) Finally, since we are interested in wavelength much larger than the radius of the cavity, we expand the above results in asymptotic series and keep only the lowest order in ka.

This is the process I have followed to calculate the Green's functions and the results are as follows:

$$\vec{s}_{11\omega} = \nabla K + \nabla\times\nabla\times\vec{a}_r rH$$

where, for $r > r_0$

$$K = P_n^m(\cos\theta)\cos m\phi h_n(k_\alpha r)$$

$$\left[- \frac{Ar_0^2}{i(\lambda_0+2\mu_0)} \frac{dj_n(k_\alpha r_0)}{dk_\alpha r_0} - \frac{B(n)(n+1)}{i(\lambda_0+2\mu_0)} r_0^2 \frac{j_n(k_\alpha r_0)}{k_\alpha r_0} \right.$$

$$- \frac{A}{i(\lambda_0+2\mu_0)} \frac{2^n n!}{(2n)!} k_\alpha^{n-1} a^{n+1} \left(\frac{a^n}{r_0^n}\right) \ell \left(p + \frac{r_0^2}{a^2} m\right)$$

$$\left. + \frac{B}{i(\lambda_0+2\mu_0)} \frac{2^n n!}{(2n)!} k_\alpha^{n-1} a^{n+1} \left(\frac{a^n}{r_0^n}\right) \ell \left(v + \frac{r_0^2}{a^2} s\right)\right]$$

and

$$H = P_n^m(\cos\theta)\cos m\phi h_n(k_\beta r)$$

$$\left[- \frac{Ar_0^2}{i\mu_0} \frac{j_n(k_\beta r_0)}{k_\beta r_0} - \frac{Br_0^2}{i\mu_0} \left(\frac{j_n(k_\beta r_0)}{k_\beta r_0} + \frac{dj_n(k_\beta r_0)}{dk_\beta r_0} \right) \right.$$

$$- \frac{A}{i\mu_0} \frac{2^n n!}{(2n)!} k_\beta^{n-1} a^{n+1} \left(\frac{a^n}{r_0^n}\right) \frac{\ell}{n} \left(p + \frac{r_0^2}{a^2} m\right)$$

$$\left. + \frac{B}{i\mu_0} \frac{2^n n!}{(2n)!} k_\beta^{n-1} a^{n+1} \left(\frac{a^n}{r_0^n}\right) \frac{\ell}{n} \left(v + \frac{r_0^2}{a^2} s\right)\right]$$

where

$$\ell = \frac{2n-1}{\lambda_0[2n^2+1]+\mu_0[2n^2+2n+2]}$$

$$p = n\left[\frac{\mu_0(n+1)^2}{(2n+1)} - \frac{(n+1)n(\lambda_0+2\mu_0)}{(2n+1)} + \frac{\lambda_0(n+1)}{2n+1}\right]$$

$$m = n\left[-\frac{(n-1)^2(2\mu_0)}{2(2n-1)} + \frac{(n^2-1)(\lambda_0+2\mu_0)}{2(2n-1)}\right]$$

$$v = \frac{n^2(n+1)}{2(2n+1)}\left[2(n+1)\mu_0 - 2n(\lambda_0+2\mu_0)+2\lambda_0\right]$$

$$s = \frac{n(n^2-1)}{2(2n-1)}\left[-2\mu_0 n+2(n-2)(\lambda_0+2\mu_0)\right]$$

The case n = 0 can be treated in a similar way and the result is as follows

$$\vec{s}_{11\omega} = \nabla K$$

where for $r > r_0$

$$K = h_0(k_\alpha r)\left[\frac{Ar_0^2}{i(\lambda_0+2\mu_0)}\, j_1(k_\alpha r_0)\right.$$

$$\left. + \frac{Ar_0^2}{i(\lambda_0+2\mu_0)}\,\frac{k_\alpha a}{3}\left(\frac{-3\lambda^-+2\mu_0+3\lambda_0}{3\lambda^-+4\mu_0}\right)\right]$$

We remark that the first part of these Green's functions is exactly the same as the one we have obtained in Section 2.4. The other terms are corrections due to the presence of the fluid cavity.

By expanding the above results in asymptotic series in terms of the parameter $k_\alpha r_0$ we remark that the correction terms are of the same order of magnitude as the first part of the Green's function when the scatterer radius, r_0, is approximately the same as the radius of the cavity, a. On the other hand, when the scattering occurs at a large distance compared to the radius of the cavity, then the corrections terms can be neglected and we thus recover the results obtained in Chapter II.

In order to see what are the effects of these correction terms, let us calculate the coefficients of the scattered wave.

The Coefficients of the scattered wave

To evaluate these coefficients, we must first integrate the effect of the equivalent body force given in eq. 2.4.3 by using the preceding Green's functions and then add to this result the surface perturbation. Since the correction terms in the Green's function just described are effective only near the source, we can calculate their contribution to the scattered wave by using the asymptotic expansion for small $k_\alpha r_0$ of the equivalent body force.

When the above calculations are made, we find that the total displacement field, in a region outside the inhomogeneities, i.e. for $r > r_f$, can be expressed as follows:

$$\vec{s}_\omega = \nabla\psi + \nabla\times\nabla\times r\vec{a}_r\psi_2 \qquad \text{(XII.1)}$$

where

$$\psi = Gh_0(k_\alpha r) + \varepsilon d_{00}h_0(k_\alpha r)$$

$$+ \sum_{n=1}^{\infty}\sum_{m=0}^{n}(\varepsilon d^1_{nm}\cos m\phi + \varepsilon d^2_{nm}\sin m\phi)h_n(k_\alpha r)P^m_n(\cos\theta) \qquad \text{(XII.2)}$$

and

$$\psi_2 = \sum_{n=1}^{\infty}\sum_{m=0}^{n}(\varepsilon g^1_{nm}\cos m\phi + \varepsilon g^2_{nm}\sin m\phi)h_n(k_\beta r)P^m_n(\cos\theta) \qquad \text{(XII.3)}$$

where

$$d_{00} = c_{00} + \frac{G}{\lambda_0+2\mu_0}\,\frac{4}{3}\left(\frac{-3\lambda^{-}+2\mu_0+3\lambda_0}{3\lambda^{-}+4\mu_0}\right)\int_a^{r_f} \mu_{00}\,\frac{a}{r_0^2}\,dr_0$$

(XII.4)

$$d_{1m}^{\sigma} = c_{1m}^{\sigma} + {}^{F}c_{1m}^{\sigma} \qquad \text{(XII.5)}$$

$$d_{nm}^{\sigma} = c_{nm}^{\sigma} + \frac{1}{\lambda_0+2\mu_0}\,\frac{2^n n!}{(2n)!}\,k_\alpha^{n-2}a^{n-2}\cdot$$

$$\int_a^{r_f} 2\mu_{nm}^{\sigma}\left(\frac{a^{n+3}}{r_0^{n+4}}\right)\ell\left[2(n+3)p+v+\frac{r_0^2}{a^2}\,(2(n+1)m+s)\right]dr_0$$

$$n > 1 \qquad \text{(XII.6)}$$

$$g_{1m}^{\sigma} = f_{1m}^{\sigma} + {}^{F}f_{1m}^{\sigma} \qquad \text{(XII.7)}$$

$$g_{nm}^{\sigma} = f_{nm}^{\sigma} + \frac{G}{\mu_0}\,\frac{2^n n!}{(2n)!}\,\frac{k_\beta^{n-1}}{k_\alpha}\,a^{n-2}\cdot$$

$$\int_a^{r_f} 2\mu_{nm}^{\sigma}\left(\frac{a^{n+3}}{r_0^{n+4}}\right)\frac{\ell}{n}\,\left[2(n+3)p+v+\frac{r_0^2}{a^2}(2(n+1)+s)\right]dr_0$$

$$n > 1 \qquad \text{(XII.8)}$$

The terms c_{00}^{σ}, c_{nm}^{σ}, f_{nm}^{σ} are the same as the ones given in Section 2.7. The other terms are a correction to these values due to the presence of the fluid cavity. We note that we have not given the explicit form of the terms $F_{c}{}_{1m}^{\sigma}$ and $F_{f}{}_{1m}^{\sigma}$. Indeed, to calculate these coefficients, we must keep more terms in the asymptotic expansion of the Green's functions in powers of the small parameter, $k_{\alpha}a$. This work will not be done in this report.

We remark that there are two special cases of interest relative to long wave scattering near the source, i.e. n=0 and n=2. Indeed, for each of them, the correction terms depend on frequency only through the spectrum of the source whereas for other values of n we have a low frequency cut-off.

Since the case n = 2 is discussed in Chapter IV, let us restrict our consideration here to the case n = 0.

If we examine the scattered wave produced within a wavelength from the source, then we can use the asymptotic expansion of c_{00} given in 3.2.2. But since this contribution to d_{00} has a low frequency cut-off, we can neglect it compared to the correction term. We then obtain, for the sum of the potential due to the main wave and the scattered wave characterized by n = 0, the following result:

$$\psi = \frac{T_{rr}}{4\mu_0} a^3(1+\varepsilon b)h_0(k_\alpha r)$$

where

$$b = \frac{-1}{\lambda_0+2\mu_0} \frac{4}{3} \left(\frac{-3\lambda^-+2\mu_0+3\lambda_0}{3\lambda^-+4\mu_0} \right) \int_a^{r_f} \mu_{00} \frac{a}{r_0^2} \, dr_0$$

and here we have used the notation of Appendix I.

Thus the field observed is the same as if the medium was homogeneous, provided we define an effective pressure and radius of the cavity such that

$$(T_{rr}a^3)_{eff} = T_{rr}a^3(1+\varepsilon b).$$

BIBLIOGRAPHY

1. Aki, K., A note on surface wave generated from the Hardhat nuclear explosion, J. Geophys. Res., 69, p. 1131-1134, 1964.

Aki, K., P. Reasenberg, T. De Fazio, and Y. B. Tsai, Near field and far field seismic evidence for triggering an earthquake by the Benham explosion, Bull. Seism. Soc. Am., 59, p. 2197-2207, 1969.

Aki, K., Y.B. Tsai, The mechanism of Love wave excitation by explosive source, J. Geophys. Res., 1971, in press

2. Archambeau, C. and Sammis, C., Seismic radiation from explosion in prestressed media and the measurement of tectonic stress in the earth, Rev. of Geophys. and Space Physics, 8, p. 473-500, 1970.

3. Brune, J.N., and P.W. Pomeroy, Surface wave radiation patterns for underground nuclear explosions and small magnitude earthquake, J. Geophys. Res., 68, p. 5005-5028, 1963.

4. Dunkin, J.W., Scattering of a transient spherical P wave by a randomly inhomogeneous elastic half-space, Geophysics, Vol. 34, p. 357-382, 1969.

5. Geyer, R.L., and S.T. Martner, SH waves from explosive sources, Geophysics, 34, 893-905, 1964.

6. Karal, F.C. and Keller, J.B., Elastic wave propagation in homogeneous and inhomogeneous media, J. Acoust. Soc. Am., 31, p. 694-705, 1959.

Karal, F.C. and Keller, J.B., Elastic electromagnetic and other waves in random medium, J. Math. Phys., 5, p. 537-547, 1964.

7. Kisslinger, C., Katekar, E.J., Jr., and T.V. McEvilly, SH motion from explosions in soil, J. Geophys. Res., 66, p. 3487-3496, 1961.

8. Knopoff, L., and J.A. Hudson, Scattering of elastic waves by small inhomogeneities, J. Acous. Soc. Am., 36, p. 339-343, 1964.

9. Morse, P.M. and Feshback, H., Methods of theoretical physics, McGraw-Hill Publishers, 1953.

10. Orkild, P.P., F.M. Byers, Jr., D.L. Hoover, and K.A. Sargent, Subsurface geology of Silent Canyon Caldera Nevada Test Site, Nevada, ed. by E.B. Eckel, Geol. Soc., Am. Memoir, 110, p. 77-86, 1968.

11. Sato, Y., Boundary conditions in the problem of generation of elastic waves, Bull. Earthq. Res. Inst., 27, p. 1-9, 1949.

12. Sezawa, K., Dilatational and distortional waves generated from a cylindrical or spherical origin, Bull. Earthq. Res. Inst., 2, p. 13-20, 1927.

13. Sharpe, J.A., The production of elastic waves by explosion pressure, II Results of observation near an exploding charge, Geophysics, 7, p. 311-321, 1942.

14. Smith, S.W., Generation of seismic waves by underground explosions and the collapse of cavities, J. Geophys. Res., 68, p. 1477-1483, 1963.

15. Stauder, W., Smaller aftershocks of the Benham nuclear explosion, Bull. Seism. Soc. Am. 61, p. 417-428, 1971.

16. Toksöz, M.N., D.G. Harkrider, and A. Ben Menahem, Determination of source parameters by amplitude equalization of seismic surface waves, 2. Release of tectonic strain by underground nuclear explosions and mechanisms of earthquakes. J. Geophys. Res., 70, p. 907-922, 1965.

17. Wright, J.K., and E.W. Carpenter, The generation of horizontally polarized shear waves by underground explosions, J. Geophys. Res., 67, p. 1957-1963, 1962.